

E 7.5 - 1 0.1 5.5

CR-142205

N75-18667

(E75-10155) APPLICATION OF ECOLOGICAL,
GEOLOGICAL AND OCEANOGRAPHIC ERTS-1 IMAGERY
TO DELAWARE'S COASTAL RESOURCES MANAGEMENT
Final Report, Sep. 1972. - Jun. 1974
(Delaware Univ.) 140 p HC \$5.75 CSCL 08A G3/43

Unclas
00155

APPLICATION OF ECOLOGICAL, GEOLOGICAL
AND OCEANOGRAPHIC ERTS-1 IMAGERY
TO DELAWARE'S COASTAL RESOURCES MANAGEMENT

by Vytautas Klemas, David S. Bartlett, William D. Philpot, Gary R. Davis,
Robert H. Rogers, and Larry Reed

CMS-NASA-4-74

"Made available under NASA sponsorship
in the interest of early and wide dis-
semination of Earth Resources Survey
Program information and without liability
for any use made thereof."



COLLEGE OF MARINE STUDIES
UNIVERSITY OF DELAWARE
NEWARK, DELAWARE 19711

This work is the result of research sponsored by the ERTS and Skylab
Programs of the National Aeronautics and Space Administration.

TECHNICAL REPORT STANDARD TITLE PAGE

1. Report No. Final - 1	2. Government Accession No.	3. Recipient's Catalog No.	
4. Title and Subtitle APPLICATION OF ECOLOGICAL, GEOLOGICAL AND OCEANOGRAPHIC ERTS-1 IMAGERY TO DELAWARE'S COASTAL RESOURCES MANAGEMENT		5. Report Date December 1974	
		6. Performing Organization Code	
7. Author(s) V. Klemas, D. Bartlett, W. Philpot R. Rogers, L. Reed *		8. Performing Organization Report No.	
9. Performing Organization Name and Address College of Marine Studies University of Delaware Newark, Delaware 19711		10. Work Unit No.	
		11. Contract or Grant No. NAS5-21837	
12. Sponsoring Agency Name and Address F. Gordon Goddard Space Flight Center National Aeronautics & Space Administration Greenbelt, Maryland 20771		13. Type of Report and Period Covered Final (Type III) Sept. 1972-June 1974	
		14. Sponsoring Agency Code	
15. Supplementary Notes * R. Rogers and L. Reed Bendix Aerospace Division Ann Arbor, Michigan 48107			
16. Abstract Data from twelve successful ERTS-1 passes over Delaware Bay have been analyzed with special emphasis on coastal vegetation, land use, current circulation, water turbidity and pollution dispersion. Secchi depth, suspended sediment concentration and transmissivity as measured from helicopters and boats were correlated with ERTS-1 image radiance. Multispectral signatures of acid disposal plumes, sediment plumes and slick were investigated. Current circulation patterns observed in the ERTS-1 imagery were compared to predicted current conditions. To map the ecological communities of Delaware's coastal zone, ten vegetative cover and water discrimination classes were selected: 1) Forest-land, 2) <u>Phragmites communis</u> , 3) <u>Spartina patens</u> & <u>Distichlis spicata</u> , 4) <u>Spartina alterniflora</u> , 5) Cropland, 6) Plowed Cropland, 7) Sand and Bare Sandy Soil, 8) Bare Mud, 9) Deep Water, and 10) Sediment--laden and shallow water. Canonical analysis predicted good classification accuracies for most categories. The actual classification accuracies were very close to the predicted values with 8 of the 10 categories classified with greater than 90% accuracy indicating that representative training sets had been selected.			
17. Key Words (Selected by Author(s)) Coastal Vegetation Mapping Land Use Mapping Current Circulation Sedimentation Transport Pollution Dispersion		18. Distribution Statement	
19. Security Classif. (of this report) None	20. Security Classif. (of this page) None	21. No. of Pages 140	22. Price*

*For sale by the Clearinghouse for Federal Scientific and Technical Information, Springfield, Virginia 22151.

APPLICATION OF ECOLOGICAL, GEOLOGICAL AND OCEANOGRAPHIC ERTS-1
IMAGERY TO DELAWARE'S COASTAL RESOURCES MANAGEMENT

ERTS-1 Investigations of Coastal Vegetation, Land Use, Current
Circulation, Sediment Transport and Pollution Dispersion

Vytautas Klemas
David S. Bartlett
William D. Philpot
Gary R. Davis

College of Marine Studies
University of Delaware
Newark, Delaware 19711

Robert H. Rogers
Larry Reed

3300 Plymouth Road
Bendix Aerospace Systems Div.
Ann Arbor, Michigan 48107

Original photography may be purchased from:
EROS Data Center
1014 and Dakota Avenue
Sioux Falls, SD 57198

December 1974

Final Report for Period September 1972 - June 1974

Prepared for
Goddard Space Flight Center
Greenbelt, Maryland 20771

iii. Preface

(a) Objective

There is a need for information on the natural state of Delaware Bay and its surroundings to form the basis for rational decisions on utilization. The need is made acute by present and proposed projects destined to affect the system. Among these are: an ensemble of off-shore developments associated with deep-draft vessels, including off-shore oil terminals; prospecting and mining activities along the Continental Shelf; the enlargement of the Chesapeake and Delaware Canal; the installation of waste treatment plants and nuclear generating stations; and general dredging and the construction activities in the coastal zone.

All of these projects have supporting engineering studies associated with them and some have ecological surveys as well. The difficulty is that these studies have restricted themselves in the past to the immediate vicinity of a project and have not related to the Bay as an interdependent system. The objective of this study was to determine which environmental parameters could be reliably monitored with the synoptic, repetitive coverage of ERTS-1, in order to establish a scientific baseline defining the present condition of the coastal zone, bay and shelf as an interrelated system. ERTS-1 applications to coastal resources management are shown in Table 1.1.

(b) Scope of Work

Imagery and digital tapes from thirteen successful ERTS-1 passes over Delaware Bay have been analyzed with special emphasis on water turbidity, current circulation, pollution dispersion, coastal land use and vegetation. During ERTS-1 overpasses, ground truth was collected with boats and helicopters along three transects across the bay, including measurements of Secchi depth, suspended sediment concentration, transmissivity, temperature, salinity, and water color. Nine major medium and high altitude aircraft overflights were conducted during the same period. Coastal land use and vegetation maps prepared from ERTS-1

digital tapes were annotated and verified using training sets obtained from detailed maps derived from aircraft imagery and ground checks. The scope of our ERTS-1 applications is summed up in Table 1.1.

(c) Conclusions

ERTS-1 image radiance (microdensitometer trace) correlated well with Secchi depth and suspended sediment concentration. Under atmospheric conditions encountered along the East Coast of the United States, MSS band 5 seemed to give the best representation of sediment load in the upper one meter of the water column. Maps of suspended sediment concentration were prepared by relating the measured sediment concentration values to the radiance in band 5 and fitting the data to an exponential by a non-linear regression. Color density slicing of 70mm transparencies of all four MSS bands helped delineate the suspended sediment patterns more clearly and differentiate turbidity levels. The four bands were found to penetrate to different depths, ranging from several centimeters to several meters, respectively.

Current circulation patterns were observed during different parts of the tidal cycle, using suspended sediment as a natural tracer. The current direction in the ERTS-1 imagery generally agreed with predicted and measured currents throughout Delaware Bay, except on those days when the wind caused surface currents to differ from predicted tidal currents.

Convergent shear boundaries between different water masses have been observed from ERTS-1, with foam lines containing high concentrations of lead, mercury, and other toxic substances. The dispersion and movement of plumes of acid and sludge dumped at various intervals before ERTS-1 and Skylab overpasses have been studied.

Work carried out over the past two years at the University of Delaware indicated that the coastal zone of Delaware and, in particular, its extensive tidal wetlands, offer a unique opportunity to evaluate ERTS-1 sensing capabilities and the feasibility of using digital processing techniques to map and inventory coastal vegetation and land-use. Analysis of ERTS color-composite images using analogue processing equipment confirmed that all the major wetlands plant species were distinguishable at ERTS scale. Furthermore, human

alterations of the coastal zone were easily recognized since such alterations typically involve removal of vegetative cover resulting in a change of spectral signature. The superior spectral resolution of the CCTs as compared with single band or composite imagery has indeed provided good discrimination through digital analysis of the CCTs with added advantage of rapid production of thematic maps and data.

Digital land-use analysis of ERTS data shows great potential as an inventorying and planning tool on the state, regional and federal level. While resolution problems generally restrict analysis to scales smaller than 1:100,000, ERTS data has the considerable advantages of regular, frequent coverage and easy, rapid data handling. Further, the digital techniques developed for use with ERTS data can be easily applied to data at larger scales if necessary.

Land-use data can be accumulated and updated at a fraction of the time and cost of conventional techniques. The ERTS digital format allows rapid, inexpensive data handling and offers the potential for automated change detection. Data products produced are generally cartographically precise and presented in a variety of formats easily used by planners and other government officials.

ERTS-1 results including applications are summarized in Table 1.1.

(d) Recommendations

1. To continue monitoring environmental properties with ERTS-1 or ERTS-B in order to determine man-made and natural changes from the baseline provided by ERTS-1 and other systems and to extrapolate environmental impact towards future, more intense development.

2. To launch a stationary, synchronous orbit satellite which would enable the continuous observation of current circulation and other water properties over complete tidal cycles under different wind, flow and wave conditions. Such operational systems would also significantly improve our ability to detect, track and clean-up accidental oil spills and provide flood warnings.

3. To add a thermal infrared mapping capability to the next satellite that is launched.

4. To develop an all-weather observation capability from future Earth Resources Observation Satellites.

5. To develop sensors which will help penetrate coastal waters more effectively and thus reduce the number of boats required for intensive oceanographic studies.

6. To accelerate the dissemination of ERTS imagery and digital tapes to users and investigators.

PARAMETERS
DISCRIMINATED AND CORRELATED

1. **SUSPENDED SEDIMENT CONCENTRATION**
Concentration maps prepared by matching band 5 image radiance to concentrations and other data obtained from boats and helicopters.
2. **CURRENT CIRCULATION PATTERNS**
Good agreement with predicted current circulation as a function of tide and wind during 13 good overpasses.
3. **WATER MASS BOUNDARIES AND SLICKS**
Foam lines along convergent boundaries found to contain toxic substances.
4. **WASTE DISPOSAL PLUMES**
Plumes 40 miles off coast best visible in bands 4 and 5.
5. **WETLANDS VEGETATION**
Maps of Delaware's wetlands completed showing 6 vegetation species and 3 other properties.
6. **LAND USE AND ENVIRONMENTAL IMPACT**
About 12 coastal land use categories mapped using ERTS digital tapes.
7. **INTERNAL WAVES**
Internal waves detected during several passes over the Continental Shelf.

APPLICATION
TO COASTAL RESOURCES MANAGEMENT

To verify and extend sediment transport model of Delaware Bay and monitor water quality. (U.D. and EPA).

To extend and verify predictive model for oil slick movement in Delaware Bay. (U.D. and NSF-RANN).

Boundaries used to modify hydrodynamic model of bay; toxic substances affect oyster beds. (U.D. and State).

Sludge and acid dumps coordinated with ERTS-1 overpasses to study dispersion of wastes dumped along continental shelf. (U.D. and EPA).

To develop marsh relative value model and plan wetlands development. (U.D. and State).

To monitor land use, its impact on marsh environment, and coastal erosion. (U.D. and State).

To study interaction between water masses at the edge of shelf and in its canyons.

ORIGINAL PAGE IS
OF POOR QUALITY

Table of Contents

1.0	INTRODUCTION	
2.0	DESCRIPTION OF THE DELAWARE BAY TEST SITE	2
2.1	Socio-Economic Characteristics of Delaware Bay	2
2.2	Physical Characteristics of Delaware Bay	7
3.0	ACQUISITION OF IMAGERY AND GROUND TRUTH	12
3.1	Imagery from ERTS-1 Overpasses	12
3.2	Aircraft Overflights	15
3.3	Measurements from Boats and Helicopters	17
4.0	ESTUARINE HYDRODYNAMICS AND WATER PROPERTIES	27
4.1	Physical and Optical Properties of Suspended Sediments	27
4.2	Suspended Sediment Concentration	29
4.3	Current Circulation and Coastal Fronts	37
4.4	Dispersion of Acid and Sludge Disposal Plumes	39
4.5	Off-shore Oil Terminal Site Dye Studies	40
4.6	Enhancement of Water Features	41
5.0	COASTAL VEGETATION AND LAND USE	68
5.1	Digital Data Analysis and Classification	68
5.2	Coastal Vegetation and Land-Use Mapping	76
6.0	CONCLUSIONS	90
7.0	RECOMMENDATIONS	93
8.0	REFERENCES	94
9.0	LIST OF PUBLICATIONS	96
10.0	NEW TECHNOLOGY	98
11.0	APPENDIX	110

List of Illustrations

- Figure 2.1 Delaware Bay test site for ERTS-1 and Skylab/EREP investigations.
- Figure 2.2 Delaware Bay bathymetry. Tongues of deeper water radiate from the bay entrance into the bay.
- Figure 3.1 R. V. Skimmer measuring water properties during an ERTS-1 overpass.
- Figure 3.2 Collecting water samples from a hovering helicopter.
- Figure 3.3 Organization of ground truth collection and data interpretation effort.
- Figure 3.4 Boat and helicopter sea-truth collection transects across Delaware Bay.
- Figure 3.5 Transmissometer flow-through system.
- Figure 4.1 Photographs taken at 65,000 feet altitude by a NASA U-2 aircraft, 41 minutes after the December 3, 1972 ERTS-1 overpass. The mouth of Delaware Bay is shown in three spectral bands.
- Figure 4.2 MSS band 4 of ERTS-1 overpass of Delaware Bay on October 10, 1972. (I.D. 1079-15133)
- Figure 4.3 MSS band 5 of ERTS-1 overpass of Delaware Bay on October 10, 1972. (I.D. 1079-15133)
- Figure 4.4 MSS band 6 of ERTS-1 overpass of Delaware Bay on October 10, 1972. (I.D. 1079-15133)
- Figure 4.5 MSS band 7 of ERTS-1 overpass of Delaware Bay on October 10, 1972. (I.D. 1079-15133)
- Figure 4.6 Microdensitometer traces of October 10, 1972, ERTS-1 imagery from Cape Henlopen, Delaware, to Cape May, New Jersey, using MSS bands 4, 5, and 6.
- Figure 4.7 Correlation of ERTS-1 image radiance (microdensitometer scan) with suspended sediment concentration and Secchi depth.
- Figure 4.8 Spectral signatures. The representation of the spectral signature becomes more accurate as the number of bands increases and the band width decreases. (a) actual reflectance spectrum; (b) typical signature using 4 ERTS bands; (c) signature using 1st nine of the 13 S 192 bands.
- Figure 4.9 Choosing a training set. Each symbol on this computer printout of ERTS band 5 represents a range of radiance. The training set is chosen in an area where all of the symbols are identical.

- Figure 4.10 Map of Delaware Bay. The solid lines show the transects along which ground truth was collected on July 7, 1973. The numbers show the points at which the training sets were chosen.
- Figure 4.11 Suspended sediment concentration map.
- Figure 4.12 Spectral signatures of the training sets. The signatures which are most similar in form and which are probably representative of different concentrations of the same type of sediment are shown by solid lines. The dotted lines are signatures which deviate from the sediment signature pattern.
- Figure 4.13 Predicted tidal currents and ERTS-1 MSS band 5 image of Delaware Bay obtained on October 10, 1972 (I.D. Nos. 1079-15133).
- Figure 4.14 Comparison of bottom contours and ERTS-1 image radiance during flood tide across the mouth of Delaware Bay.
- Figure 4.15 Temperature, salinity and turbidity gradients across frontal system.
- Figure 4.16 Coastal frontal system inside Delaware Bay.
- Figure 4.17 Predicted tidal currents and ERTS-1 MSS band 5 image of Delaware Bay obtained on January 26, 1973 (I.D. Nos. 1187-15140).
- Figure 4.18 Predicted tidal currents and ERTS-1 MSS band 5 image of Delaware Bay taken on July 7, 1973 (I.D. Nos. 1349-15134).
- Figure 4.19 Predicted tidal currents and ERTS-1 MSS band 5 image of Delaware Bay obtained on August 12, 1973 (I.D. Nos. 1385-15131).
- Figure 4.20 Predicted tidal currents and ERTS-1 MSS band 5 image of Delaware Bay taken on December 3, 1972 (I.D. No. 1133-15141).
- Figure 4.21 Predicted tidal currents and ERTS-1 MSS band 5 image of Delaware Bay taken on February 13, 1973 (I.D. No. 1205-15141).
- Figure 4.22 Acid waste dumped from barge about 40 miles east of Indian River Inlet appears clearly as a fishhook-shaped plume in MSS band 4 image of January 25, 1973. Due to its predominantly greenish component, the acid plume shows less contrast in band 5.
- Figure 4.23 Enlarged digital enhancement of acid waste plume of Figure 4.22.
- Figure 4.24 A 300-meter diameter Rhodamine WT dye patch being spread at the 8-mile offshore oil terminal site by the R. V. Delaware.
- Figure 4.25 The dye patch is caught in a boundary, stretched into a long line and being carried two miles toward the bay.

- Figure 4.26 A coastal front with a foam line between two masses of different water properties observed near the proposed 8-mile offshore oil terminal site from an altitude of 3000 meters.
- Figure 4.27 ERTS-1 image of the mouth of Delaware Bay showing several water mass boundaries and high concentrations of suspended sediment in shallow waters. (Band 5, August 16, 1972, I.D. 1024-15073).
- Figure 4.28 Aquatic boundaries and suspended sediment plumes identified in the ERTS-1 image of August 16, 1972, shown in Figure 4.22.
- Figure 5.1 Portion of grey scale printout showing training sets selected for: Spartina alterniflora, Mud and Fresh Water.
- Figure 5.2 Canonical analysis printout.
- Figure 5.3 Delaware Bay - decision land-use and vegetation image.
- Figure 5.4 Water boundary printout at 1:24,000 scale superimposed on USGS topographic map.
- Figure 10.1 Attenuation coefficient versus wavelength for pure water and sea water.
- Figure 10.2 Spectral Attenuation Board.
- Figure 10.3 Spectral Attenuation Board with green, white, and red stripes in water adjacent to Henlopen fishing pier, without camera support structure on float.
- Figure 11.1 Transmissometer flow-through system.
- Figure 11.2 Measuring global irradiance (H) with RPMI - ZTY steradian field of view for measuring downwelling radiation in ERTS MSS bands. Bubble level aids this measurement. Sky irradiance (H_{sky}) is measured by blocking direct sunlight in every ERTS MSS band. Angle from zenith to sun is also measured in this mode by reading sun shadow on sun dial.
- Figure 11.3 Radiance from narrow solid angles of sky (L_{meas}) - handle serving as field stop, permits direct measurements through a 7.0° circular field of view. This mode also used to measure direct beam irradiance, H_{sun} .
- Figure 11.4 Reflected radiation measurement at ground truth site.
- Figure 11.5 InterOcean Marine Illuminance Meter used for comparing luminosity at the surface and under water. Interchangeable filters allow for measurements in the ERTS MSS bands.

1.0 INTRODUCTION

There is a need for information on the natural state of the Delaware Bay and its surroundings to form the basis for rational decisions on utilization. This need is recognized by most of those concerned with the conservation, regulation, or development of Delaware's Coastal Zone. It is made more acute by present and proposed projects destined to affect the system. Among these are: an ensemble of off-shore developments associated with deep-draft vessels, including off-shore oil terminals; prospecting and mining activities along the Continental Shelf; the enlargement of the Chesapeake and Delaware Canal; the installation of waste treatment plants and nuclear generating stations; and general dredging and the construction activities in the coastal zone.

All of these projects have supporting engineering studies associated with them and some have ecological surveys as well. The difficulty is that these studies have restricted themselves in the past to the immediate vicinity of a project and have not related to the Bay as an interdependent system. We have used ERTS-1 to help establish a scientific baseline defining the present condition of the Bay and River as an inter-related system, and will employ ERTS-B to monitor changes from this baseline as a function of time and to extrapolate environmental impact towards future, more intense development.

Since its launch in July of 1972, NASA's Earth Resources Technology Satellite (ERTS-1) has made about thirty passes over Delaware, ten of which were favored by nearly cloud-free conditions. The second Skylab crew made three EREP passes over the same area, one of which produced imagery of the highest quality. During ERTS-1 and Skylab passes, aircraft underflights were conducted and ground truth was collected by teams on helicopters, boats and in the marshes. The purpose of this article is to review our investigations of current circulation patterns, suspended sediment concentration, coastal frontal systems and waste disposal plumes based on visual interpretation and digital analysis of ERTS-1 and Skylab/EREP imagery.

2.0 DESCRIPTION OF THE DELAWARE BAY TEST SITE

2.1 Socio-Economic Characteristics of Delaware Bay

The Delaware River and Bay is the water gateway to a great industrial and commercial complex of the Delaware Valley. The coastal bays of Delaware are part of a system of shallow water estuaries which are the nursery and rearing ground for most fin fishes important to both commercial and sport fishermen along the East Coast of the United States. In fact, about two-thirds of the fish landed by U. S. fishermen spend part of their lives in an estuary. The tidal wetlands in Delaware, encompassing about 120,000 acres, are an important link in these grounds and provide breeding areas for birds, mammals and shellfish, produce food for all of these and are part of the aesthetic quality of the shore region.

The Atlantic Ocean, Delaware Bay and other coastal bays and their surroundings are prime attractions for persons seeking water-based recreation adjacent to the East Coast megalopolis. Many early residences, industries and other places of historical and cultural significance are closely associated with the Coastal Zone because the tidal streams and bays provided the principal transportation routes for early settlers. To this day, the prosperity of municipalities such as Wilmington, New Castle, Delaware City, Odessa, Smyrna, Dover, Milford, Milton, Lewes, Rehoboth Beach, Bethany and Fenwick Island is closely linked to one or more coastal assets such as water transportation, water-based recreation and water-based industry. When considered together with the general absence of other significant topographic features and the lack of traditional mineral resources, Delaware Bay and other coastal bays represent not just a factor in the State's geography, but a determining factor in its history, economy and way of life.

However, the Delaware Bay Region is threatened by the impact of rapid industrial and domestic development.¹ Adjacent to the Delaware Estuary is one of the major oil refining areas in the Eastern United States. Seven oil companies operate large refineries whose combined daily throughput is about 900,000 barrels or 3,780 million gallons. As of 1967, the

Federal Water Quality Administration estimated that traffic of cargo ships, barges, naval vessels, and tankers on the Delaware exceeded 200 vessels per day, many of which either use petroleum products or are involved in refinery operations thereby contributing to oil spillage. Oil slicks involving surface patches of oil exceeding 1,000 feet in length and 50 angstroms in thickness, are recorded during routine sampling runs. During 1970, oil slicks were reported in 33 of 38 runs. Although few catastrophic spills have been recorded in the area in recent years, the growing literature on the biological effects of oil in aquatic systems points to significant insidious incorporation of hydrocarbons in the marine food chain as the result of low level chronic pollution.

The petrochemical, utility and other industries are discharging increasing amounts of oil, exotic chemicals and trace metals, as well as thermal effluent, all of which upset the ecology of the Bay and its estuaries. For instance, in the foam along water boundaries we have found toxic metals, such as mercury and lead, at concentrations two to four orders of magnitude greater than the averages for Delaware Bay water.² Current methods of sewage treatment remove only 75 to 90 percent of the suspended solids and B.O.D., and very little of the nitrogen and phosphorous. This stimulates obnoxious plant life (algae), depletes oxygen, and endangers fish life. Historical catch statistics provided by the Fish and Wildlife Service show that shad catches in the middle Atlantic fishery increased from over 5 million pounds in 1880 to 21 million pounds by 1901. However, by 1904, the catches had dropped to less than 7 million pounds and never again exceeded that level. In 1965, catches totaled 635,000 pounds. The severe decline in both the shad and sturgeon fisheries was most probably due to the blockage of their anadromous spawning runs to the headwaters of the Delaware by substantial stretches (up to ten miles) of anoxic river water and other man-made barriers. Undoubtedly, toxic pollutants, the destruction of food organisms, and the destruction of spawning grounds have also contributed to the decline in shad and sturgeon.

Waste disposal in the waters of the Delaware drainage system has been one of the foremost historical abuses of the environment. Under the

guidance of the Delaware River Basin Commission, a pollution-abatement plan is now in effect which is designed to have a significant effect on the quality of the upper estuary by 1973. The cities of Trenton, Philadelphia, Camden, Chester, and Wilmington each have combined sewer systems which were built nearly 100 years ago. These systems carry sewage during dry periods and a mixture of storm water and sewage after the start of precipitation. When the sewage and storm-water mixture reaches a predetermined level, some of the flow is diverted directly into the nearest natural water course without any further treatment. In 1964, it was estimated that 76,000 pounds per day of the Delaware River's ultimate oxygen demand was contributed by storm-water overflows. As a result of the chemical and biological oxygen demands, decreased oxygen levels are observed in the river near Philadelphia. In fact, anaerobic conditions persist over a 10-mile stretch of the river during the summer months. Obviously this low to zero oxygen band can eliminate anadromous fish spawning runs involving shad, sturgeon, etc.

Additionally, nutrient enrichment occurs involving nitrate reduction to nitrite under anaerobic conditions and high phosphate levels. The combination of oxygen depletion and nutrient enrichment has a predictably debilitating effect on aquatic ecosystems.

Another crucial aspect of waste disposal and other sources is the discharge of heavy metals such as zinc, copper, chrome, nickel, cadmium, mercury, and lead into the aquatic environment. Bopp and Biggs, in a study of trace metals in bottom sediments near shellbanks in Delaware Bay, concluded that iron, zinc, lead, cadmium, mercury, and nickel have their primary sources in the Delaware River with high concentrations accumulating near the mouths of the Cohansey, Murderkill, and St. Jones Rivers.³ Additionally, they point out that so little is currently known about the biochemistry of trace metals, that it is impossible to state what the danger levels are.

Other major man-made environmental impacts are major dredging projects, thermal additions due to power plant cooling needs, use of pesticides, sediment production, and diversion of freshwater from the headwaters

of the Delaware. The basic impact of maintenance dredging on the marine habitat includes: 1) the utilization of tidal marshes for disposal of dredged material; 2) changes in mixing of fresh and salt water in areas where channels affect stream gradients; and 3) increase in suspended sediments which can adversely affect marine fishes particularly during spawning. Major thermal discharges resulting from use of the Delaware Estuary as a source of cooling water for industrial operations and power generation are increasing. The combined usage presently requires over 7 billion gallons of water per day and of course increasing power needs will drive that usage up. Additionally, fresh water diversions out of the Delaware River watershed to the Hudson and Raritan watersheds amount to approximately 0.5 billion gallons per day. The State of Delaware annually uses approximately \$3 to \$4 million worth of agricultural chemicals and at least \$1 million of household pesticides. This level of pesticide use can be extrapolated to the entire Delaware watershed and undoubtedly affects food chains in the estuaries, although specific research in Delaware on this point is lacking. Lastly, it has been estimated that the total mineral sediment delivered to Delaware Bay is 2,296,000 tons annually. Much of this sediment is the result of land grading operations, agricultural practices and other man-induced erosional factors.

Economic development of coastal regions has presented public officials and planners with difficult and demanding environmental and land-use problems; yet information on ecological deterioration in a coastal region is difficult to acquire by conventional survey methods. The instantaneous areal distribution, and the variations in flow rate of waters from various sources, the unique meteorological conditions along sea-coasts, and the variety of land uses and land forms that exist from the tidal zone to the upland hinterlands all combine to present a highly complex picture. This is complicated further by human activity, especially that involving emissions into the air and water, and by the wide-spread reworking of the land and the shoreline that has resulted from increasingly intensive land use. Of particular concern are plans for offshore oil terminals, sewage and power plants, dredging and commercial marsh development which threaten to further degrade the coastal environment unless the environmental impact of each is carefully assessed and extrapolated in area and time.

We have found that ERTS-1 imagery offers an opportunity for simultaneous observation and measurement of large-scale features and their associated spectral patterns, their distribution, and spatial and temporal variance relative to the natural environment and to centers of man's activities. Having established that the wide-area synoptic imagery of ERTS-1 can be used to areally extrapolate and map coastal vegetation, land use, coastal erosion, suspended matter and water circulation, we are now proceeding to a more operational mode to study natural and man-made changes in the coastal environment.

2.2 Physical Characteristics of Delaware Bay

Delaware Bay is an estuary on the East Coast of the United States, bordered by the states of New Jersey and Delaware and situated between the major estuaries of New York Harbor and Chesapeake Bay. The geography of this region, including the locations of several convenient reference points, is shown in Figure 2.1 and 2.2. Trenton, New Jersey is generally taken to define the upper limit of the estuary, so that its total length is over 200 kilometers. Delaware Bay itself may be distinguished as a less extensive body of water by defining an upper limit in the vicinity of the Smyrna River entrance. The length of the Bay is 75.2 km with mean and maximum widths of 24.6 km and 43.6 km respectively. The Bay encompasses approximately 1864.8 sq. km and has a volume of about 1.78×10^{13} liters.

Fresh water input to the system is derived mainly from the Delaware River at an average rate of 316 cu.m/sec which, in terms of volume flow, ranks this as one of the major tributaries on the eastern plain. Together with this large volume of fresh water, the river also discharges a heavy load of suspended and dissolved material, since its effective watershed encompasses an area typified by intensive land use, both agricultural and industrial.⁴ Seaward of the Smyrna River, the bay undergoes a conspicuous exponential increase in both width and cross-sectional area so that the strength of the river flow is rapidly diminished beyond this point. Ketchum has computed the flushing time of the bay (defined in this case as the time required to replace the total fresh water volume of the bay) to be roughly 100 days.⁵ Seasonal variations in river flow cause this figure to fluctuate within a range of from 60 to 120 days. Consequently, river flow is not a significant factor in determining the current pattern in the bay except in the consideration of time-averaged flow. In terms of short-period studies it is mainly important as a source of suspended sediment and contaminants.

The seaward boundary of the bay extends from Cape May southeast to Cape Henlopen -- a distance of eleven miles. Tidal flow across this boundary profoundly affects the dynamic and hydrographic features of the entire estuary. The effect is especially pronounced toward the mouth where conditions are generally well mixed. The dynamic behavior of the tides is closely approximated

by the model described by Harleman.⁶ In this model, the upper end of the estuary is assumed to act as an efficient reflecting boundary. Consequently, the actual tidal elevation at any given point is a result of the interaction of both a landward directed wave entering from the ocean and a reflected wave traveling back down the estuary. The tidal range is a maximum at the reflecting boundary and decreases toward the mouth in a manner dependent upon the relative phase of the two components. Observations of the tide at Trenton show a 2.3 m range compared to 1.2 m range at the mouth. A relative maximum appears at roughly the location of Egg Island Point, where the phase relationship is temporarily optimal. An important consequence of this behavior is the occurrence of strong reversing tidal currents in the Delaware River. The tidal wavelength, as compared by Harleman, is 330 kilometers, so that both peak currents and slack water may occur simultaneously at either end of the bay.

In general, waters of the Delaware Bay circulate in a large rotary current, which normally flows southward along the western shore and northward along the eastern New Jersey shore. Due to the Coriolis effect, the flood tide reinforces the northerly flow component while the ebb tide reinforces the southerly current. During the flood tide, the maximum tidal current reaches 4.3 km/hr and 4.4 km/hr northwestward at the Cape May and Cape Henlopen entrance, respectively. During ebb tide, the maximum exit velocity reaches 5.0 km/hr and 5.2 km/hr southeast at Cape May and Cape Henlopen, respectively. Levels of 1.2 meters above the mean high water have been caused by extratropical cyclones. Strong easterly and southeasterly winds sometimes contribute to higher tides in the bay, resulting in the flooding of lowlands.

The tidal flow is also modified by the bay's rather complex bathymetry (Figure 2.2). Most prominent are several deep finger-like channels which extend from the mouth into the bay for varying distances.⁷ Depths of up to 46 meters are present, making this one of the deepest natural embayments on the east coast. The channels alternate with narrow shoals in a pattern which is shifted noticeably toward the southern shore. On the northern side, a broad, shallow mudflat extends from Cape May to Egg Island Point. Considerable transverse tidal shears result from these radical variations in bottom contours.

As a consequence, a marked gradient structure may form normal to the main axis of the bay as a function of tidal phase. This intrinsic two-dimensional character, together with the complex, superimposed time variations, represents an almost insurmountable task when it is confronted with the tools of conventional hydrographic surveys. The problem is ready-made, however, for the techniques of high-altitude photography.

There are approximately 115,000 acres of tidal wetlands in the State of Delaware forming an almost continuous band along the western shore of Delaware Bay from Cape Henlopen north to Wilmington. The width of this band varies from a few hundred yards to three to four miles, with an average width on the order of one mile. In addition, there are small fringes of marsh associated with the barrier beach-lagoon complexes along the Atlantic Shore in the southern portion of the state.⁶ The most abundant plant species found in the marshes are salt marsh cord grass (Spartina alterniflora), salt marsh hay (Spartina patens), spike grass (Distichlis spicata) and reed grass (Phragmites communis).

There are, of course, many other species present but in most cases their occurrence is limited to small patches scattered within areas dominated by one or more of the above-mentioned primary species. In the north, Delaware's coastal zone is dominated by heavy industrial development, while its Atlantic coastline is feeling pressure from recreational builders.

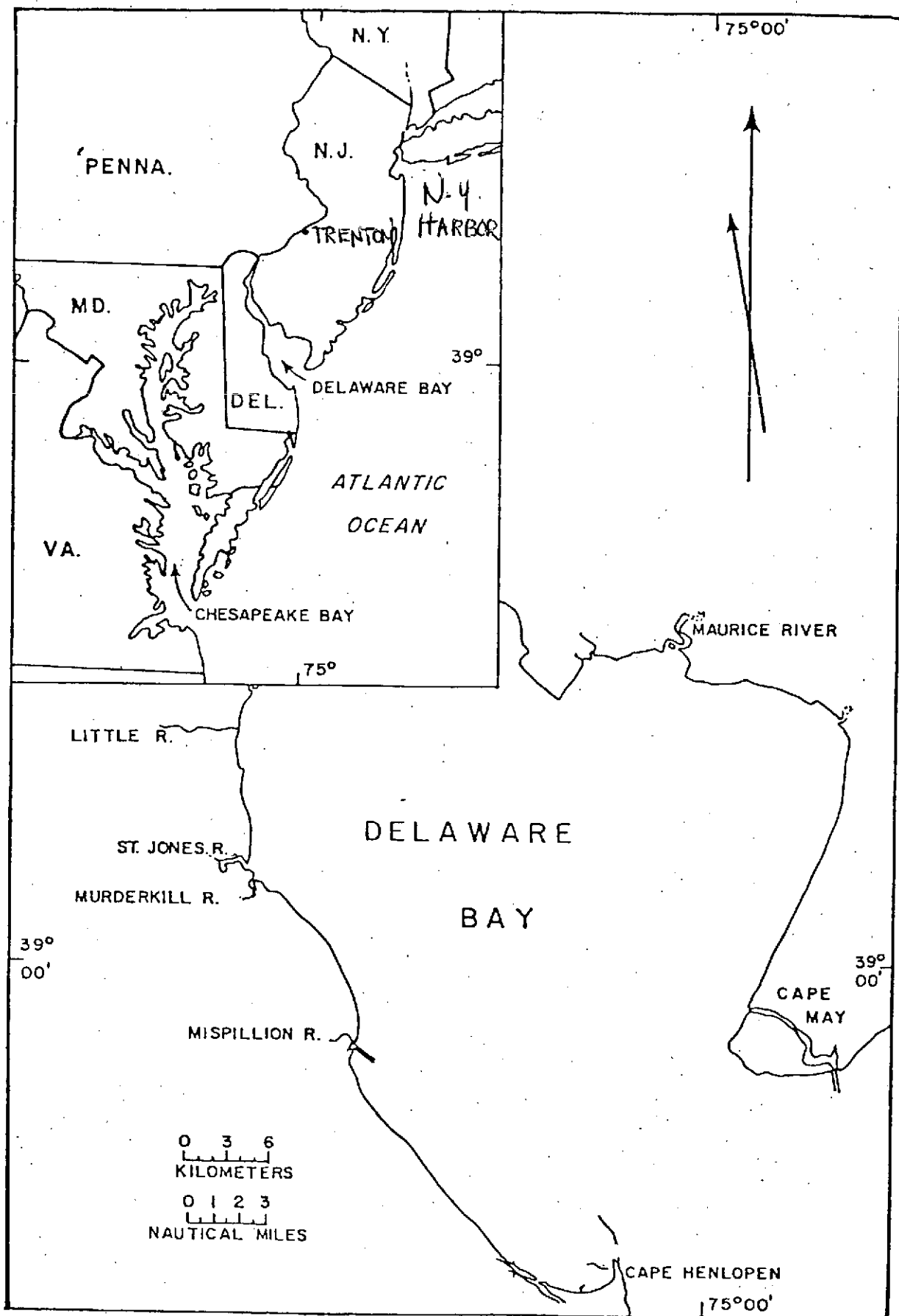
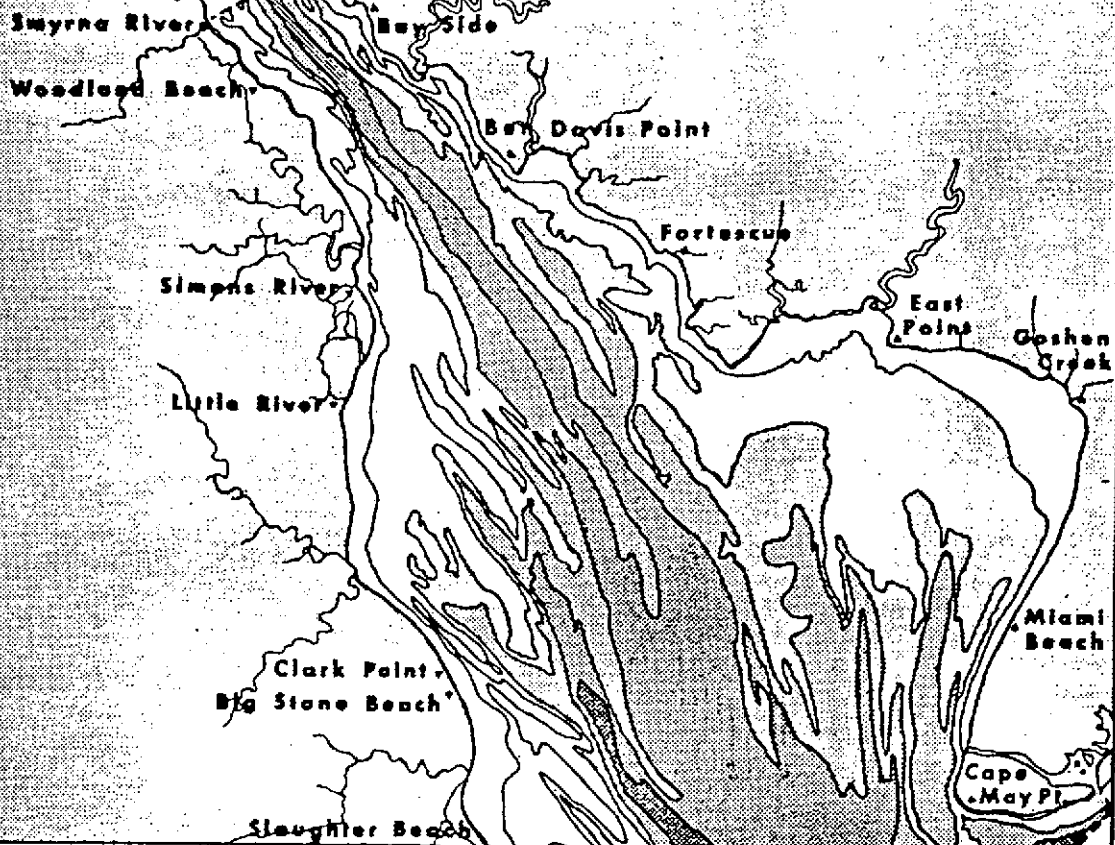


Figure 2.1 Delaware Bay test site for ERTS-1 and Skylab/EREP investigations...

FIGURE 2.2

Delaware Bay bathymetry - Tongues of deeper water radiate from the the bay entrance into the bay itself.



Delaware Bay

Scale in Miles

0 5 10

Submerged Contours with
Depths in Fathoms

A1	0 to 1	A4	3 to 5
A2	1 to 2	A5	5 to 10
A3	2 to 3	A6	10 to 25

ORIGINAL PAGE IS
OF POOR QUALITY

3.0 ACQUISITION OF IMAGERY AND GROUND TRUTH

3.1 Imagery from ERTS-1 Overpasses

As shown in Table 3.1 about thirty ERTS-1 passes over Delaware Bay produced imagery with less than 60% cloud cover. The quality ratings indicate that thirteen passes produced data under atmospheric conditions suitable for digital analysis (Quality A), ten passes were suitable for visual interpretation only (Quality B), and during seven overpasses cloud cover obscured the primary features, making the imagery worthless for these investigations (Quality C).

The ERTS-1 imagery used in our work was produced by the four-channel multispectral scanner having the bands shown in Table 3.2. From an altitude of 920 km each frame covered an area of 185 km by 185 km. In addition to the 9-track 800 bpi magnetic tapes, reconstructed negative and positive transparencies in 70 millimeter format and prints in 9-inch format were obtained from NASA. No Return-Beam Vidicon Camera data were used. Before visual interpretation, some of the imagery was enhanced optically, using density slicing and color additive techniques. Annotated thematic maps were prepared by computer analysis of digital tapes and by direct photo-interpretation of the transparencies reconstructed by NASA.² Computer analysis of digital tapes was performed under subcontract by the Bendix Aerospace Systems Division at Ann Arbor, Michigan.

TABLE 3.1
IMAGERY FROM
ERTS-1 SATELLITE OVERPASSES
OF DELAWARE BAY REGION

<u>Date of Pass</u>	<u>Region</u>	<u>I.D. Number</u>	<u>Bands</u>	<u>%Cloud Cover</u>	<u>Quality</u>
8/16/72	DO	1024-15073	M	30	B
9/3/72	DO	1024-15074	M	80	B
9/22/72	DB	1061-15133	M	60	C
10/9/72	DO	1078-15075	M	10	B
10/10/72	DB	1079-15133	M	10	A
*10/27/72	DO	1096-15081	M	40	C
12/2/72	DO	1132-15083	5,6,7	20	C
12/3/73	DB	1133-15141	5,6,7	0	A
1/25/73	DO	1186-15081	M	10	A
*1/26/73	DB	1187-15140	M	0	A
2/13/73	DB	1205-15141	M	0	A
3/2/73	DO	1222-15084	M	30	B
3/20/73	DO	1240-15085	M	20	B
4/7/73	DO	1258-15085	M	10	B
5/13/73	DO	1294-15083	M	10	A
*5/14/73	DB	1295-15142	M	30	C
5/31/72	DO	1312-15082	M	10	B
*6/1/73	DB	1313-15141	M	10	B
7/6/73	DO	1348-15080	M	10	B
*7/7/73	DB	1349-15134	M	10	A
7/24/72	DO	1366-15074	5,6,7	30	B
*7/25/73	DB	1367-15133	M	60	C
8/11/73	DO	1384-15073	M	60	C
8/12/73	DB	1385-15131	M	10	A
*8/29/73	DO	1402-15071	M	10	A
8/30/73	DB	1403-15125	M	10	A
*9/17/73	DB	1421-15123	M	50	C
2/26/74	DB	1583-15091	M	10	A
4/03/74	DB	1619-15083	M	10	A
4/21/74	DB	1637-15080	M	10	A
5/26/74	DO	1672-15012	M	20	A

M= MSS Bands 4,5,6, and 7

Region DB Delaware Bay -
DO Delmarva Coast

* Ground truth available for these dates.

Table 3.2 ERTS-1 Multispectral Scanner Bands

<u>Band</u>	<u>Spectral Range</u>
4	0.5 - 0.6 microns
5	0.6 - 0.7 "
6	0.7 - 0.8 "
7	0.8 - 1.1 "

3.2 Aircraft Overflights

A total of fourteen major aircraft overflights were conducted over the Delaware Bay test site, seven of which were directly in support of ERTS-1 and Skylab overpasses. A summary of aircraft overflights is presented in Table 3.3. Since the remote sensing instrument payload of each aircraft is well known, no attempt is made to describe them in this table. The ERTS-1 underflights were conducted primarily by U-2 and C-130 aircraft. During ERTS-1 overpasses the University also rented two-seater and four-seater aircraft for low altitude photography. Table 3.3 does not include helicopter flights used for collecting water samples. As will be discussed in the result sections, U-2 imagery proved valuable in delineating grass-water features, such as current circulation patterns and suspended sediment plumes. The C-130 multispectral capability was used successfully in preparing wetland and coastal land-use training sets and more clearly defining water pollution plumes.

TABLE 3.3

NASA AIRCRAFT OVERFLIGHTS
OF DELAWARE BAY TEST SITE

<u>Date</u>	<u>Aircraft and Altitude</u>	<u>Agency</u>
September 14, 1970	RB-57 at 60,000 ft. altitude	(NASA-Houston)
November 4, 1971	U-2 at 65,000 ft. altitude	(NASA-Ames)
August 26, 1971	C-54 at 11,500 ft.	(NASA-Wallops)
September 15, 1972	U-2 at 65,000 ft. altitude	(NASA-Ames)
October 27, 1972	C-130 at 10,000 ft. altitude	(NASA-Houston)
December 3, 1972	U-2 at 65,000 ft. altitude	(NASA-Ames)
March 24, 1973	U-2 at 65,000 ft. altitude	(NASA-Ames)
April 5, 1973	C-130 at 10,000 ft.	(NASA-Houston)
May 14, 1973	C-130 at 10,000 ft.	(NASA-Houston)
April, 1973 - November, 1973	Sidelooking Radar Overflights	(NASA-Wallops-Navy)
June 1, 1973	C-54 at 11,500 ft.	(NASA-Wallops)
August 17, 1973	Laser Wave Profiling Overflights	(NASA-Wallops-Navy)
August 23, 1973	Laser Chlorophyll and Oil Detection Overflights	(NASA-Wallops)
August 29, 1973	C-130 at 3,000 to 25,000 ft.	(NASA-Houston)

* This list does not include helicopters provided for water sampling during ERTS-1 overpasses, nor small aircraft used by the University of Delaware for low altitude photographic overflights.

3.3 Measurements from Boats and Helicopters

Most ground truth collection transects (point A to point B) were scheduled to have the overpasses and underpasses at their midpoint in time. Table 3.4 describes the various transects.

Table 3.4

<u>Date</u>	<u>EST Time Span</u>	<u>Location</u>	<u>Type of Vehicle</u>
Oct. 22, 1972	1145-1308	Cape Henlopen to Cape May	R/V Wolverine
Jan. 26, 1973	0950-1050	Bombay Pt. to Cohansey River	Whaler
May 14, 1973	0906-1319	Cape Henlopen to Cape May	R/V Skimmer
June 1, 1973	0958-1030	Bombay Pt. to Cohansey River	Whaler
July 7, 1973	1010-1043	Bombay Pt. to Cohansey River	Whaler
July 7, 1973	0829-0851	Cape Henlopen to Cape May	Helicopter
July 7, 1973	1006-1036	Bowers to Egg Island Point	Helicopter
July 7, 1973	0920-1108	Cape Henlopen to Cape May	R/V Skimmer
July 25, 1973	1008-1253	Cape Henlopen to Cape May	R/V Wolverine
Aug. 29, 1973	0922-0942	Cape Henlopen to Cape May	Helicopter
Aug. 29, 1973	0901-1033	Cape Henlopen to Cape May	R/V Skimmer
Oct. 22, 1973	0927-1238	Cape Henlopen to 10 miles out into the ocean	R/V Skimmer
Oct. 23, 1973	0944-1243	Cape Henlopen to Cape May	R/V Skimmer
July 2, 1974	1000-1300	Joe Flogger Shoals to Hen and Chicken Shoals	Individual Boaters

Ground truth collection employs the use of either the Research Vessel Skimmer, or the Research Vessel Wolverine, a sixteen-foot Boston Whaler; a Cessna 172 airplane; an Army NASA jet-powered Bell-Huey Helicopter, and interested pleasure boaters. The R/V Skimmer is a forty-two foot aluminum-hulled craft equipped for plankton trawls, dredging, geologic and hydrographic sampling, Seismic profiling, and Loran positioning. It has a top speed of twelve kts. and can withstand moderate (3'-4') swells. It also has a three-foot draft which allows shallow work around shoaled areas. The R/V Wolverine is a forty-eight foot wooden-hulled trawler equipped for exploratory fishing, geological sampling, and limited hydrographic work. The Boston Whaler is

sixteen feet long, powered by a fifty-five horsepower engine. The Cessna airplane employed is a 172 four-seater with high wings, which allows easy access to photography of the ground. It can bank sixty degrees which gives fairly vertical pictures. The NASA helicopter is a jet-powered Bell-Huey piloted by a two-man NASA team from Wallops Island, Virginia. It is equipped with pontoons and many navigational tools. It can hover for short periods and travel from station to station at approximately 90 mph. which facilitates speedy sampling during the overflights. The scientist can be harnessed directly to the pontoon to work from that position during hovers and high-speed traveling.

Although more widely dispersed water samples can be obtained from a hovering helicopter than by boat, to further increase the number and dispersion of samples at the exact time of the ERTS-1 pass over Delaware Bay, pleasure crafts were organized to obtain samples over the entire test site. Problems in the past with using boaters were that they were asked to be at a specific location and to sample over several hours. We eliminated this problem by asking the boaters to take only two samples between 11 and 11:15 and to take them wherever they were at the time.

On the ERTS-1 pass of July second, scientists were stationed at three public boat launches along the bay (Woodland Beach, Bowers Beach, and the Lewes Public Boat Ramp) to hand out sampling packets to interested boaters. The packets contained two litre sampling bottles, a map, data card, and a pen. After filling the two bottles at the appropriate time the boaters were asked to mark their location on the map and fill out the data card with the time and their name and address. Boxes were placed at the ramps for the return of the bottles.

The two packets handed out at Woodland Beach, were either not returned or removed from the drop off point before we could pick them up. At Bowers Beach 19 packets were handed out and 16 had been returned by evening (84.2%). In Lewes 28 packets were handed out of which 24 came back (85.7%). A total of 49 packets were handed out and 40 of these were returned. Only 4 (10%) of the 40 were not in the allotted time range. This gave 36 (90% of packets returned, 73% of packets handed out) real time data points covering approximately 30 nautical miles. In the future, pleasure craft sampling will be

used in conjunction with other sampling techniques discussed previously to further increase our amount of sea truth.

Instrumentation and Sampling Techniques

The instrumentation utilized in analyzing ground truth samples includes a transmissometer, a Bendix radiant power measuring instrument, an interoceanic Marine Illuminous meter, Secchi discs, Pentax Spotmatic cameras, centigrade bucket thermometers, Loran, a sonar bathymetry transducer, analyzer.

A Hydro-Products Model 612S transmissometer system was used in situ for turbidity measurements. The instrument consists of a projector light source, a ten-cm cell path, and a photo cell detector. The housing chamber is baffled to eliminate external stray light. Optics in the projector housing present a lightbeam which is collimated sufficiently to illuminate only the detector optics. The detector optics are such that only light coming directly from the projector is "seen". This optical arrangement minimizes effects of forward and backscatter due to ambient light and divergent beam light. The sensor is designed to allow the water sample to circulate freely into the optical path where transmissivity is determined (%T) such that:

$$T = \frac{I_2}{I_1} \times 100$$

where: T = % Transmission

I_1 = intensity at projector

I_2 = intensity at detector

This measurement is related to the average optical attenuation coefficient of the water (α) by the equation:

$$T = 100e^{-\alpha d}$$

where: α = attenuation coefficient in Ln/Meter

d = cell path lengths in meters.

The 612 Sensor was designed for lowering from a static platform or it can be towed from a moving boat at speeds up to 5 knots, but our needs required a more sophisticated sampling technique in order to cover a large surface area in a short amount of time. The transmissometer was placed in a flow-

through pump system on board the R/V Skimmer for use with ERTS-1 data gathering (see Fig. 3.1). The ship's bilge pump supplied ocean water from a constant depth of 3 feet to the case which housed the instrument sensors. The case was air-tight which allowed a great volume of water to be passed through the sensor in a short period of time. This allowed the boat to travel its course at high speeds (10 kts.). The %T values represented integrated masses of water from point A to point B along the transect. In other words, the water sample was not at a point in the transect, but it was from a segment of water approximately 50 feet long. These average values are very realistic considering the resolution of ERTS-1 imagery.

The Bendix Radiant Power Measuring Instrument (RPMI) is a lightweight, portable instrument which is calibrated to measure down-welling and reflected radiation in each of the four ERTS MSS bands. The handle folds over to provide narrow-angle (7.0° circular) measurements from sky and ground targets as well as wide-angle sky and ground irradiance. The wide range of the RPMI allows for measurements as high as direct-beam-solar irradiance of $25\text{mw}/\text{cm}^2$ in Band 7 to as low a radiance from surface water as $0.02\text{mw}/\text{cm}^2$ in Bands 6 and 7.

The RPMI measurements are taken during the time of the ERTS pass. These measurements include, (1) global irradiance, H ; (2) sky irradiance, H_{sky} ; (3) radiance from a narrow solid angle of sky, $L_{\text{meas}}(\phi)$; and (4) direct-beam-solar irradiance, $H_{\text{sun}}(m)$. From these measurements the following parameters can be determined: beam transmittance, τ ; path radiance, L_a ; and direct-beam-solar irradiance above the atmosphere, H_o . Now the measurements can be combined in the following equation to transform the ERTS radiance measurements, L , into absolute target reflectance units, ρ :

$$\rho = \frac{(L - L_a) \cdot \pi}{\tau (H_o \tau^m \cos Z + H_{\text{sky}})}$$

where Z is the solar zenith angle read from the sun dial on the side of the RPMI or determined by a sextant.

The Inter-Ocean Marine Illuminance Meter (MIM) is a light, compact, and portable unit designed to measure and compare luminosity both onboard and underwater. Operation is independent of any power source other than incident light on the photocells.

Once both the surface cell and the underwater cell are calibrated, relative incident radiance is measured by the surface cell and the underwater cell is lowered to the desired depth where relative radiance is again measured. When the two measurements are compared the transparency of the water is determined. Both cells are designed so that filters of different wavelengths can be attached in order that measurements can be made in the same spectral regions as the ERTS MSS bands.

White Secchi discs .49 cm in diameter, were used for relative visual turbidity readings. This size worked well in turbulent waters where swells were a few feet high. Also, green and red discs of the same diameter and color matched well with the green and red bands of the ERTS-1 MSS were employed to correlate light transmission of the scanners.

The R/V Skimmer's Loran was used to aid in transect alignment and radar aided in station positioning. These tools allowed mapping of stations to be ± 50 feet in precision. The sonar transducer aboard the boat was utilized in plotting the bathymetry along the transect.

Bucket thermometers were used for temperature measurements. The transmissometer case had an auxillary outlet for sampling of the water for temperature, salinity, and sediment load.

During sampling runs, the R/V Skimmer sped along a transect at approximately 10 knots non-stop gathering data at equal intervals. As a result, the cape-to-cape transect took about one hour allowing data gathering to be accomplished one-half hour on each side of the overpasses. For shorter runs the Boston Whaler was used and transect runs lasted about one hour. The NASA helicopter was utilized best for long transect distances up to 25 miles. With its speed and accuracy of locating positions, 25-30 miles was easily covered in less than one hour. The helicopter would hover two feet above the surface while a scientist would sample the water with a plastic bucket. Temperature was a problem due to strong prop wash winds.

Sample Analyses

Samples collected under the ground truth program were analyzed for 1) sediment load, 2) salinity, 3) volatile content, and 4) total carbon.

The sediment load weight was determined from a one-litre sample immediately after sampling took place. This insured that bacterial action

and the formation of salts would not occur quickly enough to add error to the results. One litre was filtered through pre-dried and pre-weighed glass membrane filter pads (Gelbman) under suction. The pads and sediment were then dried at ambient temperatures and then weighed on a Mettler balance. Sediment load was then calculated in terms of weight (mg) per one litre of sample. Salinity was determined by a salinometer on fresh unfiltered samples. Volatile content of the sediment suspended in the water column was achieved by high temperature heating of the sample. The weight loss per sample weight times 100 gave % ignition loss. Total carbon was determined on a Coleman Carbon-Hydrogen Analyzer. The principle of analysis was based on the total combustion of the sample giving off CO_2 gas which was absorbed on an ascerite medium. Carbon was then calculated by converting the weight of CO_2 to weight of carbon.

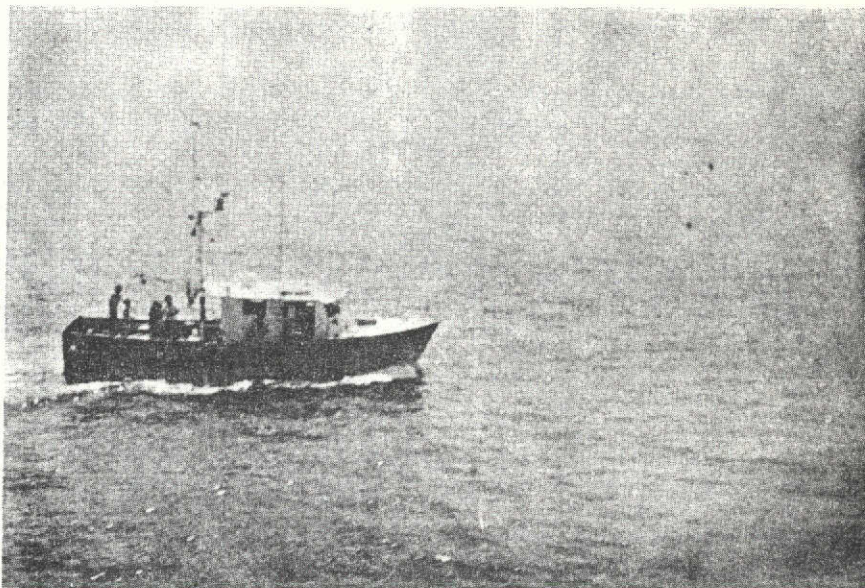
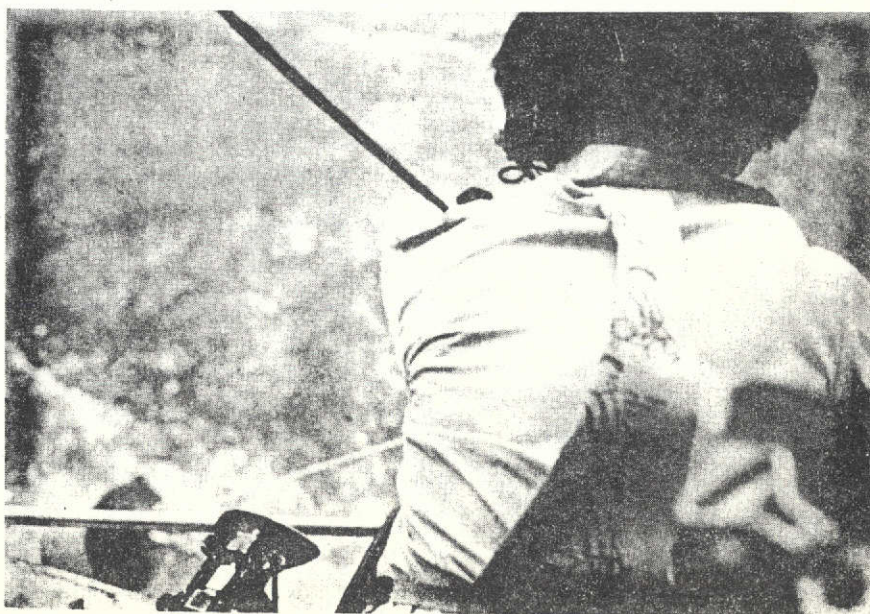


Fig. 3.1 R. V. Skimmer measuring water properties during an ERTS-1 overpass.



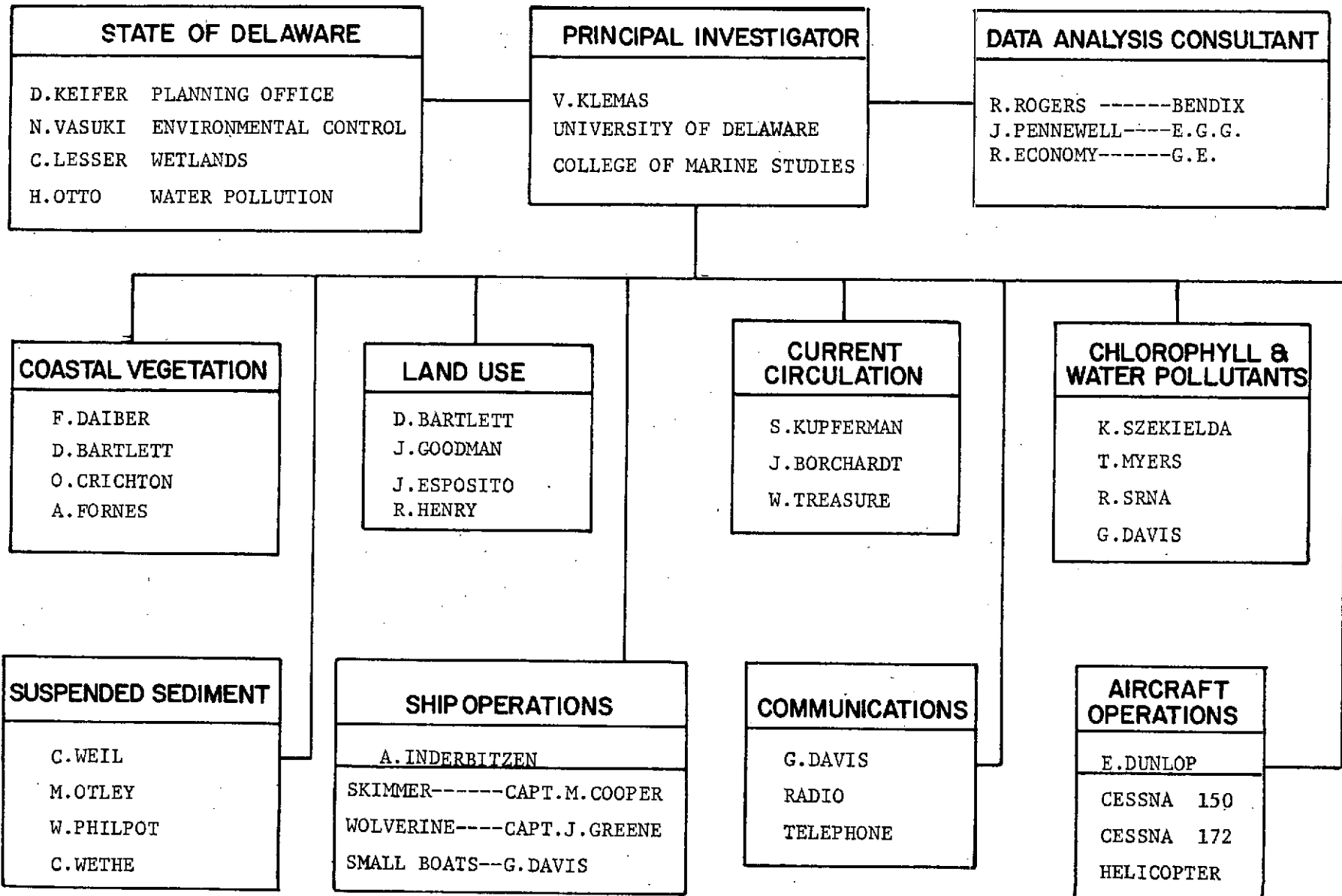
ORIGINAL PAGE IS
OF POOR QUALITY

Fig. 3.2 Collecting water samples from a hovering helicopter.

ORIGINAL PAGE IS
OF POOR QUALITY

Figure 3.3

Organization of Ground Truth Collection & Data Interpretation Effort:



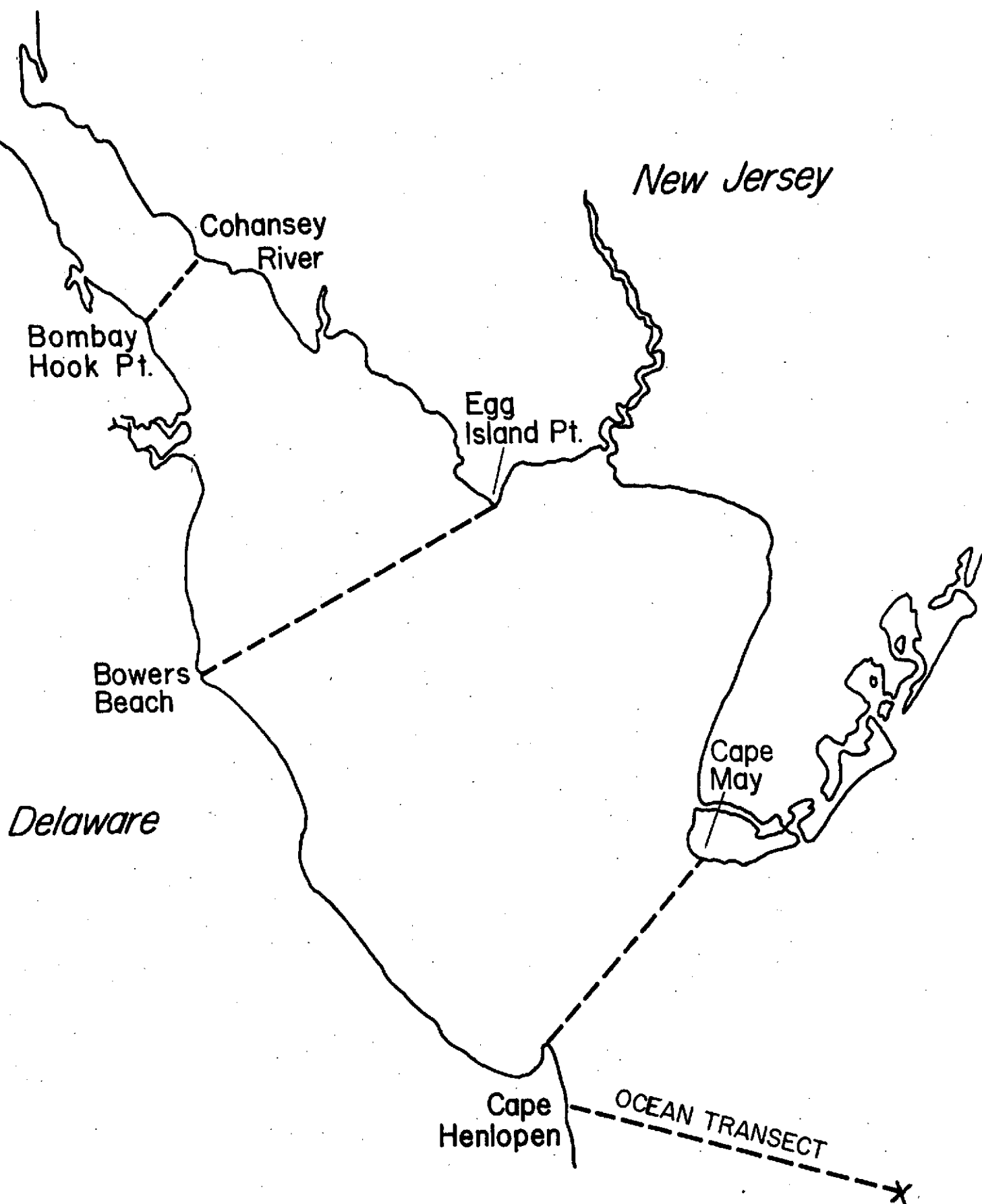


Figure 3.4 Boat and Helicopter Sea-truth Collection Transects Across Delaware Bay.

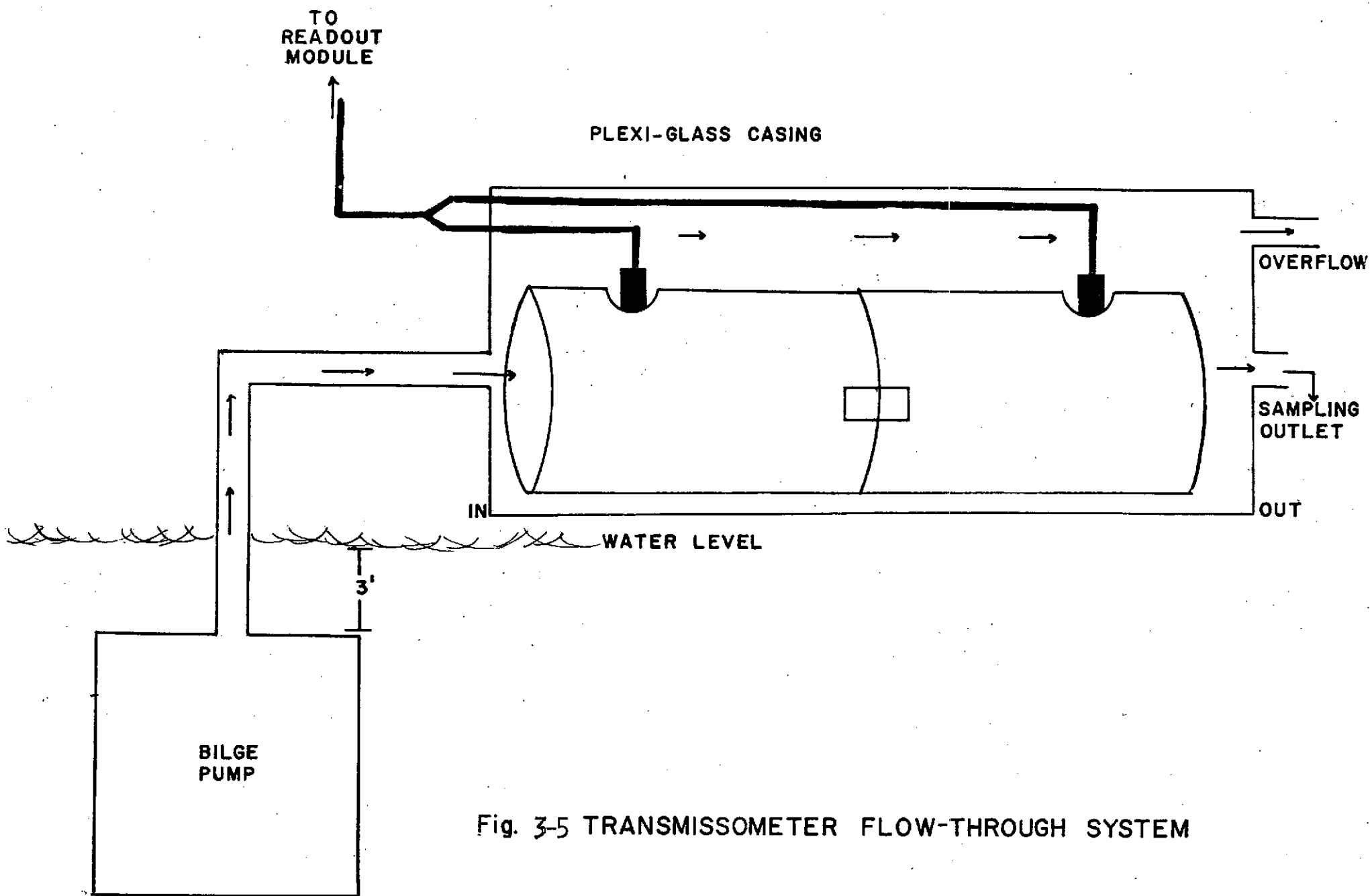


Fig. 3-5 TRANSMISSOMETER FLOW-THROUGH SYSTEM

4.0 ESTUARINE HYDRODYNAMICS AND WATER PROPERTIES

Oceanographic studies have always been plagued by the inability to collect synoptic data. This difficulty is particularly devastating in estuarine investigations where there may be significant changes within a period of less than half an hour. The data from ERTS-1 and Skylab overcome this difficulty, allowing the possibility of analysis of such complex phenomena as suspended sediment concentration and current circulation patterns over entire estuaries.

4.1 Physical and Optical Properties of Suspended Sediments

Extensive investigations of suspended sediments in Delaware Bay and laser transmission tests in a test tank facility have been conducted respectively by Oostdam and Hickman. The results can be summarized as follows:

Suspended sediments in Delaware Bay averaged 30 ppm. During July-August the average sediment level was 18 ppm.

Turbidity increased with depth in the water column, except during periods of bloom, when surface turbidities at times exceeded those greater depths.

Suspended sediment concentration gradients were greater during ebb than during flood because of greater turbulence and better mixing during flood stage.

The turbidity decreased from winter to summer.

Marked increases in turbidity which were observed during May and September were caused mainly by plankton blooms.

Suspended sediments were silt-clay sized particles with mean diameters around 1.5 microns.

The predominant clay minerals are chlorite, illite and kaolinite.

Reflectivities for the Delaware Bay sediments were measured to be about 10%.

At the time of the ERTS-1 overpasses, Secchi depth readings ranged from about 0.2 meters near the shore up to about 2 meters in the deep channel. Preliminary "equivalent Secchi depth" measurements with green and red boards indicated that neither "color" exceeded the readings obtained with the white Secchi disc. Therefore, it is quite unlikely that the bottom will be visible in any of the ERTS-1 channels and, at least in Delaware Bay, most of the visible features will be caused by light reflected off the surface or backscattered from suspended matter.

"Red" filters, such as the Kodak Wratten No. 25A, have frequently been used in aerial photography to enhance suspended sediment patterns (Klemas et al., Bowker et al.).^{2,8} In Delaware Bay red filters have been particularly effective for discriminating light-brown sediment-laden water in shallow areas from the less turbid dark-green water in the deep channel, as illustrated in the U-2 photographs in Figure 4.1. Comparing the ERTS-1 images of Delaware Bay in Figures 4.1, 4.2, 4.3, and 4.4, it becomes apparent that MSS band 5 gives the best representation of suspended sediment patterns in the upper portions of the water column. Along the east coast of the United States, Band 4 seems to be masked by haze-like noise, while bands 6 and 7 penetrate less than 10 cm into the water column, as compared to one to two meters for band 5.

Figure 4.1 contains microdensitometer scans between Cape Henlopen and Cape May across the mouth of the bay of the ERTS-1 images shown in Figures 4.2, 4.3, 4.4, and 4.5. ERTS-1 images taken in band 4, 5, and 6 were scanned, and grey scales equalized, to enable comparison on the same set of coordinate axes. Band 5 is clearly most sensitive to suspended sediment features. Even in band 5, however, the sediment patterns are caused by only four to five neighboring shades of grey in the negative transparencies and about twice that number in the digital tapes.

4.2 Suspended Sediment Concentration

4.2.1 Introduction

A simple visual study of ERTS band 5 imagery is sufficient to distinguish the most general features of the sediment distribution in Delaware Bay. For this purpose it is sufficient to assume that waters with a high sediment load appear as light-tinted areas on the ERTS imagery, while waters relatively low in sediment appear dark. For example, in the imagery for January 26 and July 7, 1973 (Figures 4.17 and 4.18 respectively) the sediment load, which is highest in the Delaware River and upper bay, decreases toward the mouth of the bay. Waters with differing sediment loads form boundaries and striated patterns throughout the bay. These features are essential to the current circulation study. Other obvious features are the sediment plumes at the mouths of rivers and inlets most easily seen along the Atlantic coast of New Jersey (Figure 4.18), the complex sediment patterns around Cape May which can be related to the intricate bottom topography at this point (Figure 2.2), and the high sediment load on the New Jersey side of the lower bay (Figure 4.17) which is due largely to the shallowness of the water in this region.

A more convincing technique in displaying the relationship between sediment load and band 5 imagery "brightness" is to take a microdensitometer trace across the band 5 imagery through points at which ground truth was collected on the day of the satellite overpass. A comparison between such a trace and ground truth collected during the January 26, 1973 overpass is shown in Figure 4.7. As might be expected there is a fairly good correlation between sediment concentration*, inverse Secchi depth and the densitometer readings. Although these results were not sufficient to define the relationship they were sufficiently good to warrant further study.

In order to more accurately determine the relationship between sediment concentration and imagery "brightness", more detailed information is necessary. First of all we must be able to distinguish between sediment and such things

*Sediment concentration is in units of mg/l. It is measured by filtering a known volume of a water sample through a millipore filter and drying and weighing the residue.

as oil slicks, acid plumes, sewage sludge and shallow water, all of which are capable of changing the reflectance characteristics of the water. Secondly, we must have more precise information about the radiance from the water than the purely relative measure obtainable from the microdensitometer readings.

It should be noted that in generally turbid water such as is typical of Delaware Bay, that any aircraft or satellite imagery is going to be a sensitive measure of effects in only surface waters.

The fact that different wavelengths penetrate to different depths adds another dimension to the analysis albeit a rather small one.⁹ The maximum penetration depth of any visible wavelength in turbid water is less than a few meters. The maximum Secchi depth recorded in this study of Delaware Bay was 2.04 m and was measured at the mouth of the Bay in the middle of the ship channel. McCluney has estimated penetration depths of 1.8 and 0.16 m for bands 4 and 5 respectively on the basis of a quasi-single scattering model.¹⁰ Penetration depths for bands 6 and 7 are typically even less than for bands 4 and 5. Thus a water mass which shows a high radiance in band 7 probably has a surface film (for instance, oil).

In order to distinguish sediment from oil slicks, etc. (and perhaps even to differentiate between different sediment types), it is necessary to use information from more than just one band, that is, we must seek distinct spectral signatures for waters with sediment and waters with oil and so on.* The greater the number of bands and the smaller the band width, the greater will be the detail in the spectral signature.¹¹ Figure 4.8 illustrates this point. Over similar spectral regions use of 9 of the 13 Skylab bands yields a better defined signature than could be obtained using only the 4 ERTS bands. Of course, an even more complete signature would be available using all 13 Skylab bands.**

*At the very least it is necessary to find a typical signature for sediment-laden water which is distinguishable from other water types whether or not their particular signature is known.

**More appropriate to the study of water features would be an increase in the number of bands in the visible region. Although the signature would then be limited to a smaller spectral region, the resolution would improve in the very region where the best information might be expected. Such a system has recently been made available by NASA on U-2 flights.

However, conventional photo-interpretation techniques are not equal to the task of correlating multispectral imagery. Even if it were feasible to use conventional techniques for multispectral analysis, the photographic reproductions contain far less detailed information than that available using the digital tape format for which computer analysis is necessary. Not only is the resolution better with the tapes, but the data is in terms of absolute radiance measurements which are extremely difficult to get from the photographs. Thus computer analysis of the digital tapes is the most promising technique available to us.

4.2.2 Procedure

At the time of an ERTS-1 overpass, ground truth is collected at predetermined points in the bay. Until recently, due to limits of equipment and personnel, ground truth consisted of, at best, 4 distinct points at which water samples were taken. At one (and occasionally more than one) station further measurements were taken which regularly included Secchi depth and transmissometer readings. Recent improvements in our collection techniques and additional equipment have greatly increased both the extent and reliability of our sampling. However, since the results to be presented depend on the older data, the refinements will be covered later.

At the site of each sample taken during the time of the overpass a training set is taken from the ERTS-1 imagery. That is, in a region on the imagery, surrounding the sampling site, over which the radiance readings are relatively constant in each band, an average spectral signature is found. This spectral signature, which is taken to be characteristic of water similar to that in the water sample, is called a training set. Once training sets have been found for all the sampling sites, the computer can compare each pixel with the various training sets and then classify each pixel which is similar to the training set.* As a result of this type of analysis the computer can generate maps of the bay which differentiate various water types on the basis of their differing spectral characteristics.

*A pixel is the smallest area of a scene over which radiant power is integrated for measurement.

4.2.3 Results

For our initial study of Delaware Bay using the computer analysis technique, the data from the July 7, 1973 ERTS overpass was chosen as most suitable because the ERTS data was excellent and sufficient ground truth was collected on that day to make an attempt at correlation between sediment and radiance. Although the Skylab data has more bands and would have yielded a better defined spectrum, ERTS data was used rather than Skylab, since the Skylab data was too noisy and would have to be filtered first to remove noise components which interfere with quantitative studies.

The ground truth for the July 7 overpass was collected in three transects across the bay (Figure 4.10). The best data is from the middle transect from the Murderkill River to Egg Island Point where the water samples were obtained from a low-flying helicopter, and the upper bay transect from Bombay Hook Pt. to the Cohansey River. The upper bay transect was done by boat and included 11 stations. Both of these transects were completed in about half an hour and included several stations within 10 minutes of the overpass which can be taken as being synoptic.

The data from the Cape May to Cape Henlopen transect suffers from two problems in particular. First, the transect, which is 11 miles in length, was taken by boat and took nearly 2 hours to complete. Thus, of the 21 stations taken only 4 could be taken as being synoptic with the ERTS data. Secondly all 4 of these stations were in a region of complex bottom topography. The resulting irregular sediment pattern made it difficult to choose a training set in the immediate region of the sampling sites.

Four training sets, then, were chosen on the basis of ground truth. These are marked 1, 2, 4, and 9 in Figure 4.10. After classification of all the pixels conforming to these training sets, there remained large unclassified regions in the bay. These remaining unclassified regions were then systematically classified by the method described earlier based entirely on radiance readings. The technique is illustrated in Figure 4.9. Once this classification procedure had been carried out each class was assigned a color. The computer system was capable of assigning 15 colors: 14 classified types and 1 unclassified (black). The resulting map is shown in Figure 4.11. Table 4.1 gives the relationship between the colors, the

TABLE 4.1. COLOR ASSIGNMENTS

File #	Color	Band 4	Band 5	Band 6	Band 7	Measured	Concentration
						concentra- tion (mg/l)	from non- linear regression
1	dk. green	.659	.358	.178	.211	25mg/l	24mg/l
2	blue green	.642	.341	.153	.147	20mg/l	21mg/l
3	turquoise	.587	.310	.164	.187		16mg/l
4	green	.703	.410	.223	.255	40mg/l	39mg/l
5	yellow	.719	.406	.177	.145		
6	lt. blue	.539	.250	.125	.112		9.7mg/l
7	dk. gray	.504	.223	.108	.093		7.7mg/l
8	med. gray	.496	.247	.157	.150		
9	orange	.782	.486	.251	.280	70mg/l	72mg/l
10	red	.790	.530	.301	.335		104mg/l
11	purple	.853	.613	.341	.370		211mg/l
12	lt. gray	.797	.549	.368	.492		
13	white	.627	.343	.222	.374		
14	blue	.462	.192	.096	.104		5.6mg/l

* The table shows the actual radiance values in each band, the four measured concentrations and the extrapolated concentration values. The values in parenthesis are for areas whose spectral signature varies only slightly from the sediment signature pattern. No sediment values are given for regions with anomalous signatures.

position of the corresponding training set and the sediment concentration of the 4 known sampling sites.

The spectral signatures of the training sets are shown in Figure 4.12. The dark solid lines are the signatures which are all of the same general form although they are distinctly different in radiance levels. If we assume for a moment that the radiance difference is due chiefly to sediment concentration, we find as expected that the training sets which are farthest up the bay have the highest radiance.

By relating the measured sediment concentration values to the radiance in band 5, it is possible to fit the data to an exponential by a non-linear regression. Band 5 was chosen because, of the two bands that penetrate the water appreciably (bands 4 and 5), band 5 is less affected by atmospheric effects. Fitting the data by the method of least squares we have:

$$y = a e^{bx}$$

where y = sediment concentration (mg/l)

x = radiance (mw/cm²)

a = 1.169

b = 8.481

correlation coefficient = 0.99598

We find that the resulting values for sediment concentration in areas of the bay for which there is no ground truth are generally quite reasonable. Training set 11, which is the farthest up the bay of all the training set, yields a concentration of 211 mg/l which is not an unusual value, and training set 14, which is in ocean waters, corresponds to a predictably low concentration. The 7.7 mg/l concentration for the training set between the capes, however, is somewhat lower than might be expected. Concentrations of 15 mg/l have been observed in this region, but of the ground truth collected on July 7, no concentration measured was less than 22 mg/l. It is rather unlikely that the concentrations were quite as low as estimated by the curve. Still the correlation is good enough for the rest of the data to demonstrate the relationship between sediment concentration and radiance. A more rigorous relationship between suspended sediment concentration, material size, sphericity and composition will be defined during follow-on work.

One thing which, if you will, clouds the analysis somewhat is the effect of the atmosphere. Thus far we have made the tacit assumption that the atmospheric effects have been reasonably uniform over the area of interest. However, in a land use study using the same ERTS data and having excellent ground truth throughout the region, it was discovered that there was considerably more haze effect over the northern portion of the bay than over the southern.¹² This haze probably exaggerated the radiance gradient over the bay, increasing it more in the north than in the south. Unfortunately, there is no way of making any really quantitative statement about the effect of the haze since no radiance readings were taken as part of the ground truth.

One further thing to note is that the spectral signatures of six of the training sets do not fit the pattern set by the other eight. Two of these (sets 3 and 14) are fairly close to the pattern, being only slightly skewed in the IR. Sets 5 and 8 differ more significantly. Set eight is rather shallow water on the New Jersey side of the bay. There might be a difference in sediment here due to different sediments from the New Jersey rivers. The circulation in this area is not as good as it is in the deeper portion of the bay and the river sediment type may be more dominant.

The most obviously different spectral signatures are for training sets 12 and 13. Both are very strong in the IR. The differences in set 12 are obviously due to the river flow from the Chesapeake and Delaware Canal. Oddly enough the signature of set 13, which is in the Atlantic, is of a remarkably similar form to that of set 12. The source of these differences is unknown. No such patterns have been observed in any other ERTS or Skylab data studied.

4.2.4 Discussion

There were basically two problems which prevented our getting more precise results: the limited number of sampling stations and the lack of ground radiance measurements. We believe that both problems have been solved.

The problem of collecting enough water samples all at the same time over an area as large as Delaware Bay seemed an impossible task. Yet it

eventually lent itself to a unique solution. On the morning of an overpass we now station scientists at several boat launching ramps around the bay. After a brief explanation of the purpose of the experiment, the boaters and fishermen are asked to take water samples for us. They are requested to fill two sampling bottles at the time of the overpass and to mark the time and their position on charts which are provided.

This method has, as of this writing, been tried only once and the response was excellent. Most of the people were happy to help and 85% of the sample packets handed out were returned. Even though several of the samples were taken in the same areas (which is still useful as a measure of the homogeneity of a region), the number of valid sample points was tripled at the very least. We intend to continue to use this sampling method -- hopefully, with continued success.

The second problem, that of ground radiance measurements, has been solved at least partially by our acquisition of a radiance meter. The meter, a Bendix RPMI, is designed to measure radiance in the same bands as ERTS-1 sensors. The most important result of using this meter is that it will make it possible to correct for atmospheric effects. Although problems such as those encountered with the July 7th overpass with a varying haze effect over the bay still pose difficulties, it should be possible now to compare data from two different overpasses directly.

4.3 Current Circulation and Coastal Fronts

Using suspended sediment as a natural tracer, it is possible to study current circulation in the surface layers of Delaware Bay by employing ERTS-1 imagery and predicted tide and flow conditions. Only MSS band 5 images are shown, since the "red" band was found to give the best contrast in delineating suspended sediment concentrations in the upper one meter of the water column. Adjacent to ERTS-1 pictures, Figures 4.13 to 4.21 contain tidal current maps for Delaware Bay.¹³ Each ERTS-1 picture is matched to the nearest predicted tidal current map within ± 30 minutes.¹⁴ The current charts indicate the hourly directions by arrows, and the velocities of the tidal currents in knots. The Coast and Geodetic Survey made observations of the current from the surface to a maximum depth of 6 meters in compiling these charts.¹³

The satellite picture in Figure 4.13 was taken on October 10, 1972, two hours after maximum flood at the entrance of Delaware Bay. Masses of highly turbid water are visible around the shoals near the mouth of the bay and throughout the shallow areas on both sides of the bay. Since at that time flood currents were prevailing throughout the bay, much of the suspended matter appears to be local sediment brought into temporary suspension by flood currents and waves. During flood tide at the mouth of the bay, considerable correlation was found between the depth profile and image radiance, as shown in Figure 4.14. During flood tide most of the sediment in suspension seems to be locally generated over shoals and shallow areas of the bay resulting in a higher degree of backscatter from shallower waters. No such correlation was found during ebb tide when finer sands and silt are carried down the rivers into the bay. At the time of this ERTS-1 picture, the wind velocity was 13 to 22 km per hour from the north causing surface currents in nearly the opposite direction to the tidal flow. Peak flood current velocity is occurring in the upper portion of the bay, causing sharp boundaries along the edges of the deep channels to form.

Boundaries or fronts (regions of high horizontal density gradient with associated horizontal convergence) are a major hydrographic feature in Delaware Bay and in other estuaries. Fronts in Delaware Bay have been investigated using STD sections, dye drops and aerial photography. Horizontal salinity gradients of 4‰ in one meter and convergence velocities of the order of 0.1 m/sec have been observed.¹⁵ Underwater visibility improved

from 1 meter to 2 meters as certain boundaries were crossed (Figure 4.15). Several varieties of fronts have been seen. Those near the mouth of the bay are associated with the tidal intrusion of shelf water. The formation of fronts in the interior of the bay (Figure 4.16) appears to be associated with velocity shears induced by difference in bottom topography with horizontal density difference across the front influenced by vertical density difference in the deep water portion of the estuary. Surface slicks and foam collected at frontal convergence zones near boundaries contained concentrations of Cr, Cu, Fe, Hg, Pb, and Zn higher by two to four orders of magnitude than concentrations in mean ocean water.¹⁶

Figure 4.17 represents tidal conditions two hours before maximum flood at the mouth of the bay observed by ERTS-1 on January 26, 1973. High water slack is occurring in the upper portion of the bay, resulting in less pronounced boundaries there as compared to Figure 4.13. The shelf tidal water is not rushing along the deep channel upstream anymore as in Figure 4.13, but is caught between incipient ebb flow coming down the upper portion of the river and the last phase of the flood currents still entering the bay. On the morning of January 26, 1973, there was a variable wind over the bay at about 9 to 11 km per hour from the south-southwest, helping tidal currents push clearer shelf water against highly turbid water masses in New Jersey's shallow flats.

About six months later, on July 7, 1973, the ERTS-1 overpass shown in Figure 4.18 occurred during the same part of the tidal cycle as that shown in Figure 4.17. Since river flow differs in the winter and summer, Figures 4.17 and 4.18 enable one to compare the effect of river flow and wind under identical tidal conditions. The wind velocity was about 7 to 14 km per hour from the west at the time of the overpass. The long bright patch having a higher radiance about 20 miles from shore in the Atlantic Ocean has not been identified yet, however it could be an area of higher sea state or higher concentration of suspended matter.

As shown in Figure 4.19, on August 12, 1973, ERTS-1 passed over Delaware Bay one hour before maximum ebb at the mouth of the bay. In addition to turbid water masses over shallow areas and shoals observed in Figures 4.13 and 4.17, plumes of suspended matter are seen in Figure 4.19 parallel to the

river flow and exiting from streams and inlets off New Jersey's and Delaware's coastline. The plumes at Indian River Inlet, Delaware and Ocean City, Maryland are particularly well defined. Shear boundaries along the deep channel are still visible in the upper portion of the bay; however they are beginning to disappear as slack sets in, resembling conditions of Figure 4.17. There was a steady wind from the west at about 22 km per hour. Figure 4.20 contains an ERTS-1 image of the bay taken on December 3, 1972, when tidal condition were the same and the wind was steady from the west at 13 to 16 km per hour. The flow patterns inside the bay are somewhat similar, but there are no north-south streaks in the ocean and the plumes along the coast extend further out without being broken up. The aircraft photograph included in Figure 4.20 was taken by a U-2 from 65,000 feet altitude at the time of the satellite overpass. It shows the additional flow pattern detail available in the red band from aircraft underflights.

The satellite overpass on February 13, 1973 occurred about one hour after maximum ebb at Cape Henlopen. The corresponding ERTS-1 image and predicted tidal currents are shown in Figure 4.21. Strong sediment transport out of the bay in the upper portion of the water column is clearly visible, with some of the plumes extending up to 30 km out of the bay. Small sediment plumes along New Jersey's coast clearly indicate that the direction of the nearshore current at that time was towards the north. The wind velocity at the time of the satellite overpass was about 13 km per hour from the west-northwest, reinforcing the tidal current movement out of the bay.

4.4 Dispersion of Acid and Sludge Disposal Plumes

Approximately forty nautical miles off the Delaware coast is located the disposal site for waste discharged for a plant processing titanium dioxide. The discharge is a greenish-brown, 15-20% acid liquid which consists primarily of iron chlorides and sulfates. The barge which transports this waste has a 1,000,000-gallon capacity and makes approximately three trips to the disposal site per week.

The frequency of this dumping made it possible for the ERTS-1 satellite to photograph the acid plume in various stages of degradation. Between 16 August 1972 and 17 September 1973 five photographs were found which show water discolorations in the general vicinity of the waste dump site. While there is no ground truth to verify that these discolorations represent the iron-acid waste plume, the position of the discoloration, the dump pattern and the time difference between the dump and photograph give strong indications that the discolorations are the acid plume. It is hopeful that in the future the ERTS-1 photographs may be used to study the dispersion patterns and drift velocities of the iron-acid plume.

Careful examination of Figure 4.22 disclosed a fishhook-shaped plume about 40 miles east of Cape Henlopen caused by a barge disposing acid wastes. The plume shows up more strongly in the green band than in the red band. Since some acids have a strong green component during dumping and turn slowly more brownish-reddish with age, the ratio of radiance signatures between the green and red bands may give an indication of how long before the satellite overpass the acid was dumped.

Enlarged enhancements of the acid waste plumes, prepared from the ERTS-1 MSS digital tapes (Figure 4.23) aided considerably in studies of the dispersion of the waste plume. Currently acid dumps are being coordinated with ERTS-1 overpasses in order to determine the diffusion and movement of the waste materials along the continental shelf.

Sludge disposal plumes in the ocean off the Delaware coast have also been detected in ERTS-1 imagery. However they are more difficult to track due to the less frequent dump schedule.

4.5 Off-shore Oil Terminal Site Dye Studies

Dye drops were used to predict the movement of potential oil spills from a proposed offshore oil terminal site near the mouth of Delaware Bay. The tracking of the dye was performed by a combined aircraft-boat team. Surface currents which may influence the movement of oil were found to differ considerably from the predicted gross current circulation at the test site, with significant environmental implications.

As shown in Figure 4.24, nearly 150 liters of Rhodamine WT dye were spread by the R.V. Delaware into a large circular slick of about 300 meters in diameter. The dye patch was made large enough to be observed from ERTS-1. Subsequent cloud cover prevented the satellite from imaging the dye slick. However, it was traced successfully by aircraft. The dye was injected about one hour before the predicted flood current peak at the mouth of the bay. An aquatic frontal system (boundary) passed over the dye slick, attracting the dye into the boundary, and carried it for about two miles in the north-west direction toward the mouth of the bay. An aerial photograph obtained by enhancing the dye with a Wratten 25A red filter is shown in Figure 4.25.

Boundaries or fronts (regions of high horizontal density gradient with associated horizontal convergence) are a major hydrographic feature in Delaware Bay and in other estuaries. Several varieties of fronts have been seen. Those near the mouth of the bay are associated with the tidal intrusion of shelf water. The formation of these fronts in the interior of the bay appears to be associated with velocity shears induced by differences in bottom topography, with the horizontal density difference across the front influenced by vertical density difference in the deep water portion of the estuary.¹⁶ Surface slicks and foam collected at frontal convergence zones near boundaries contained concentrations of Cr, Cu, Fe, Hg, Pb, and Zn higher by two to four orders of magnitude than concentrations in mean ocean water.¹¹ A similar boundary with a strong foam line is shown in Figure 4.26, near the 8-mile offshore proposed oil terminal site. As shown in Figures 4.27 and 4.28, on August 16, 1972, several such boundaries outside Delaware Bay were imaged by ERTS-1. Transmissivity measurements by divers working near the boundaries showed the visibility changed from two meters to fifty centimeters as one crossed from the clear into the turbid side of the boundary.

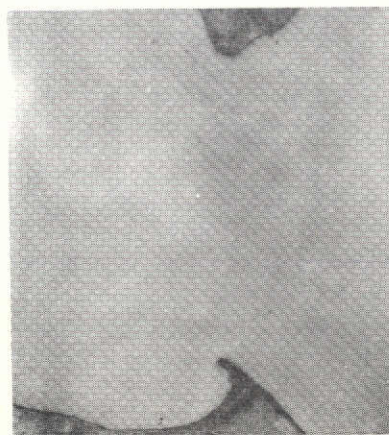
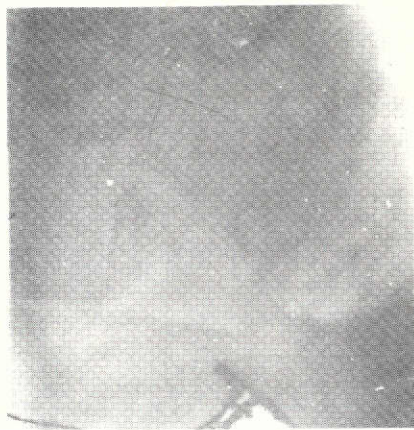
4.6 Enhancement of Water Features

Color density slicing and optical additive color viewing techniques were employed to enhance the suspended sediment patterns. Grey tone variations were "sliced" into increments and different colors assigned to each increment by using the Spatial Data Datacolor 703 System at NASA's Goddard Space Flight Center. Color density slicing helped delineate the suspended

sediment patterns more clearly and differentiate turbidity levels. Density slicing of all four MSS bands gave an indication of relative sediment concentration as a function of depth, since the four bands penetrate to different depths ranging from several meters to several centimeters, respectively.

Additive color composites of bands 4 and 5 were prepared by Photo-Science, Inc. using the photographic process silver-dye bleaching. This process bleaches out spectral separations of each MSS band to produce the color composite. The additive color rendition is then reproduced on Cibachrome CCT color transparencies. Comparison of the composite with the equivalent band 5 image indicates however that the composite does not contain more suspended sediment detail than the individual band 5 image. For similar reasons, composites prepared with the International Imaging Systems Mini-Addco Additive Color Viewer, Model 6030 did not improve contrast beyond what was attainable in band 5 directly.

As described in Section 4.2, ERTS-1 digital tapes were used by Bendix Aerospace Systems Division to prepare annotated sediment concentration maps of the bay.



ORIGINAL PAGE IS
OF POOR QUALITY

Figure 4.1 Photographs taken at 65,000 feet altitude by a NASA U-2 aircraft, 41 minutes after the December 3, 1972 ERTS-1 overpass. The mouth of Delaware Bay is shown in three spectral bands.

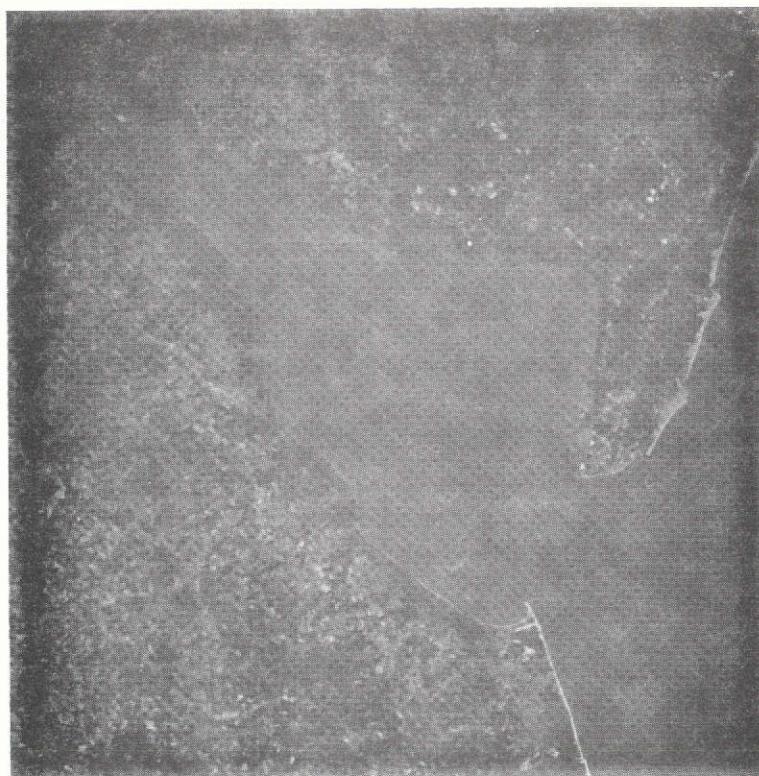


Fig. 4.2 MSS band 4 of ERTS-1 overpass of Delaware Bay on October 10, 1972. (I.D. 1079-15133)



Fig. 4.3 MSS band 5 of ERTS-1 overpass of Delaware Bay on October 10, 1972. (I.D. 1079-15133)

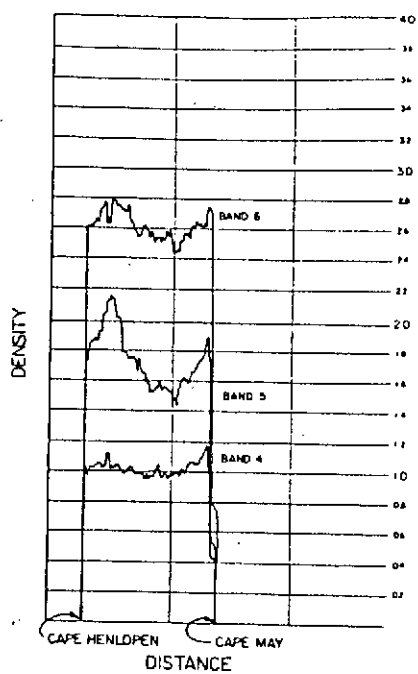


Fig. 4.4 MSS band 6 of ERTS-1 overpass of Delaware Bay on October 10, 1972. (I.D. 1079-15133)

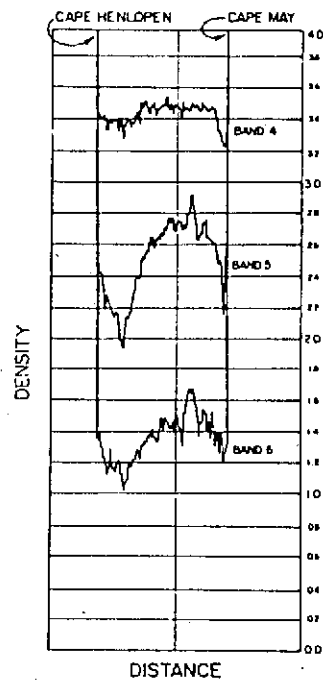


ORIGINAL PAGE IS
OF POOR QUALITY

Fig. 4.5 MSS band 7 of ERTS-1 overpass of Delaware Bay on October 10, 1972. (I.D. 1079-15133)



Positive Transparencies



Negative
Transparencies

Figure 4.6 Microdensitometer traces of October 10, 1972, ERTS-1 imagery from Cape Henlopen, Delaware to Cape May, New Jersey, using MSS bands 4, 5, and 6.

C₂₃

47

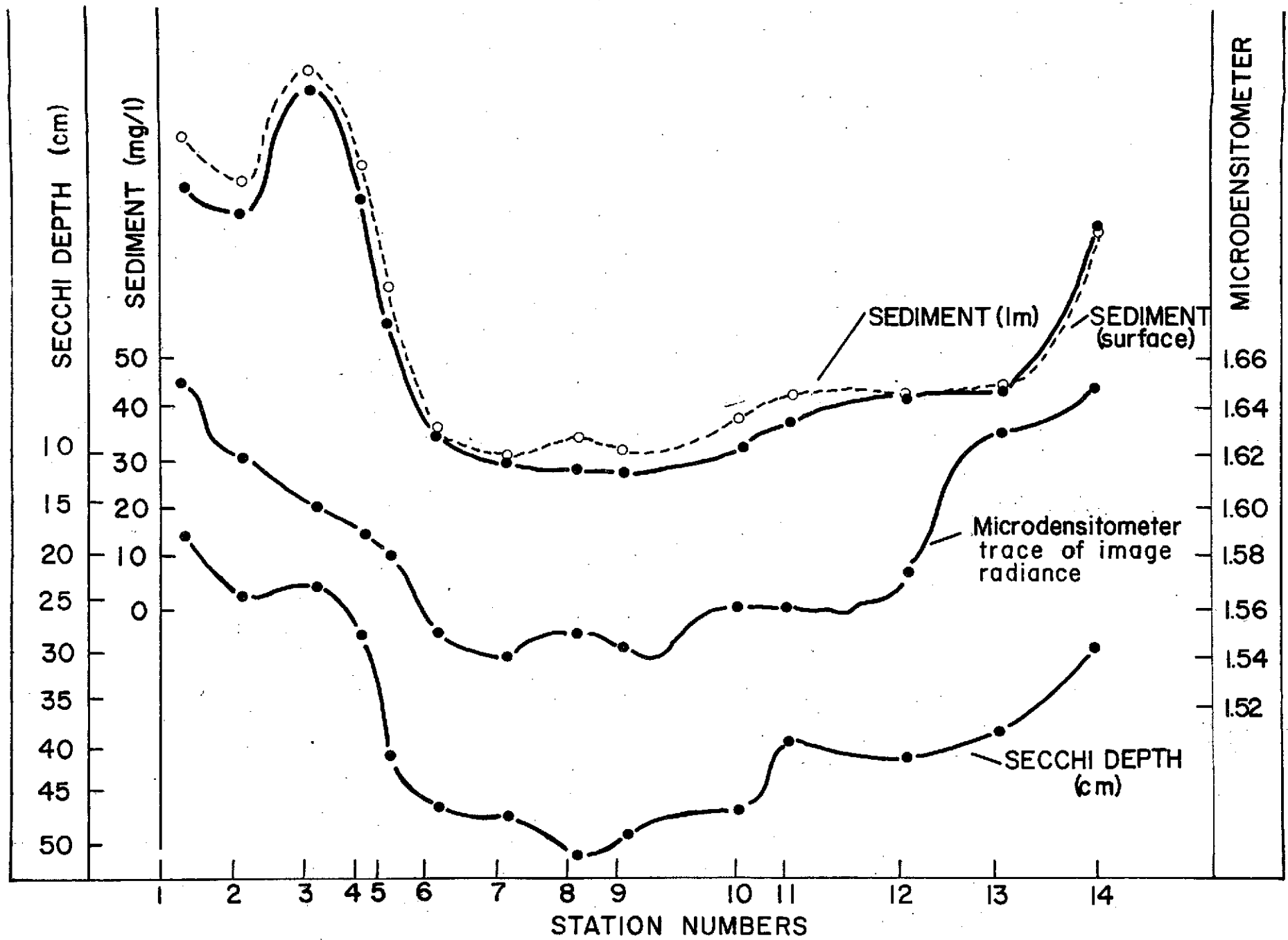


Figure 4.7 Correlation of ERTS-1 image radiance (microdensitometer scan) with suspended sediment concentration and Secchi depth.

ORIGINAL PAGE IS
OF POOR QUALITY

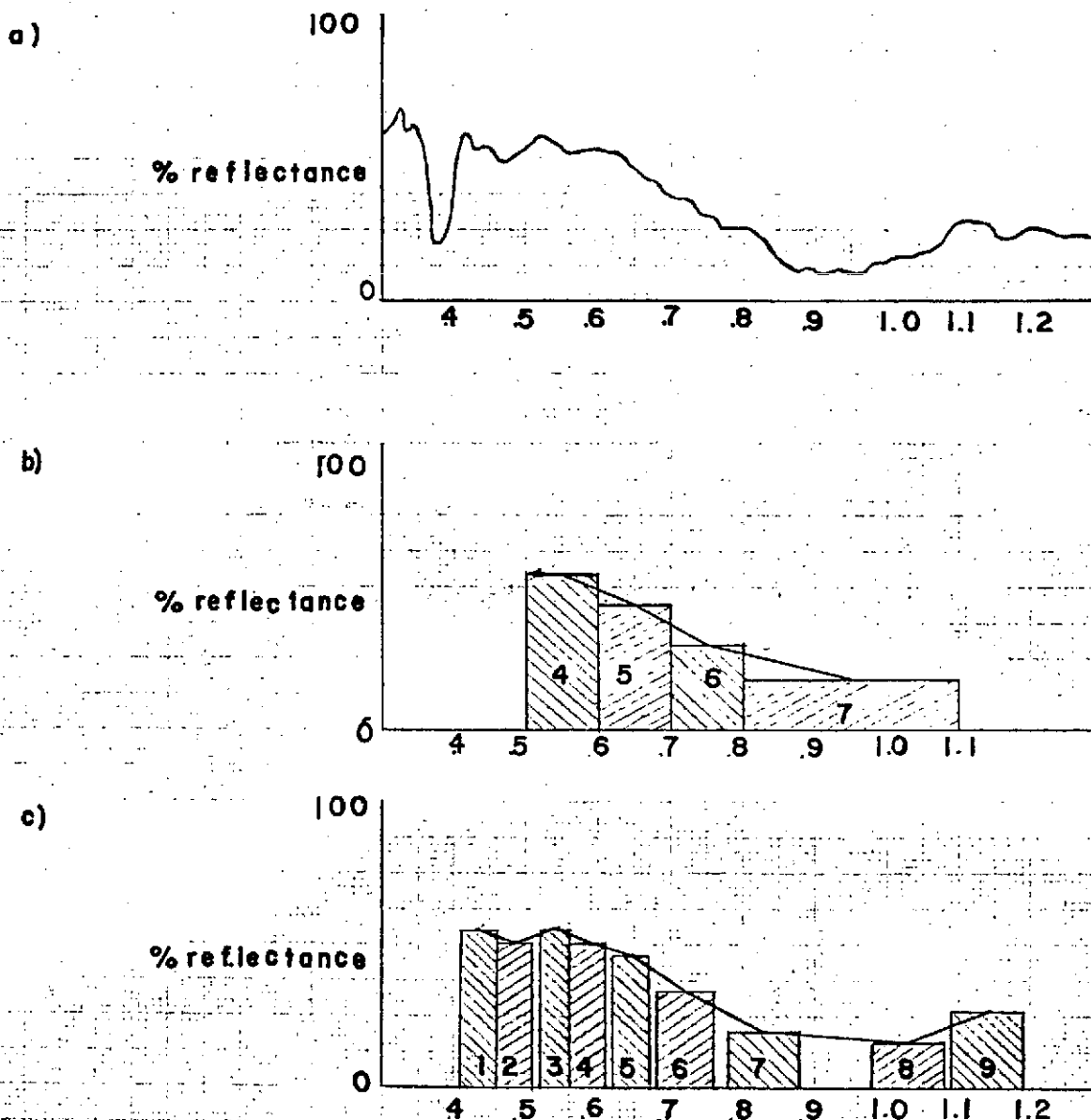


Figure 4.8 Spectral signatures. The representation of the spectral signature becomes more accurate as the number of bands increases and the band width decreases. (a) actual reflectance spectrum; (b) typical signature using 4 ERTS bands; (c) signature using 1st nine of the 13 S 192 bands.

Figure 4.9 Choosing a training set. Each symbol on this computer printout of ERTS band 5 represents a range of radiance. The training set is chosen in an area where all of the symbols are identical.

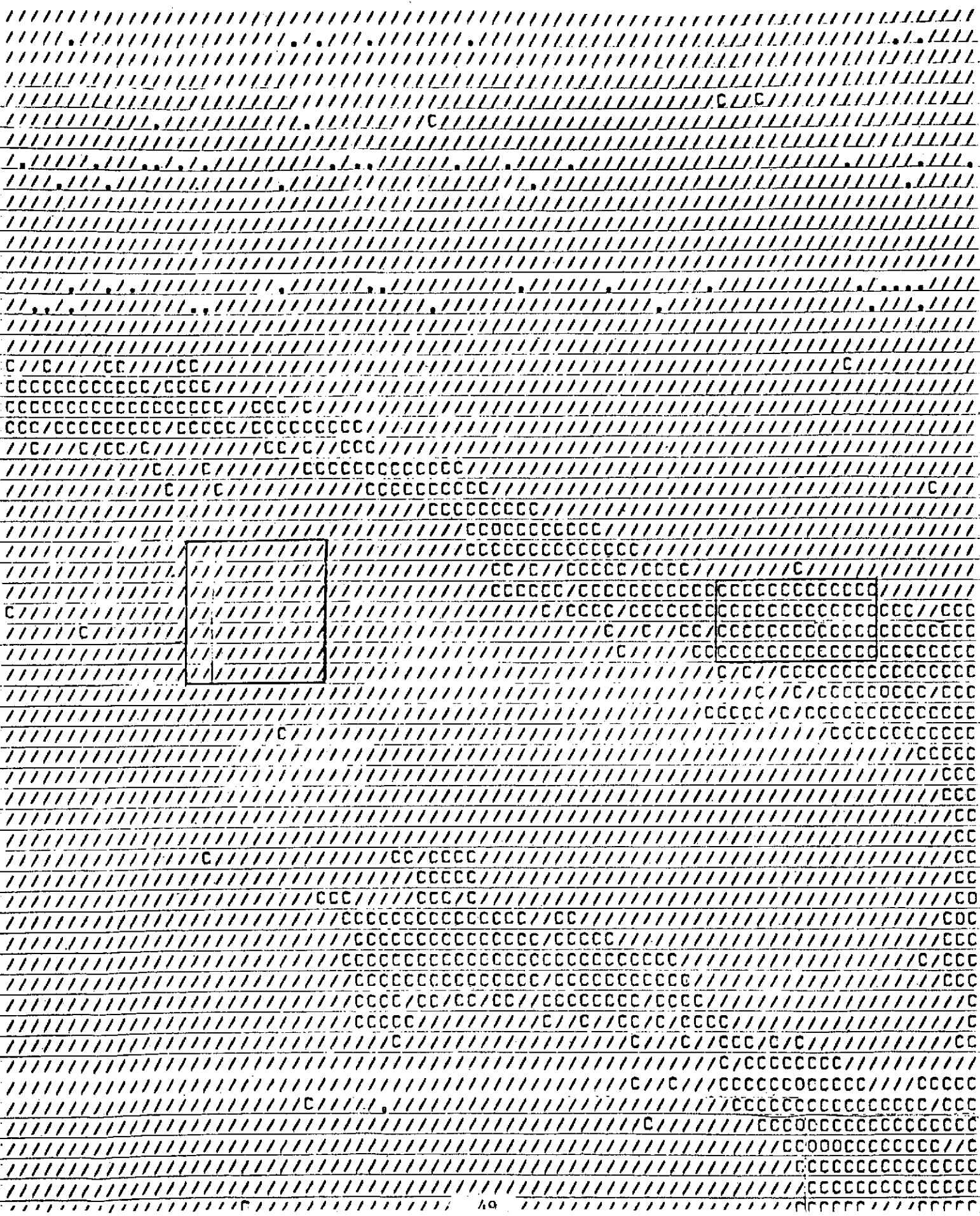
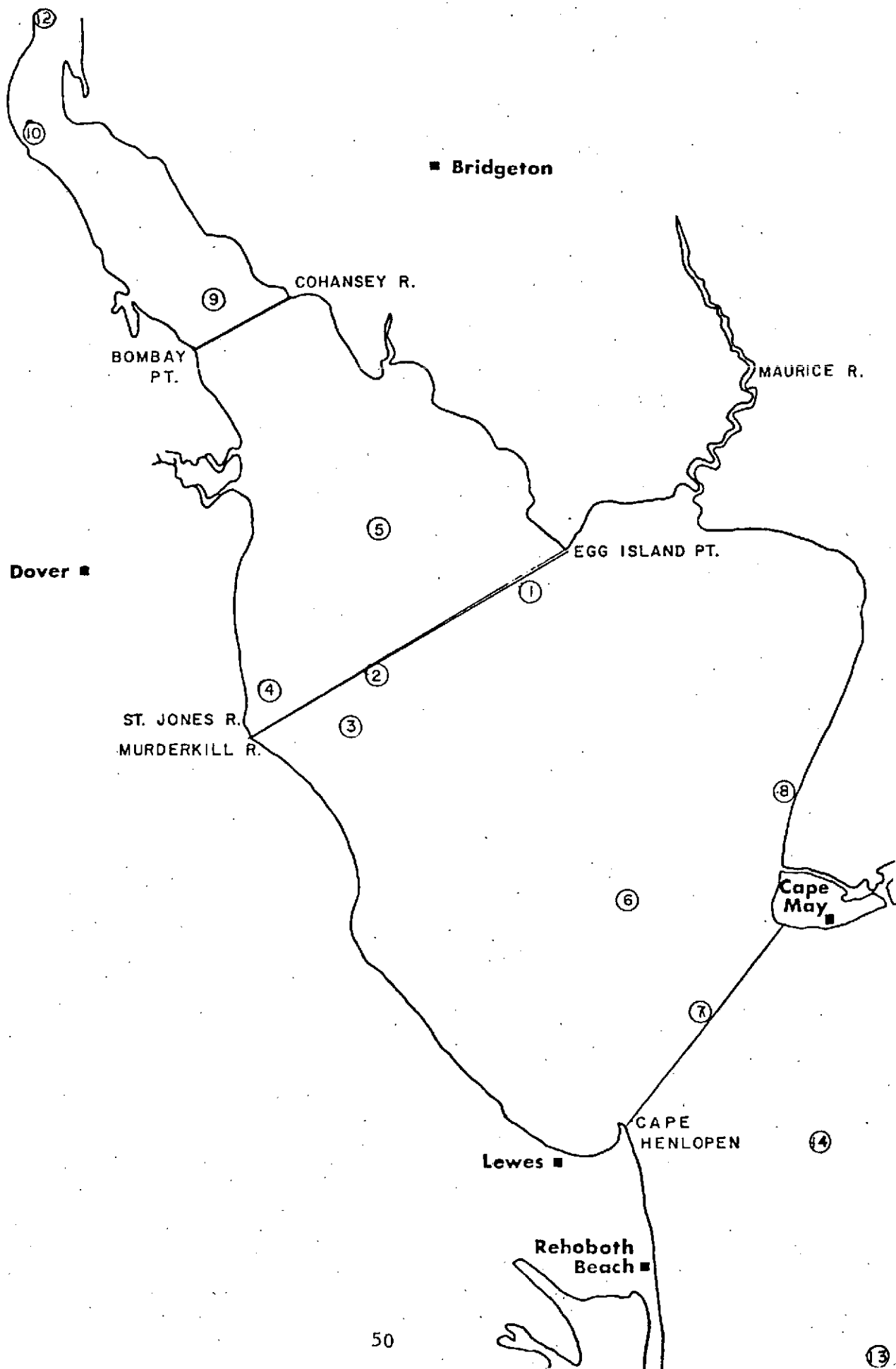


Figure 4.10 Map of Delaware Bay. The solid lines show the transects along which ground truth was collected on July 7, 1973. The numbers show the points at which the training sets were chosen.



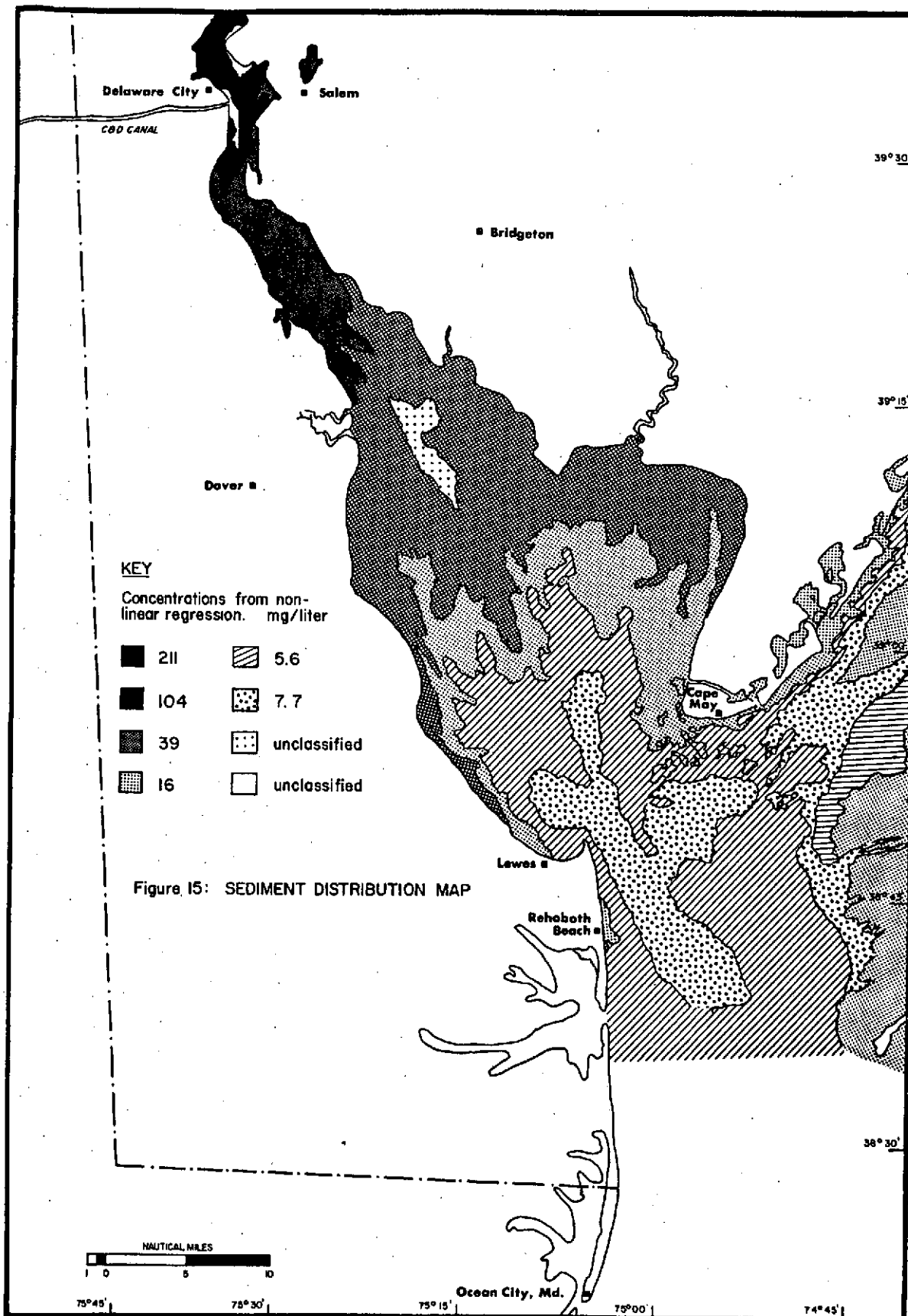
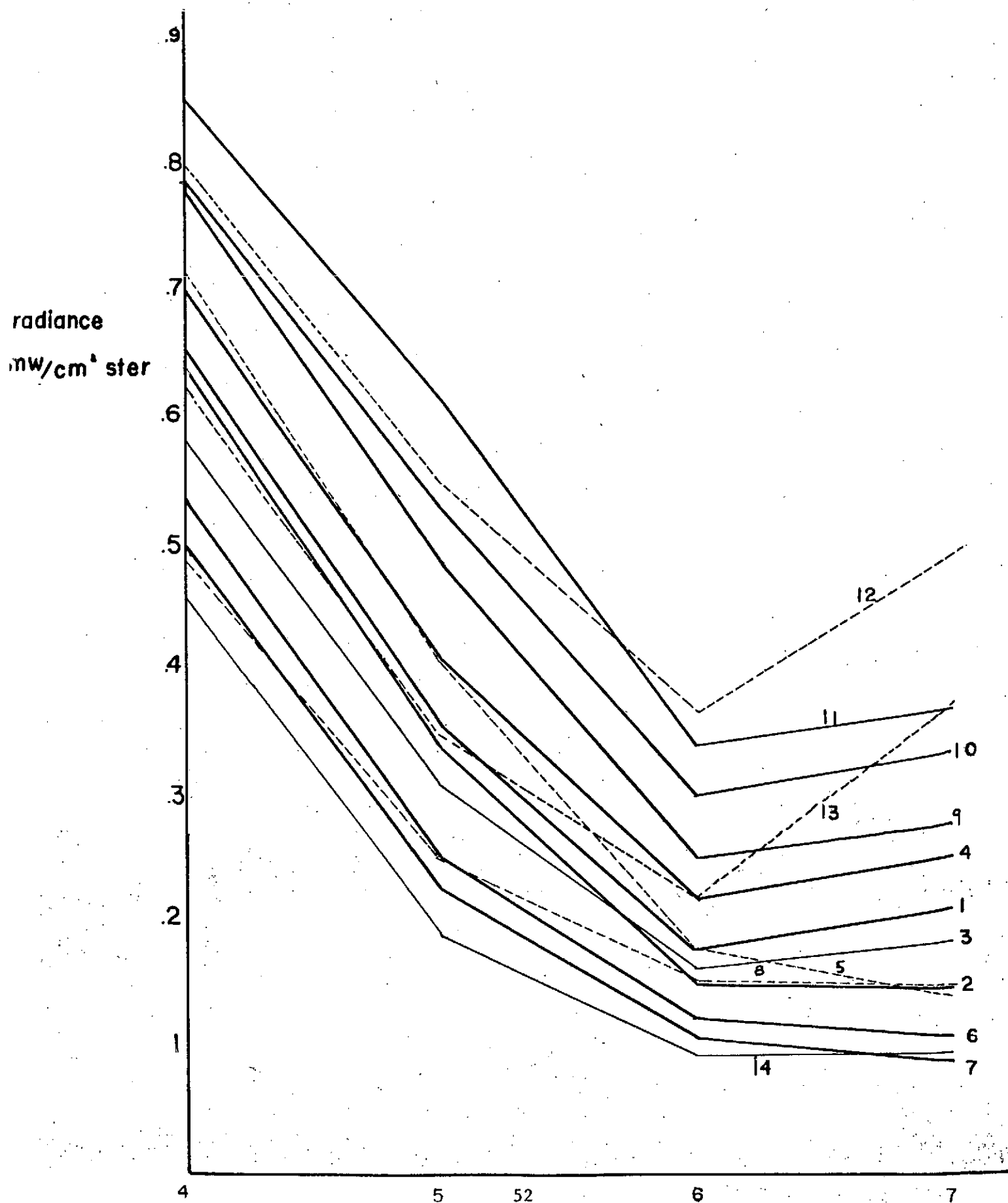


Figure 4.11 Suspended Sediment Concentration Map

Figure 4.12 Spectral signatures of the training sets. The signatures which are most similar in form and which are probably representative of different concentrations of the same type of sediment are shown by solid lines. The dotted lines are signatures which deviate from the sediment signature pattern.



ORIGINAL PAGE IS
OF POOR QUALITY

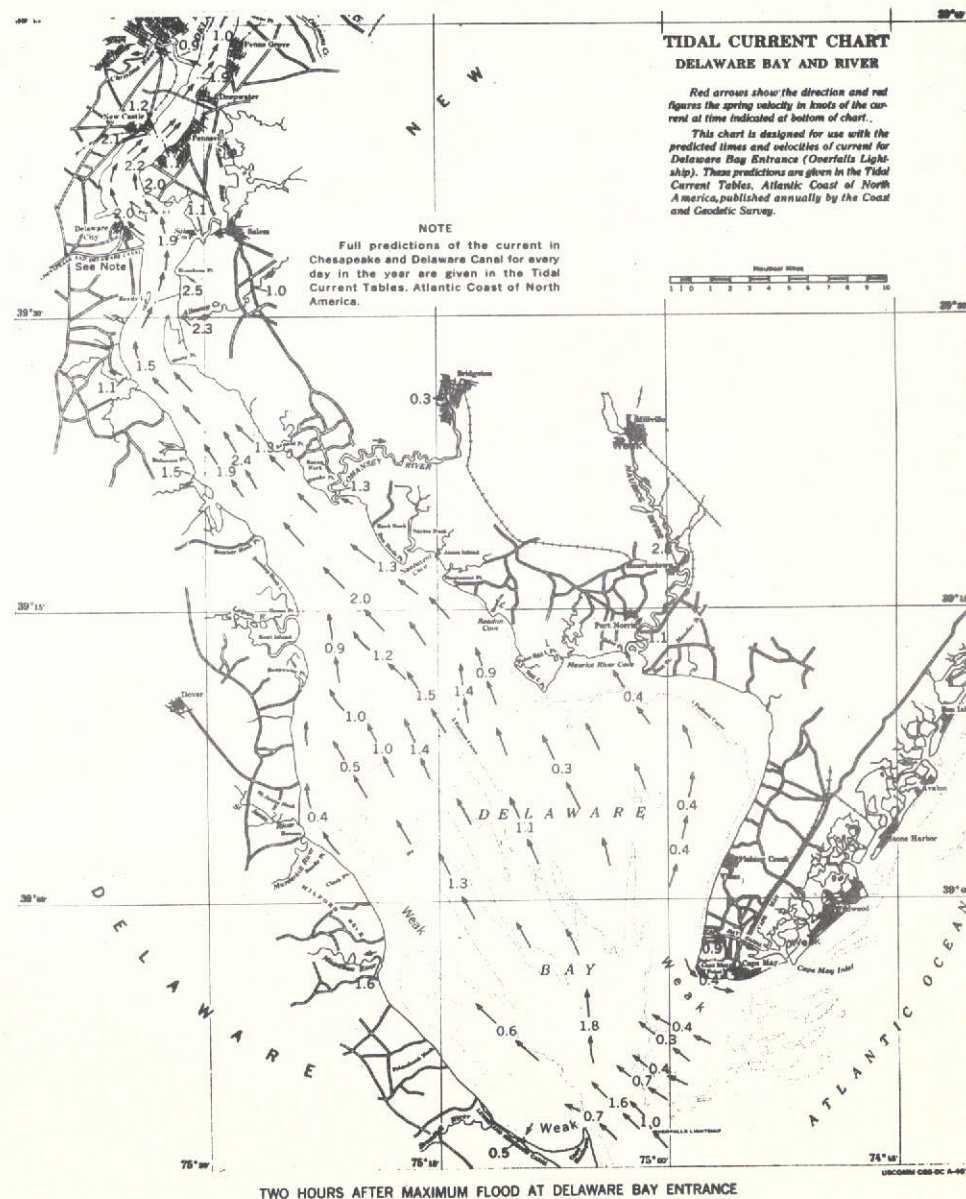
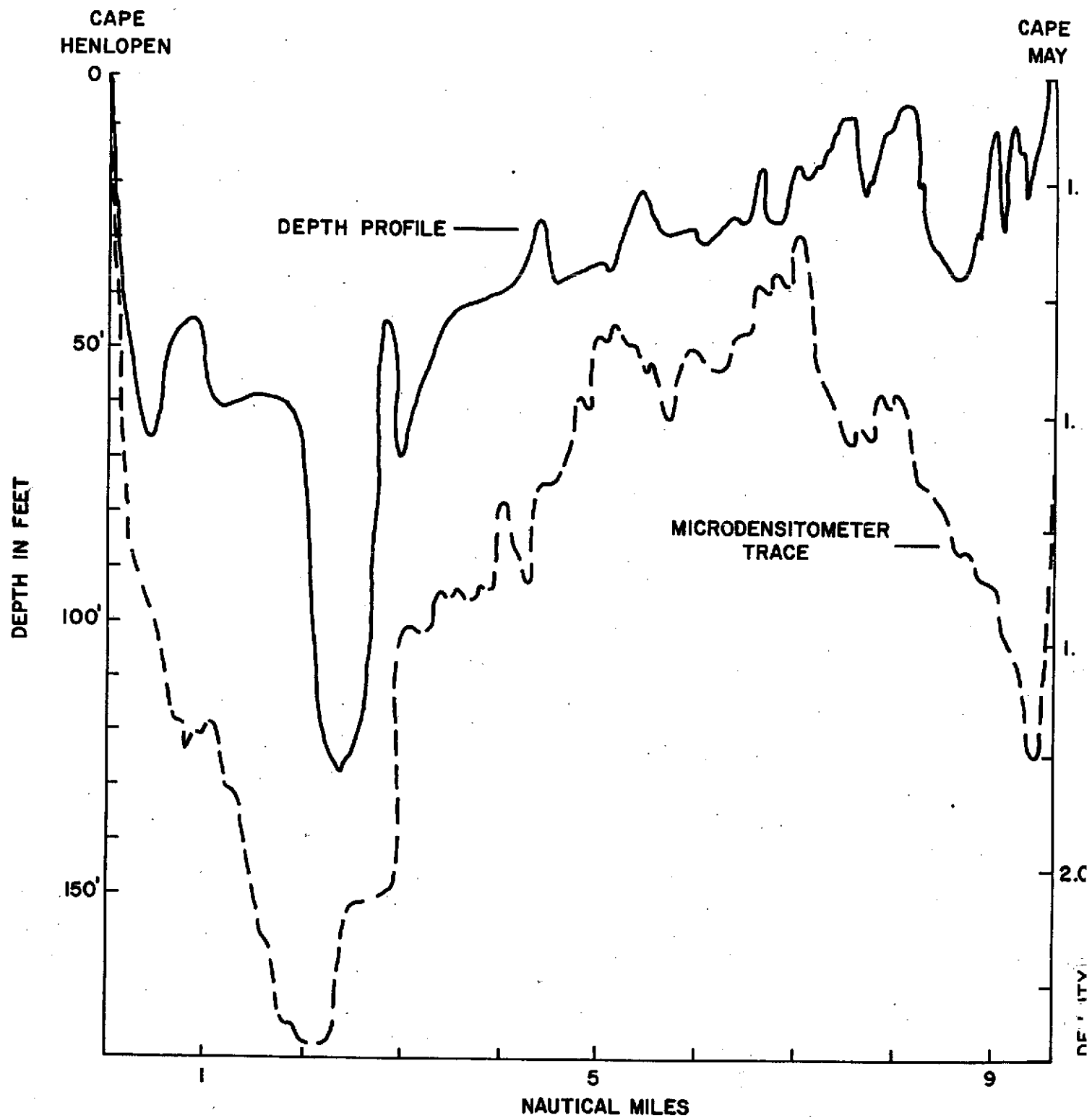
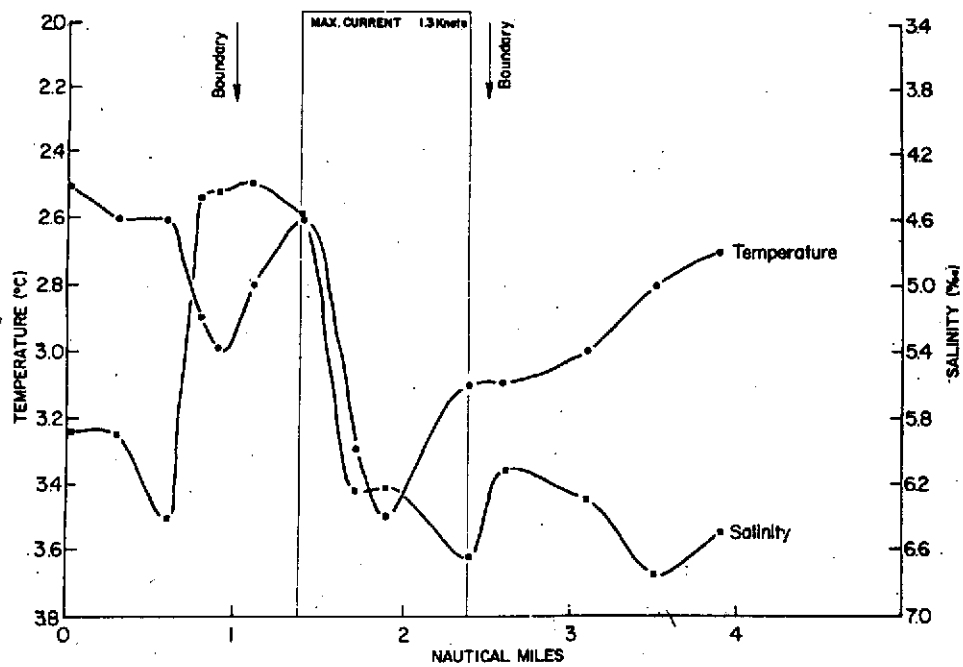


Figure 4.13 Predicted tidal currents and ERTS-1 MSS band 5 image of Delaware Bay obtained on October 10, 1972 (I.D. Nos. 1079-15133).



MICRODENSITOMETER TRACE FROM CAPE HENLOPEN, DEL. TO CAPE MAY, N. J. ERTS-1 ID. 1079-15133 (BAND 5) OCT. 10, 1972.



Whaler Transect

Bombay Hook to Cohansey River

1/26/73

Figure 4.15 Temperature salinity and turbidity gradients across frontal system.



Figure 4.16 Coastal frontal system inside Delaware Bay

ORIGINAL PAGE IS
OF POOR QUALITY

ORIGINAL PAGE IS
OF POOR QUALITY

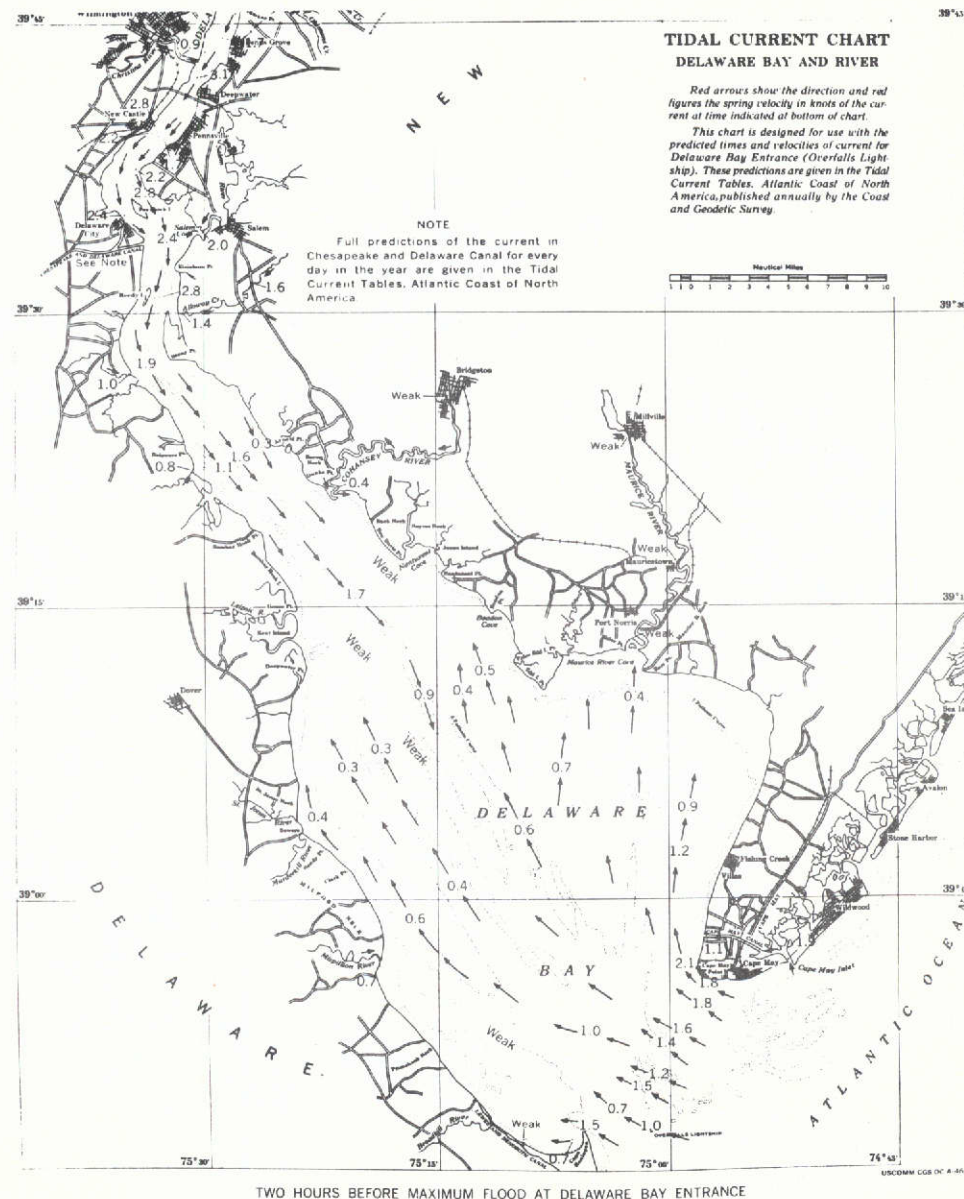


Figure 4.17 Predicted tidal currents and ERTS-1 MSS band 5 image of Delaware Bay obtained on January 26, 1973 (I.D. Nos. 1187-15140).

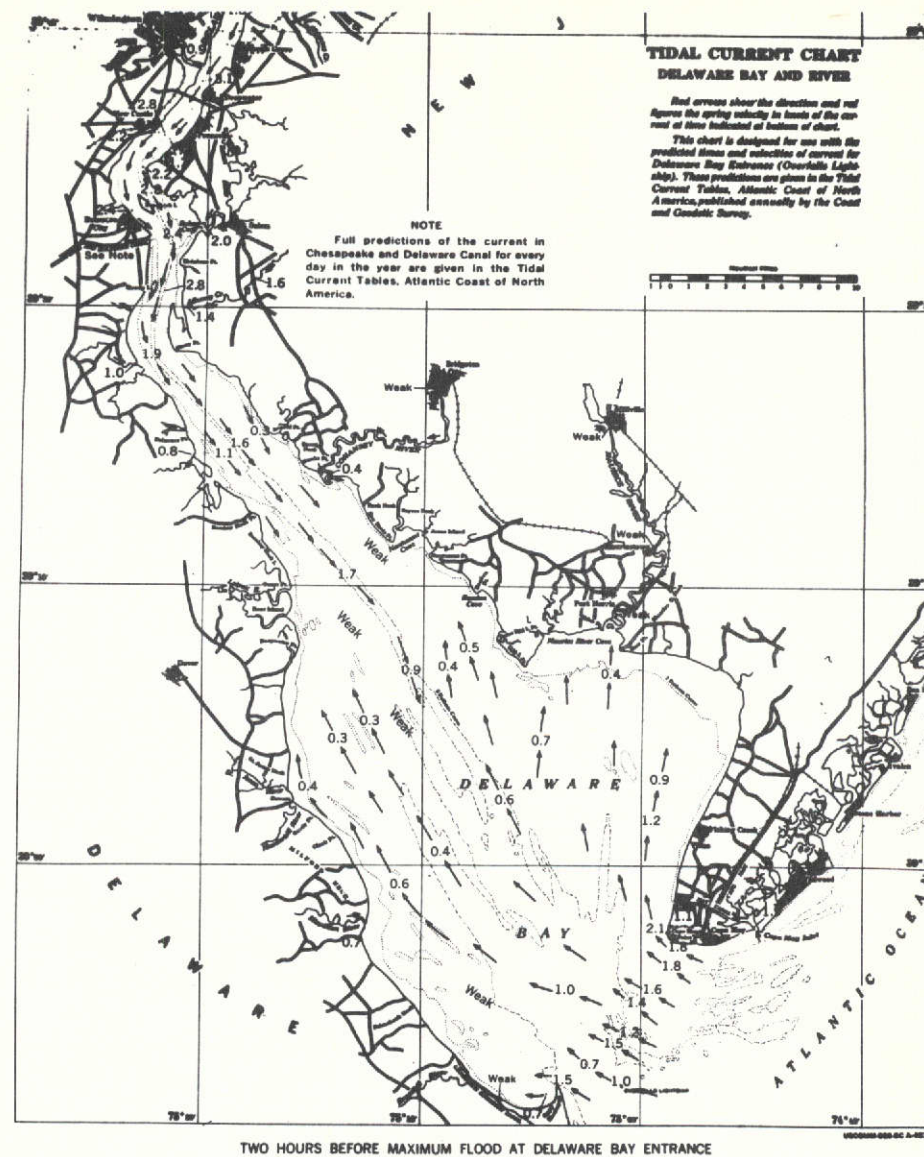


Figure 4.18 Predicted tidal currents and ERTS-1 MSS band 5 image of Delaware Bay taken on July 7, 1973 (I.D. No. 1349-15134).

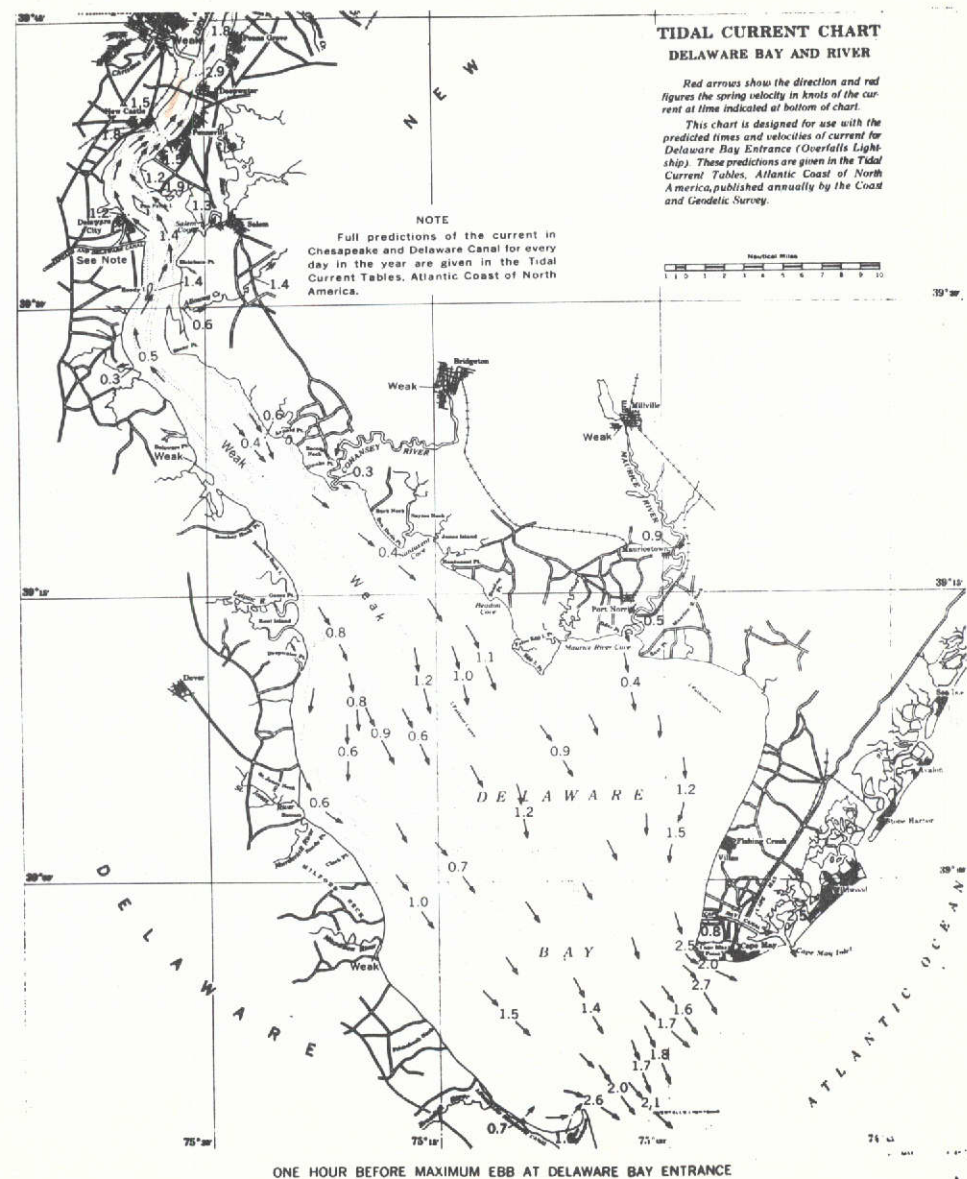


Figure 4.19 Predicted tidal currents and ERTS-1 MSS band 5 image of Delaware Bay obtained on August 12, 1973 (I.D. Nos. 1385-15131).

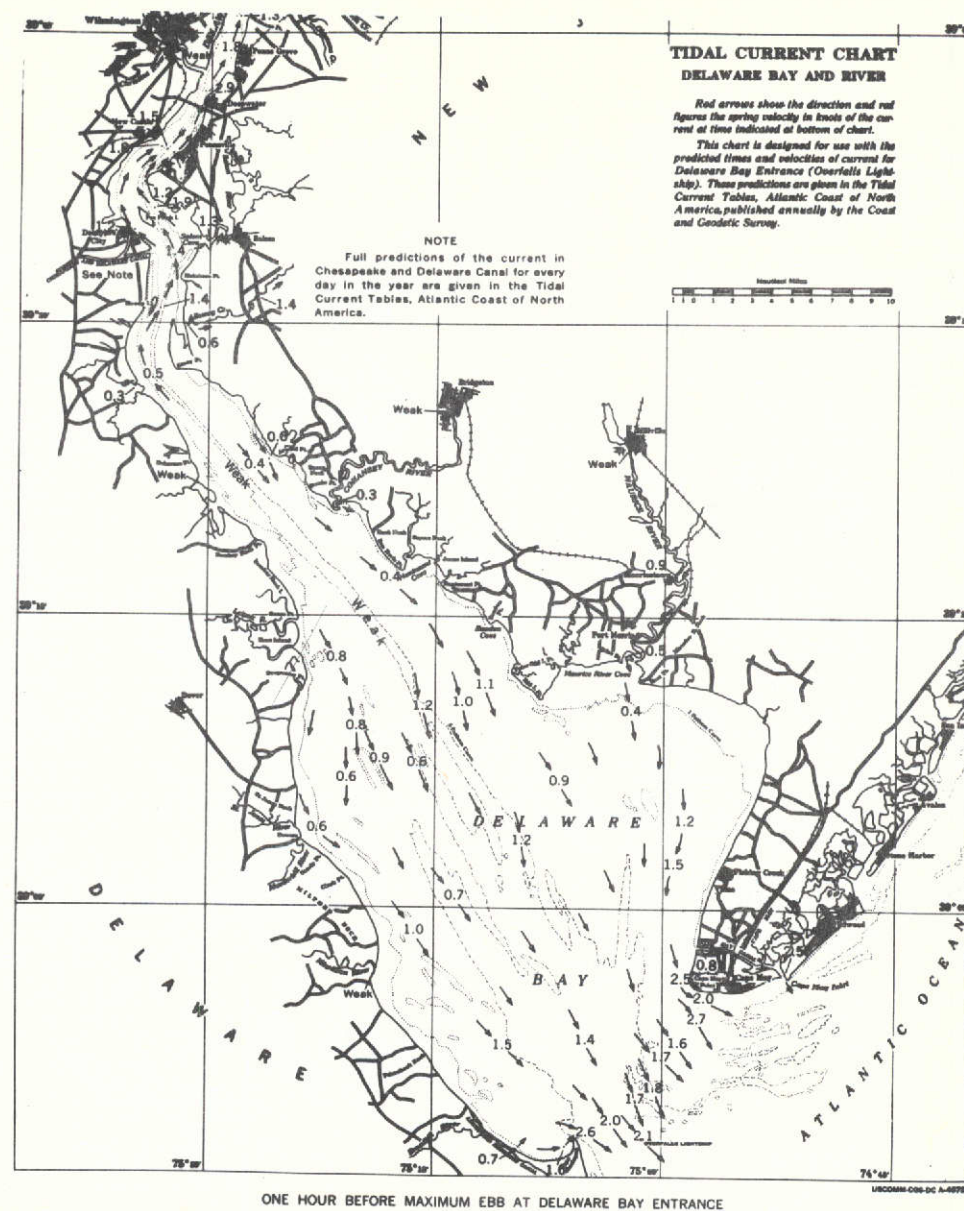
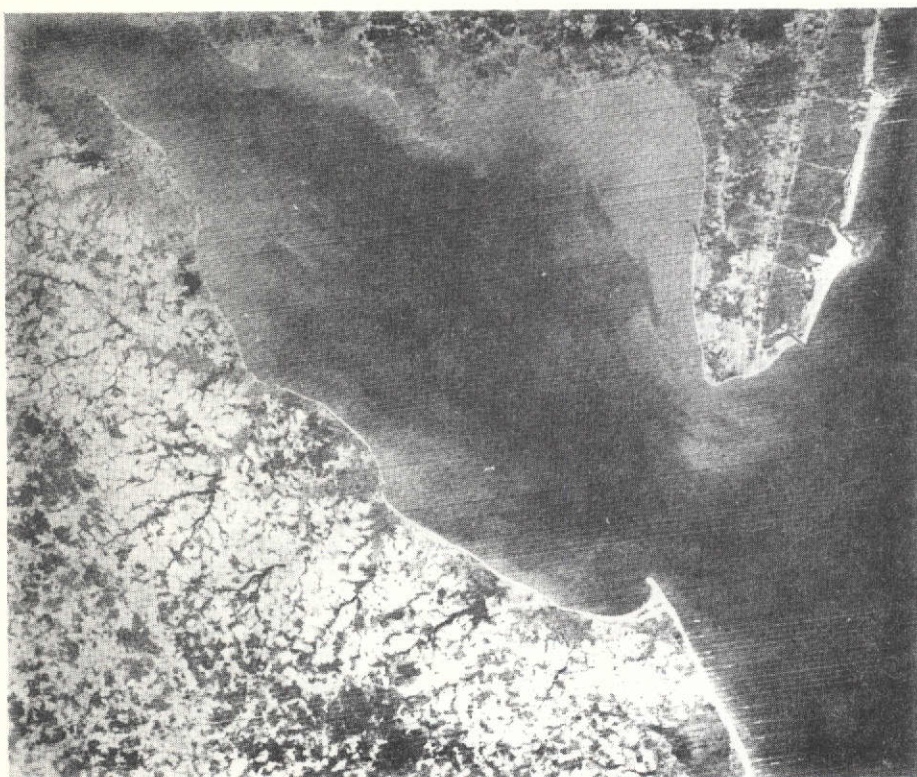


Figure 4.20 Predicted tidal currents and ERTS-1 MSS band 5 image of Delaware Bay taken on December 3, 1972 (I.D. No. 1133-15141).

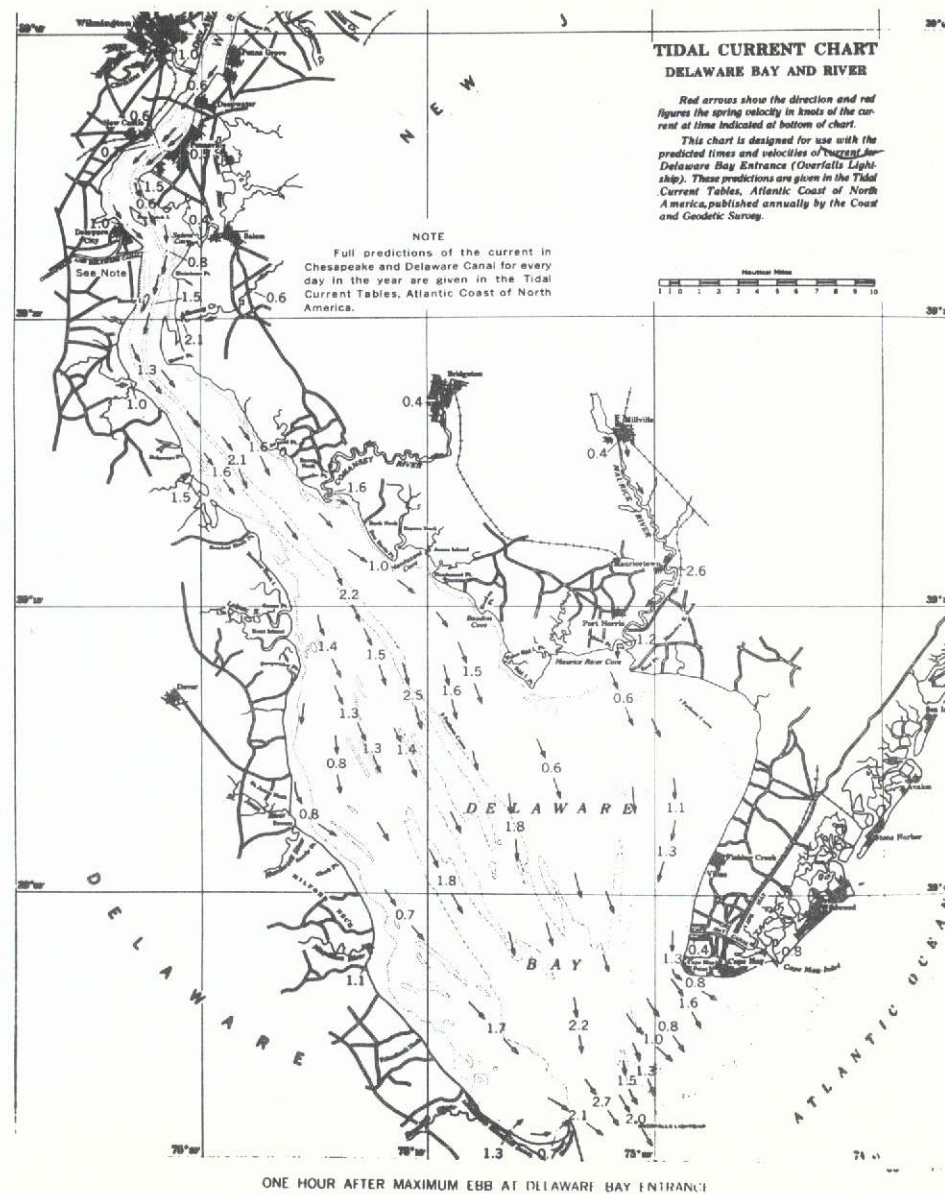


Figure 4.21 Predicted tidal currents and ERTS-1 MSS band 5 image of Delaware Bay taken on February 13, 1973 (I.D. No. 1205-15141).

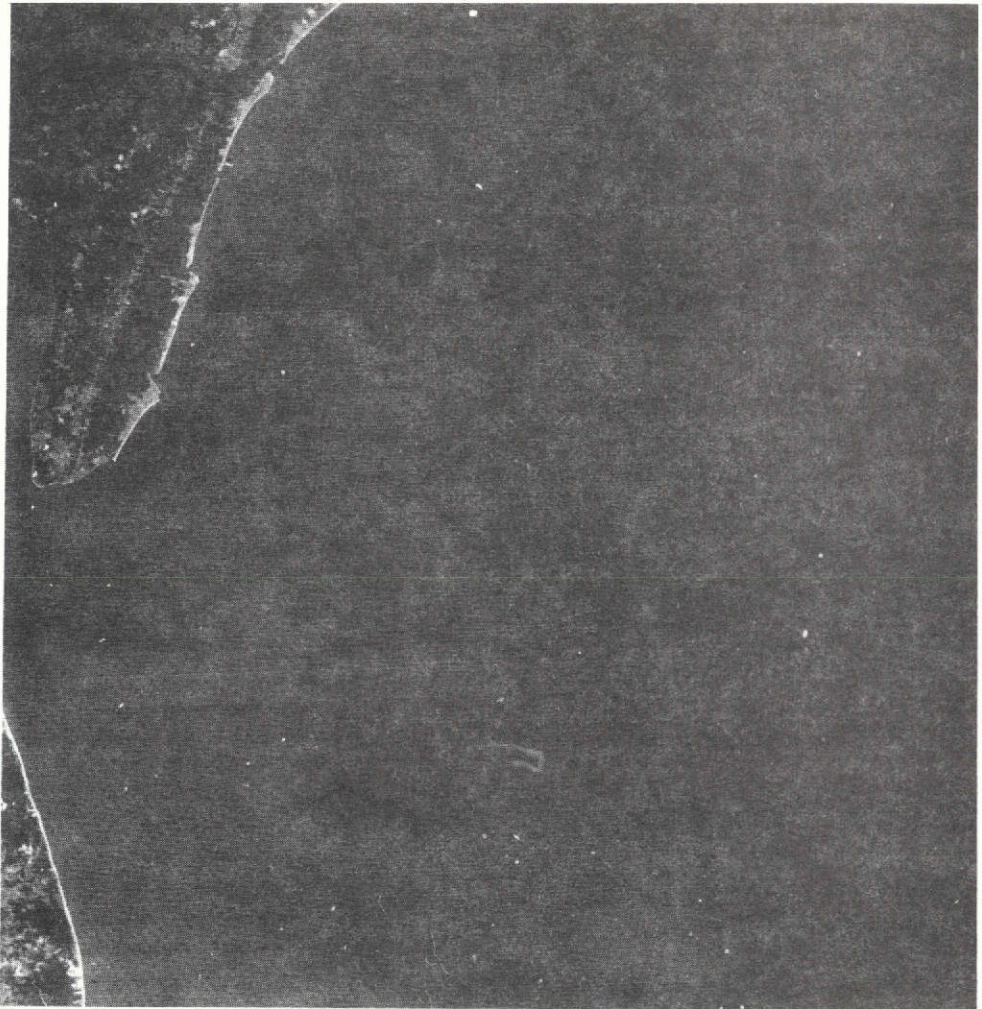


Figure 4.22 Acid waste dumped from barge about 40 miles east of Indian River Inlet appears clearly as a fishhook-shaped plume in MSS band 4 image of January 25, 1973. Due to its predominantly greenish component, the acid plume shows less contrast in band 5.

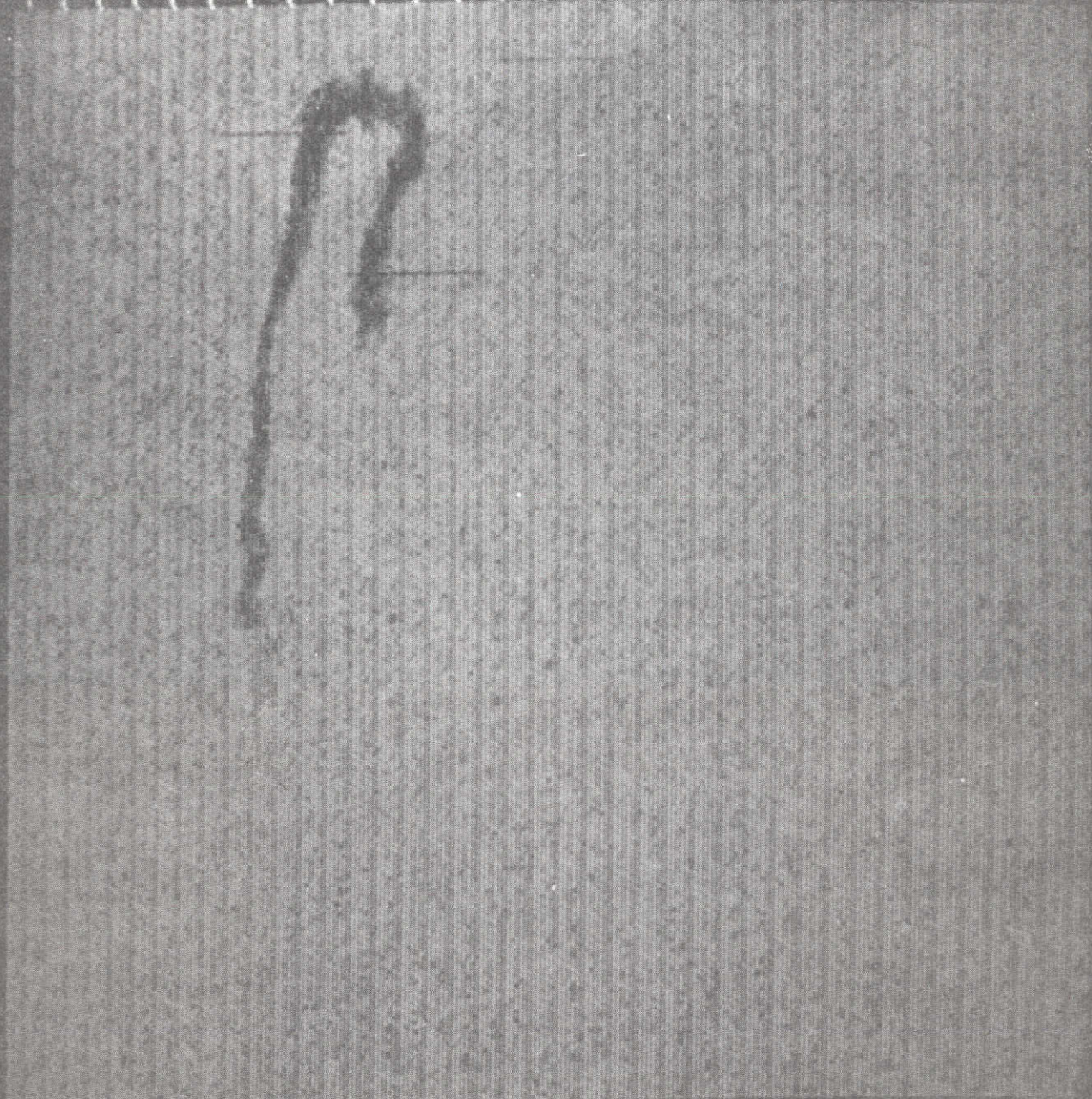


Figure 4.23 Enlarged digital enhancement of acid waste plume of
Figure 4.22.

ORIGINAL PAGE IS
OF POOR QUALITY

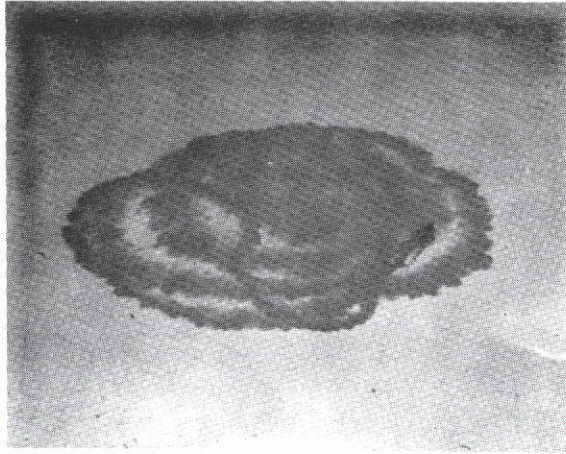


Figure 4.24 A 300-meter diameter Rhodamine WT dye patch being spread at the 8-mile offshore oil terminal site by the R. V. Delaware.



Figure 4.25 The dye patch is caught in a boundary, stretched into a long line and being carried two miles toward the bay.

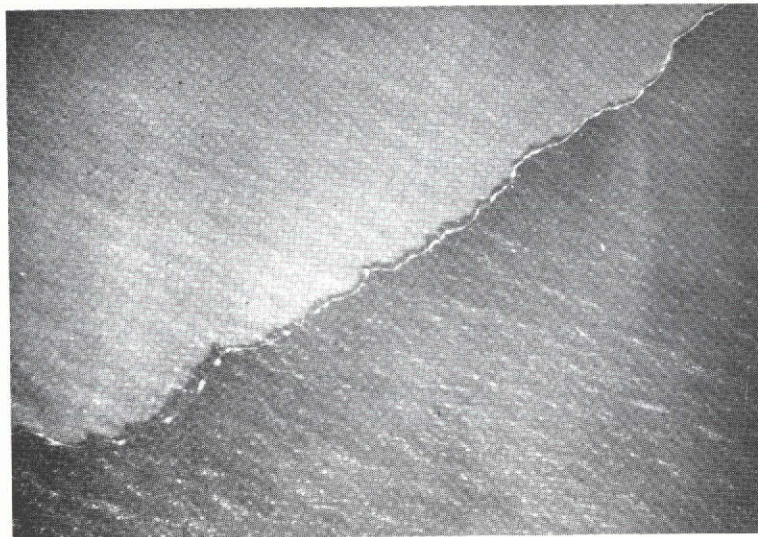


Figure 4.26 A coastal front with a foam line between two masses of different water properties observed near the proposed 8-mile offshore oil terminal site from an altitude of 3000 meters.

ORIGINAL PAGE IS
OF POOR QUALITY

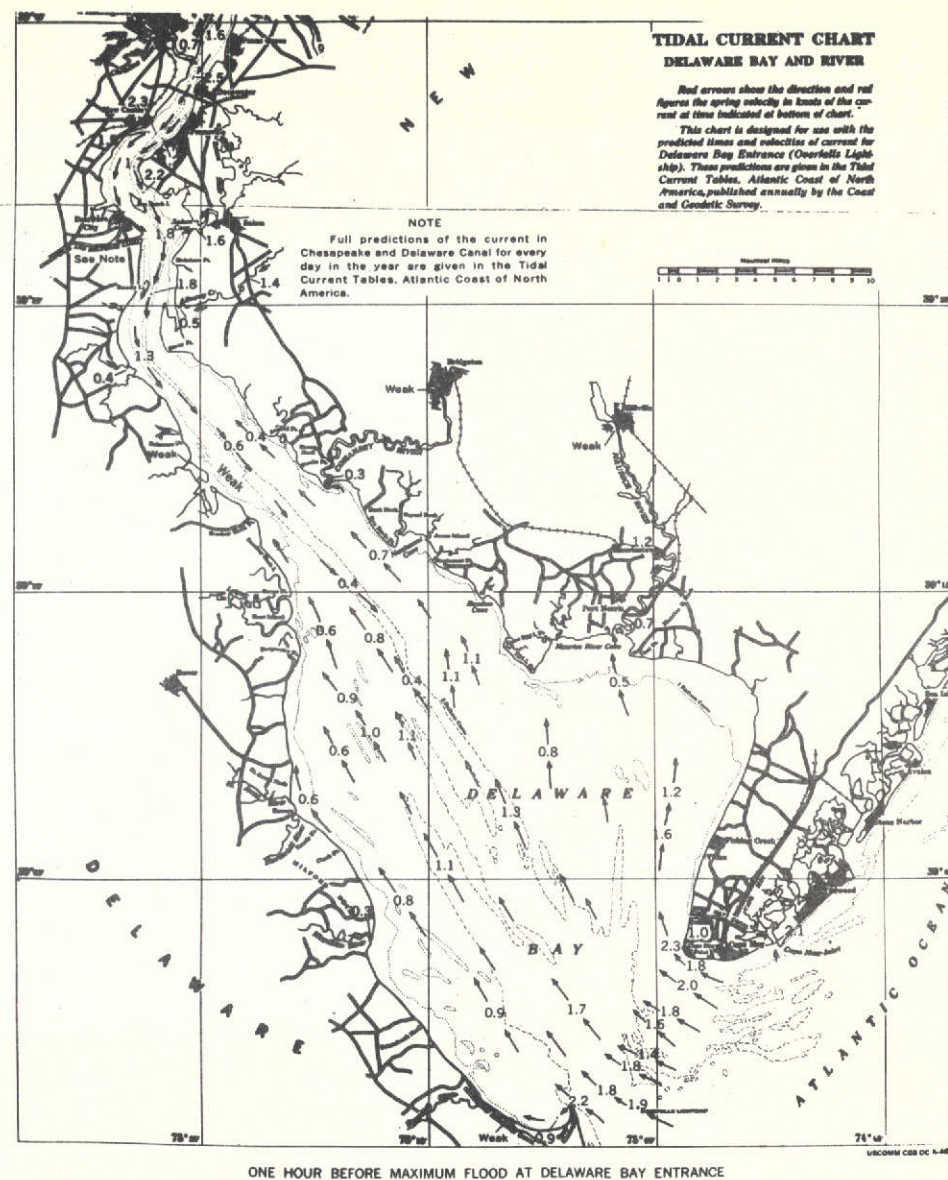
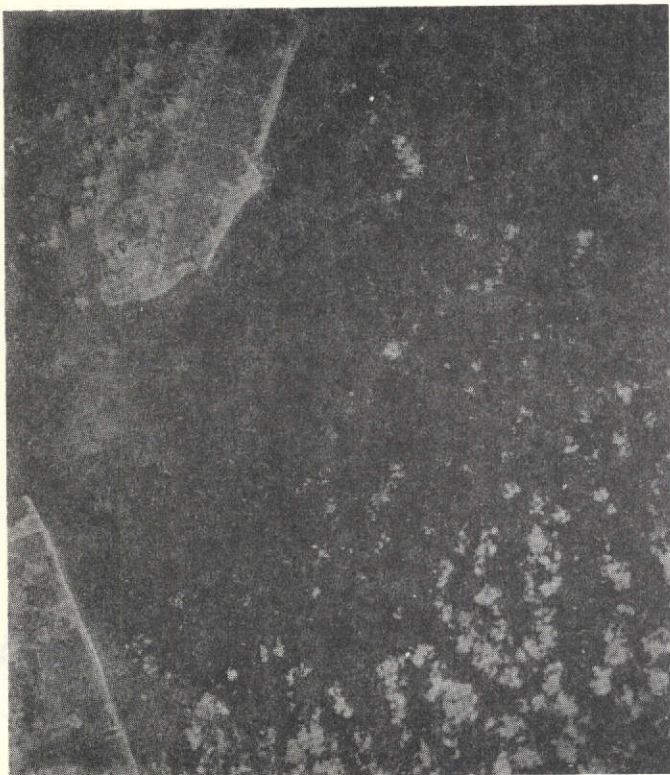


Figure 4.27 ERTS-1 image of the mouth of Delaware Bay showing several water mass boundaries and high concentrations of suspended sediment in shallow waters. (Band 5, August 16, 1972, I.D. 1024-15073).

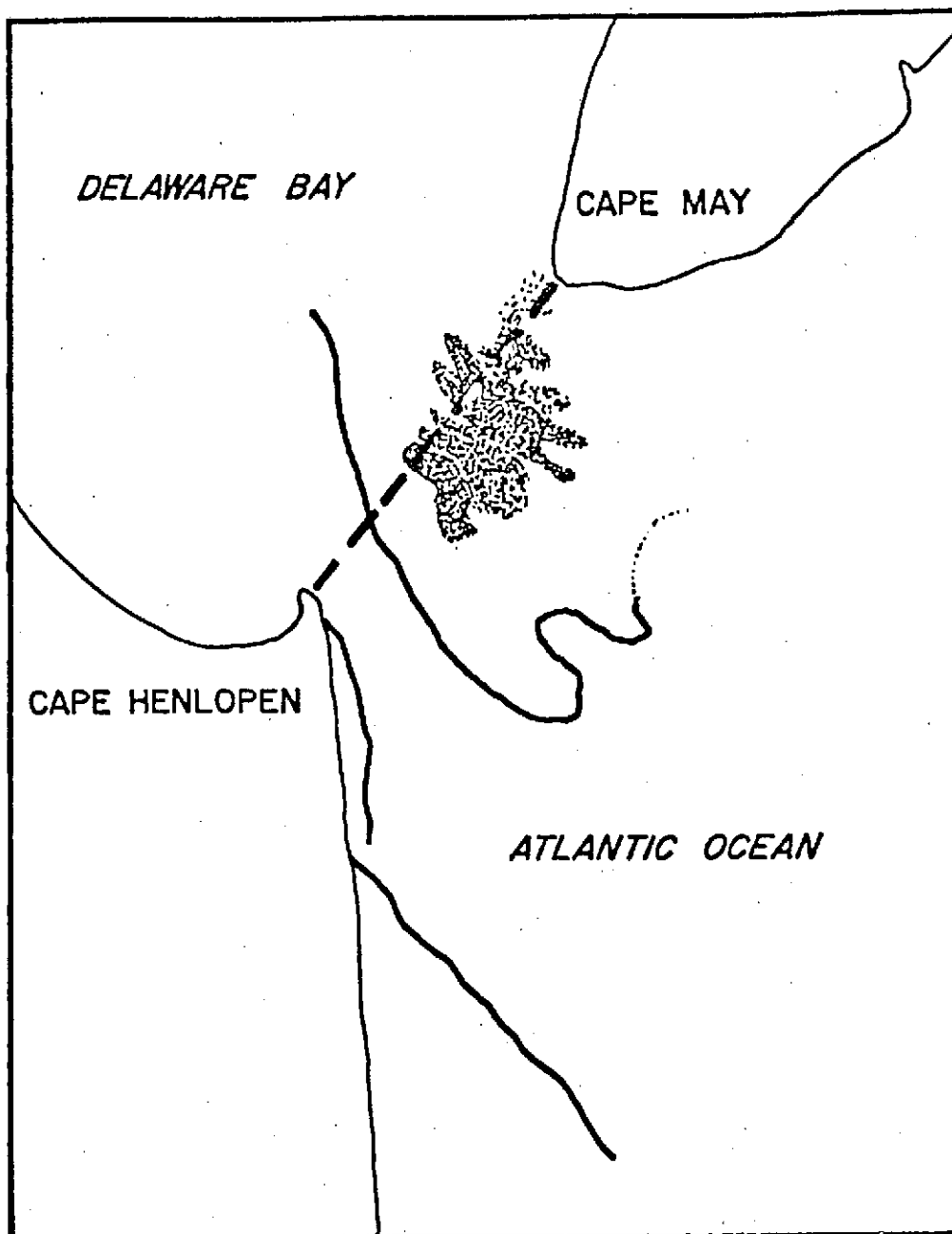


Figure 4.28 Aquatic boundaries and suspended sediment plumes identified in the ERTS-1 image of August 16, 1972, shown in Figure 4.22.

5.0 COASTAL VEGETATION AND LAND USE

5.1 Digital Data Analysis and Classification

5.1.1 Background

Present techniques for generating land-use maps are mostly manual, expensive, and time-consuming. A map is generated in several steps. If a good topographic map of the area does not exist, aerial photography is collected and the topographic map is generated, using stereo photography and a stereoplotter or orthoprinter. The land-use information is derived by either photo-interpretation of the photography, by ground survey teams, or through a combination of both. The information is then added to the topographic base to create the desired land-use map of Oakland County, Michigan, which cost \$250,000 and required two to three years to complete. These photometric mapmaking techniques are very accurate but, in high growth areas, the maps produced are usually out of date by the time the map is printed.

The same photometric techniques are now being applied by many ERTS investigators (Ref. 12) to the interpretation of ERTS imagery. As in the case of the use of aerial photography, these techniques also would be expensive and time-consuming if applied to the generation of land-use maps of large areas. Also, imagery obtained from the GSFC or EROS facilities, even though of excellent quality, may not contain all of the information being acquired by ERTS and recorded on the CCTs. Data processing techniques based on the use of this imagery (density level slicing, etc.) can only extract the information provided to them in the gray scale range, which normally varies from 12 to 16 levels.

Techniques for a faster and more economical means of interpreting ERTS data and the ready access to ERTS CCTs have led our group and a number of other organizations (Ref. 17, 18, 19) into evaluating computer target "spectral recognition" techniques as a basis for automatic target classification. These classification techniques have been under continued development at Bendix for the past 8 to 10 years, primarily using aircraft data and, more recently, using ERTS and Skylab/EREP data.

To implement these "spectral recognition" techniques, a computer is provided (trained) with a number of samples of ERTS measurements on each of the land-use categories of interest. Each MSS sample (spatial) measurement is composed of a radiance measurement in the four bands. The magnitude and variation of this radiance (or reflectance), measured as a function of band number (or wavelength), is the target "spectral characteristics" or "signature" which forms the basis for computer recognition. In the "decision-processing" mode, the probability of the spectral characteristic arising from any one of the different land-use categories of interest is computed for each spatial resolution element and a decision is reached by the computer as to the most likely target type.

Research to date in computer spectral recognition techniques has been limited to presenting the interpreted land-use data in the form of "decision imagery", either color-coded on TV or film, in which a color designates a land-use category, or in the form of a line printer output (Ref. 17, 18, 19) in which a computer symbol designates the category.

The land-use information contained within this decision imagery, to be of value for resource management, must still be geometrically corrected and transformed into a map-coordinate system. By present techniques, this is a manual, time-consuming procedure, which has been a stumbling block to automatic map making.

One of the procedures reported in this section bypasses the decision imagery/line printout stage, thereby permitting a significant breakthrough in the rate at which land-use maps can be generated. Rather than uncorrected decision outputs, the processing results in geometrically-corrected computer-driven pen drawings of land-use boundaries. The boundaries are drawn on a transparent material at a map scale specified by the operator. The overlays are placed over a base map to obtain an immediate correlation between land cover boundaries and map coordinates.

5.1.2 Earth Resources Data Center

Computer software, techniques, and procedures used to transform ERTS CCTs into the land-use maps and the data used in this report were developed in the Bendix Earth Resources Data Center.

The nucleus of this center is a Digital Equipment Corporation PDP-11/15 computer with 32K words of core memory, two 1.5 M-word disc packs, two 9-track 800 bpi tape transports, a line printer, a card reader, and a Teletype unit. Other units are an Ampex FR-2000 14-track tape recorder; a bit synchronizer and tape deskew drawers which can reproduce up to 13 tape channels of multispectral data from high-density tape recordings; a high-speed hard-wired special-purpose computer for processing multispectral data; a 70-mm laser film recorder for recording imagery on film; and a color moving-window, computer-refreshed display.

5.1.3 Locate Training Areas

The first step in the development of the Delaware Coastal Land-Cover map was to locate the CCT and the coordinates, in terms of resolution element number and scan line count number, within the CCT of the areas that best typify the land-cover target categories of interest, the "training areas".

5.1.4 Locating CCT

To identify the CCT containing the training areas, the ERTS scene provided by NASA is divided into four equal quarters in the vertical direction (North to South). Each quarter represents the area covered by one of the four CCTs. CCT number one produces the leftmost quarter, number 2 produces the scene next from the left, etc.

5.1.5 Screening Imagery

The all-color composite and black and white images provided by NASA were used in identification and location of training areas.

To define the location of the training areas still further, the CCT containing the areas of interest are screened on the color-coded TV monitor. To facilitate viewing, the ERTS band having the best target-background contrast is chosen and displayed. The signal range of interest within this band is generally sub-divided into 16 parts and displayed in 16 distinctive colors, i.e., color-sliced. The investigator can specify the signal amplitude and range into which the 16 colors are assigned.

5.1.6 Gray-Scale Printouts

When the test site of interest appears on the TV monitor, the CCT is stopped and the scene is mapped out by the line printer (Figure 5.1). The

area shown on the TV monitor and the gray-scale printout is approximately six miles wide.

The training areas are identified in the gray-scale printout, and their locations are recorded. Some of the training sets selected for the development of the Delaware Coastal Land-Cover map are marked on the Band 7 printout shown in Figure 5.1. Training areas should contain at least 25 elements or more. A number of small areas, consisting of the same type of target material, can be combined in the computer to construct a training sample of the desired size.

The locations of the training areas within the ERTS scene are conveyed to the computer by the investigator, using the resolution element number and scan line number of the upper-left and lower-right corners of each training area. These numbers are determined from the gray-scale printouts, as shown in Figure 5.1, where the scan line count numbers are the numbers running vertically down the page in the left-hand margin and the resolution element numbers run horizontally across the page.

5.1.7 Develop Target Characteristics

Inputting the training area coordinates (boundaries) to the computer permits the ERTS spectral measurements within these boundaries to be extracted (edited) from the CCTs and placed into computer disk files. One file is established for each different land-use category. The data in each file is then processed to obtain a numerical descriptor to represent the spectral characteristics of each land-use category of interest. The descriptors presently include the mean signal and standard deviation for each band and the co-variance matrix taken about the origin, which includes the four MSS bands.

5.1.8 Evaluate Target Characteristics and Classification Techniques

Once the numerical descriptions which define the spectral characteristics of each land-use category of interest are determined, the operator executes the "canonical analysis" program. This program, which has been reported previously (Ref. 20), derives, for each land-use category being sought, a set of "canonical coefficients". In the decision-processing phase discussed later, these coefficients are used by the computer to form a linear combination of the ERTS measurements to produce a "canonical variable" whose amplitude is

associated with the probability of an ERTS measurement being from the target sought. A set of canonical coefficients are derived for each land-use category of interest.

In decision processing, the probability of an ERTS measurement arising from each one of the different land-use categories of interest is computed for each ERTS spatial resolution element, and a decision is reached based on these computations. If all probabilities are below a threshold level specified by the operator, the computer is permitted to decide that the target viewed is unknown (a category undefined).

Before producing decision data on a complete ERTS CCT, a number of tests are applied to evaluate the computer's capability of performing the desired land-use classification.

5.1.9 Canonical Printout

Several tests are included in the printout provided by the "Canonical Analysis" program shown in Figure 5.2. The "Eigen Values" provide a measure, in each of the four canonical variables, of the separability of that target group (in this case #2 - Spartina alterniflora) from the background in general. Eigen values greater than 1.0 generally mean that good separability is being obtained - the value of 484.156 for target group #2 is excellent. If an "Eigen Value" of less than 1 were obtained the classification would not proceed until the training set selection or classification scheme resulting in that low value had been re-evaluated.

The "Contribution" provides a tabulation of the effect data from each of the four bands has on separating the target category from the background in each of the four canonical variables. In Figure 5.2, for instance, it can be seen that in the first (and most significant) canonical variable, band 5 had the greatest effect on signature characterization followed by bands 7, 4, and 6 in that order.

Finally, the "Canonical Variables Evaluated at Group Means" provides a measure of the separability obtained between the target group specified (#2) and each of the other target groups individually. Any value greater than one or less than negative one in the first two canonical variables indicates good separability. In Figure 5.2 it can be seen that separability is very good as expected from the very high "Eigen Value". In the case of a marginal

"Eigen Value" the "Canonical Variable . . . , etc." printout is used to identify those categories with which signature overlap is occurring.

5.1.10 Classification Accuracy Tables

Another test of the canonical coefficients is to proceed to use them in the decision processing but to limit the data processed to that which is well known, i.e., the training data which was previously edited and stored on the disk file. Processing this data and keeping an accurate record of decisions permits the computer printout shown in Table 5.1 to be developed.

The table provides the investigator with a quantitative measure of the classification accuracy achieved by the canonical coefficients in decision processing. In the case illustrated here, training set two, Spartina alterniflora, is classified correctly as Spartina alterniflora 97.5% of the time and is mistaken for bare mud 2.5% of the time. Such confusion is to be expected as S. alterniflora is a wetlands plant and one would expect patches of bare mud to be associated with wetlands, including the area in which the training data set was located.

5.1.11 Classifications on a TV Monitor

A final test of the canonical coefficient is to play back the ERTS CCT and to assign the computer decision to a color code which is displayed to the investigator on the TV monitor. By viewing the computer decisions on areas where ground truth is available, the investigator can rapidly determine the effectiveness of the decision processing.

5.1.12 Produce Decision Data Products

When the investigator is satisfied with the accuracy of the decision processing, the canonical coefficients are placed into the computer disk file and are ready to process the full ERTS CCT, portions of the CCT, or other CCTs within the same ERTS scene. It has also been established by Chase and Reed (Ref. 21) that the coefficients can be successfully applied to adjacent scenes of the same orbit. Decision products, produced for this investigation, included printouts giving the area covered by each land-use category, decision imagery, and decision map overlays. Each of the decision products are briefly discussed in the following sections.

5.1.13 Decision Data

The canonical coefficients defining each of the ten land-cover categories was applied to process the CCT's covering the Delaware Bay area. The first step in the decision processing resulted in a new or processed CCT, wherein each ERTS spatial element contained a code designating one of the ten land-use categories, and the computer generated the area measurement table shown in Table 5.2. The area measurement printout identifies each of the land-use categories of interest and the area covered by each category in terms of percent of total area processed, acres, and square kilometers.

5.1.14 Decision Imagery

The tape produced from decision processing was used to generate 70-mm imagery wherein each image shows only a specified land-use category at a scale of 1:1,000,000. This imagery is geometrically (spatially) identical to the data on the decision CCT and on the CCT provided by NASA from which it was produced. Since the NASA tape is from bulk processing, some geometrical errors exist and are carried over into the decision imagery. Also, the CCT data provided from the NASA bulk processing is not corrected for Earth rotation; consequently, the decision imagery will not directly overlay a UTM map coordinate system.

The 70-mm decision imagery forms the basis for additional image products that include decision overlays, wherein each target is color-coded and provided on a transparent overlay, and color-coded decision imagery, a composite of all targets on one image wherein each target is assigned a distinctive color. Some of these are briefly illustrated in the following section.

Figure 5.3 shows a black and white version of the color-coded thematic map for the six most important ecological communities and cover types. The other four are not included because the use of black and white restricts the number of differentiable categories which can be displayed on one map - the color product does show all ten categories. Note that, in the decision color-coded image, two types of information are presented to the investigator: the color code decision based on the spectral information content of the ERTS MSS measurements within each individual resolution element, and the spatial information, geometrical or contextual, preserved to aid the user in interpreting the land use.

5.1.15 Decision Map Overlays

To produce decision-map overlays, the decision-processed data tape is transformed into a CCT whose data are the land cover boundaries. The boundary locations are geometrically corrected for Earth rotation and other geometric distortions and are in a format capable of driving either a Cal Comp or Gerber plotter. This tape, when played back on the computer, causes the geometrically corrected pen drawing to be produced for each land-use category at a map scale specified by the investigator.

Figure 5.4 is the computer-driven pen drawing of the deep and shallow water boundaries at a scale of 1:24,000 produced on a transparent overlay material. Similar overlays have been produced for scales ranging from 1:24,000 to 1:1,000,000 and for various land-use categories. The map beneath the overlay, is a 1:24,000 USGS topographic map. The overlay placed over the base map provides an immediate correlation between land-use boundaries and map coordinates. The overlay technique is particularly useful when the task at hand is to update the base map and our interest is primarily on detecting and identifying changes, i.e., change detection, between the base map and ERTS data.

5.2 Coastal Vegetation and Land-Use Mapping

5.2.1 Background

Work carried out over the past two years at the University of Delaware indicated that the coastal zone of Delaware and, in particular, the extensive tidal wetlands found there, offer a unique opportunity to evaluate ERTS-1 sensing capabilities and the feasibility of using digital processing techniques to map and inventory coastal vegetation and land use. Major vegetation species found in the tidal wetlands have been shown to be easily distinguished on the basis of reflectance characteristics in aerial photography (Refs. 1, 22, 23) and it was thought that the same characteristics could be used to map the wetlands and other types of cover using ERTS-1 data. Analysis of ERTS color-composite images using analogue processing equipment confirmed that all the major wetlands plant species were distinguishable at ERTS scale (Ref. 24). The superior spectral resolution of the CCTs as compared with single band or composite imagery promised that good discrimination could be achieved through digital analysis of the CCTs (Refs. 24, 25) with the added advantage of rapid production of thematic maps and data.

5.2.2 Results

The primary objective of the analysis was to map and inventory the significant ecological communities of Delaware's coastal zone. To this end, ten vegetation and land-use discrimination classes were selected as follows:

1. Forest Land
2. Phragmites communis (Reed Grass)
3. Spartina patens and Distichlis spicata (Salt Marsh Hay and Spike Grass)
4. Spartina alterniflora (Salt Marsh Cord Grass)
5. Cropland
6. Plowed Cropland
7. Sand and Bare Sandy Soil
8. Bare Mud
9. Deep Saline Water
10. Sediment-laden and Shallow Saline Water

As stated in the previous section, data output may take a variety of forms - each useful to the resource or land-use planner. The results of analysis may be shown on a color-coded, thematic photo-output which displays the prominent types and patterns of land cover and water masses at scales of approximately 1:1,000,000. These color products may be produced in map form or as a series of color overlays, each showing no individual category. The excellent cartographic quality of ERTS-1 data makes these photo-products virtually equivalent to small-scale maps allowing precise evaluation of growth and degradation over time on a regional basis. Figure 5.3 shows a black and white version of one such map.

Cal Comp or Gerber digital plotters may be used to produce thematic outputs at scales considerably larger than are available in color-photo products. Plots of category boundaries at scales from 1:95,000 up to 1:24,000 have been produced and found to retain excellent cartographic quality within the resolution limits of the scanner imagery. Figure 5.4 shows a Cal Comp plot of water boundaries in the Cape Henlopen, Delaware area, overlayed onto the USGS 7-1/2' quadrangle of the same area. Note that while the resolution capability of the data is strained, it still retains good spatial relationship to the map, notably along the Lewes-Rehoboth Canal in the lower left portion of the figure. While plots at such a large scale may not be of great value, they do imply that data at smaller scales will provide cartographically reliable and accurate land-use data.

The boundary mapping has great potential in change detection. The water boundary printout in Figure 5.4, for instance, shows two water bodies in the lower right corner which are not shown on the USGS topographic maps. These areas were flooded with fresh water since the topographic maps were produced. Also shown in Figure 5.4 is a significant North-westward extension of the tip of Cape Henlopen which has occurred since the 1972 photo-revision of the topographic map. Such extension has been documented by geologists (Ref. 26) and is thought to have been occurring at an accelerating rate since 1910. The present rate of accretion is certainly large enough for the change from 1972 to the date of the ERTS data (1973) to be recorded. The potential for monitoring large scale erosion and accretion phenomena such as this appears great.

Finally, the results of analysis may be outputted in tabular form, showing the percentage of the total scene occupied by each category and the number of acres of square kilometers encompassed by each category (Table 5.2). Again, large-scale changes in distribution of cover types could be monitored through time using this capability.

5.2.3 Discussion and Evaluation of Results

Data obtained through analysis of ERTS CCT's has been compared with information from a variety of other sources in an attempt to evaluate the accuracy and reliability of the man-assisted, automatic classification system described in Section 5.1.

Table 5.3 shows a comparison of percentage of area covered by three categories obtained from the ERTS classification (Table 5.2) with percentages for the same categories obtained from the "Delaware Natural Resources Inventory" (1970) (Ref. 27). Percentages rather than the actual area measurements themselves were used because the 1970 State Inventory is limited to the political boundaries of the State of Delaware while such a restriction was not possible with the ERTS data. Therefore area measurements were not directly comparable and percentages were used instead. Recently, equipment updates by Bendix have made it possible to restrict analysis to any specified region within an ERTS tape which means that, in the future, direct comparison of area figures will be made. The ERTS percentage figures shown in Table 5.3 differ from those in Table 5.2 because they have been corrected by excluding areas encompassed by the ERTS water categories in order to make the results directly comparable to the State Inventory which does not include water.

Table 5.3

<u>Category</u>	<u>% of ERTS Scene</u>	<u>% of State Inventory</u>
Forest land	34%	31%
Wetland	14%	10%
Cropland	47%	36% (1964)

Agreement between the ERTS analysis and the State Inventory appears good, particularly in the Forest and Wetland categories. The divergence in the Cropland category probably results from differences in the way in which Cropland is defined in the Inventory or from the age (10 years) of the State data for this category. Evidence that accuracy for ERTS classification of Cropland is quite good is given later.

The classification accuracy table (Table 5.1) predicts good accuracy in classification of most categories: accuracies of greater than 90% for Spartina alterniflora (Salt Marsh Cord Grass), Phragmites communis, bare sand, cropland, (the four subcategories of cropland are combined and accuracies averaged), plowed cropland, bare mud and all water categories. Spartina patens (Salt Marsh Hay) shows a classification accuracy of 85%. Forest land shows an accuracy of 83% with all confusion occurring with the industrial category which was deleted in the final analysis for lack of an adequate training area. Thus, one would expect higher accuracy values for Forest Land and there is evidence of this shown later.

The accuracies calculated and shown in the "Classification Accuracy Table" (Table 5.1) become much more meaningful when the ERTS results are actually compared with known sites on the ground. The "Classification Accuracy Table", after all, is based only on the computer's knowledge of the scene. It is conceivable that a training area could be completely mislabeled, but the computer analysis would show good classification accuracy if that training set was spectrally distinct enough not to be confused with other training sets. Furthermore, the computer accuracy calculation is based only on the training areas and does not necessarily indicate the accuracy of classification in other areas. For these reasons, a quantitative comparison of ERTS classification results with two other sources of data, at two different scales, was performed. The two sources were the USGS - CARETS land-use map at a scale of 1:133,000 (reduced from a scale of 1:100,000) and a 1:60,000 NASA-RB57 aerial photograph. The CARETS map was compiled from photos taken in 1972 and the RB57 photo was taken in 1970. Because of the time separating these data from the ERTS overpass, the ephemeral, tide-dependent category of Bare Mud was eliminated from the comparison. Also, plowed cropland and cropland were combined into a single "Agricultural"

category for purposes of comparison, as were the two water categories. Previous work indicated that significant changes in the other categories would not occur in the intervening time. In any case, more recent land-use data was simply not available when the analysis was performed. Future attempts at this type of analysis hopefully will include concurrent ground data but acquiring such data over a large area is a difficult and time consuming task. It was thought that error analysis with the data was better than no such analysis at all. Phragmites communis and Bare Sand were not included as neither were present in the areas used for comparison. In addition, the Spartina alterniflora and Spartina patens categories were combined for comparison with the CARETS map since these maps have a Wetlands category with no species differentiation. In both cases grids were used to quantify the comparison with the grid size chosen as the finest usable pattern compatible with each scale. Thus, a grid size of .25cm (each grid representing approximately 22,500 m² on the ground) was used on the 1:60,000 photo while a finer grid size of .1cm (each grid representing 17,690 m² on the ground) was used on the 1:133,000 CARETS map. These compare with an area on the ground of approximately 10,000 m² for an ERTS pixel.

At 1:60,000, 1811 points were compared covering an area of 40.75 Km² while at 1:133,000, 8130 points were compared, covering an area of 145 Km². In both cases, the areas compared were chosen not to include areas used as training sets.

The results of comparison are shown in Table 5.4 and 5.5, presented in the same format as Table 5.1. At 1:133,000 the accuracy for Agriculture is quite good and similar to that predicted by averaging the cropland values in Table 5.1 indicating that the training sets selected were representative of the category desired. The Wetlands classification accuracy is greater than that predicted by Table 5.1, probably due to the combining of the two wetlands species differentiated by ERTS into one category. Forest accuracy is 81.5% with all confusion occurring with Agriculture, a condition which, it was observed by comparing CARETS maps with photos, is partially caused by the classification on the CARETS maps of small patches of trees within an agricultural area as agriculture. Thus the true accuracy of Forest classification is probably closer to that shown in Table 5.4 (89.9%). The low accuracy of the water classification due to confusion with urban areas is puzzling but might be caused by registration problems between the ERTS

image and the map. Evidence for this lies in the fact that accuracy values for water are also depressed in Table 5.5 with confusion occurring with two more, very different categories (S. alterniflora and S. patens). In other words, it appears that confusion is occurring randomly with whatever category happen to be geographically adjacent to the water.

At 1:60,000 the accuracies are generally higher than at 1:133,000 due perhaps to the relatively larger grid size used and to the fact that original photos rather than maps were used for comparison. As was discussed earlier, even at larger scales, the automated ERTS mapping often makes finer distinctions than a human photo-interpreter is willing to make. Thus, areas which the CARETS interpreters considered too small to distinguish are actually picked up in the ERTS analysis. This was observed to be the case with the Forest Land and thus the higher value for that category (and perhaps some of the others) seen in Table 5.5. The confusion between S. alterniflora and S. patens if not predicted spectrally by the computer analysis and so, while it is tempting to assert that mixed stands of the two included in training sets are responsible for the confusion (in fact such mixed stands rarely occur over a large area) it is more likely that registration errors between these always adjacent plant communities are the problems. It should also be noted that, as predicted in Table 5.1, there is confusion between S. patens and Agriculture. This almost certainly reflects a natural situation of signature overlap between S. patens (commonly called Salt Marsh Hay) and hay and fallow fields classified as Agriculture.

In general, the accuracy of classification of ERTS data appears quite good. Those categories compared in Tables 5.4 and 5.5 show good correlation and there is no reason to believe that bad results are being obtained in any other categories, particularly such spectrally distinct categories as Bare Sand and Mud. Visual comparison of classified imagery with known sites definitely tends to conform to the feeling that accuracies obtained for those categories not included in the quantitative study are not significantly different from those predicted on the basis of signature comparison in Table 5.1.

One significant obstacle to more accurate classification which appears to have a technical solution is contained in the present use of training sets in training the computer. Problems with mixtures of several categories inadvertently included in a training area, or the inability to find a large enough homogenous area to serve as a good training set are responsible for many

classification errors. The alternative is to use absolute reflectances of the desired targets, a procedure which would not only enhance classification accuracy but would also greatly increase the automated component and thus the speed of the classification procedure. In order to use absolute reflectances, a means must be found to correct the ERTS measurements for atmospheric and sun angle effects. Just such a means has been developed by Bendix (Ref. 28) and is currently in the early stages of testing in the Delaware Bay.

5.2.4 Conclusions

Digital land-use analysis of ERTS data shows great potential as an inventorying and planning tool on the state, regional and federal level. While resolution problems generally restrict analysis to scales smaller than 1:100,000, ERTS data has the considerable advantages of regular, frequent coverage and easy, rapid data handling. Further, the digital techniques developed for use with ERTS data can be easily applied to data at larger scales if necessary.

Land-use data can be accumulated and updated at a fraction of the time and cost of conventional techniques. The ERTS digital format allows rapid, inexpensive data handling and offers the potential for automated change detection. Data products produced are generally cartographically precise and presented in a variety of formats easily used by planners and other government officials.

CLASSIFICATION TABLE 25-JAN-74 12:21:26

REJECTION LEVEL = 0.10000 PER CENT

TRAINING SET	0	1	2	3	4	5	6	7	8	9	10	11	12	13	14	15
1	0.000	83.333	0.000	0.000	0.000	0.000	0.000	0.000	0.000	0.000	0.000	0.000	16.667	0.000	0.000	0.000
2	0.000	0.000	97.500	2.500	0.000	0.000	0.000	0.000	0.000	0.000	0.000	0.000	0.000	0.000	0.000	0.000
3	0.000	0.000	0.000	100.000	0.000	0.000	0.000	0.000	0.000	0.000	0.000	0.000	0.000	0.000	0.000	0.000
4	0.000	0.000	0.000	0.000	100.000	0.000	0.000	0.000	0.000	0.000	0.000	0.000	0.000	0.000	0.000	0.000
5	0.000	0.000	0.000	0.000	0.000	84.906	11.321	0.000	0.000	0.000	0.200	0.000	0.000	3.774	0.000	0.000
6	0.000	0.000	0.000	0.000	0.000	14.000	86.000	0.000	0.000	0.000	0.000	0.000	0.000	0.000	0.000	0.000
7	0.000	0.000	0.000	0.000	0.000	0.000	0.000	100.000	0.000	0.000	0.000	0.000	0.000	0.000	0.000	0.000
8	0.000	0.000	0.000	2.667	0.000	0.000	0.000	0.000	97.333	0.000	0.000	0.000	0.000	0.000	0.000	0.000
9	1.471	0.000	0.000	0.000	0.000	0.000	0.000	0.000	0.000	98.529	0.000	0.000	0.000	0.000	0.000	0.000
10	0.000	0.000	0.000	0.000	0.000	0.000	0.000	0.000	0.000	0.000	100.000	0.000	0.000	0.000	0.000	0.000
11	2.564	0.000	0.000	0.000	0.000	0.000	0.000	0.000	0.000	0.000	0.000	97.436	0.000	0.000	0.000	0.000
12	0.000	14.286	0.000	0.000	0.000	0.000	0.000	0.000	0.000	0.000	0.000	0.000	85.714	0.000	0.000	0.000
13	0.000	0.000	0.000	0.000	0.000	1.282	2.564	0.000	0.000	0.000	0.000	0.000	0.000	94.872	0.000	1.282
14	0.000	0.000	0.000	0.000	0.000	0.000	0.000	0.000	0.000	0.000	0.000	0.000	0.000	0.000	98.649	1.351
15	0.000	0.000	0.000	0.000	0.000	3.704	5.556	0.000	0.000	0.000	0.000	0.000	0.000	0.000	0.000	90.741

PROGRAM RUN TIME = 00:01:13

Training Set Category

- 1. Forest Land
- 2. Spartina alterniflora
- 3. Bare Mud
- 4. Impounded Fresh Water
- 5. Spartina patens
- 6. Cropland
- 7. Deep Saline Water
- 8. Bare Mud

Training Set Category

- 9. Plowed Cropland
- 10. Cropland
- 11. Sand and Bare Sandy Soil
- 12. Industrial (deleted)
- 13. Phragmites communis
- 14. Cropland
- 15. Cropland

ORIGINAL PAGE IS
OF POOR QUALITY

TABLE 5.1

TABLE 5.2

Computer Print-Out of Land Use Data Extracted from One ERTS-1 Tape

ERTS PROCESSOR	09-FEB-74	17:14:30	
ERTS SCENE ID -	1349-15134		
DATE OF SCENE -	07JUL73		
CENTER OF SCENE -	N38-50/W075-40		
SUN COORDINATES -	EL60 DEGREES		
	AZ115 DEGREES		
SPACECRAFT HEADING -	190 DEGREES		
TAPE NUMBER -	3		
STARTING SCAN LINE =	1		
ENDING SCAN LINE =	2000		
CATEGORY	PERCENT OF TOTAL	ACRES	SO. KM.
UNCLASSIFIED	0.00	0.00	0.00
FOREST LAND	27.12	491205.41	1987.83
S. ALTERNIFLORA	4.01	72567.05	293.67
WATER W/SEDIMENT	0.41	7415.00	30.01
DEEP WATER	20.44	370146.28	1497.93
S. PATENS	5.54	100319.92	405.98
CROPLAND	34.68	628073.81	2541.72
MUD	1.01	18275.35	73.96
PLOWED CROPLAND	2.59	46928.12	189.91
SAND & BARE SAND	2.36	42780.73	173.13
PHRAGMITES COMMU	1.84	33278.62	134.67
	-----	-----	-----
TOTALS	100.00	1810990.37	7328.80
PROGRAM RUN TIME =	16:40:17		

CLASSIFICATION ACCURACY TABLES DERIVED BY
COMPARISON OF THEMATIC MAPS WITH AERIAL
PHOTOGRAPHY & USGS-CARETS LAND USE MAPS

TABLE 5.4

Compared with USGS-CARETS Land Use Maps
Scale = 1:133,000

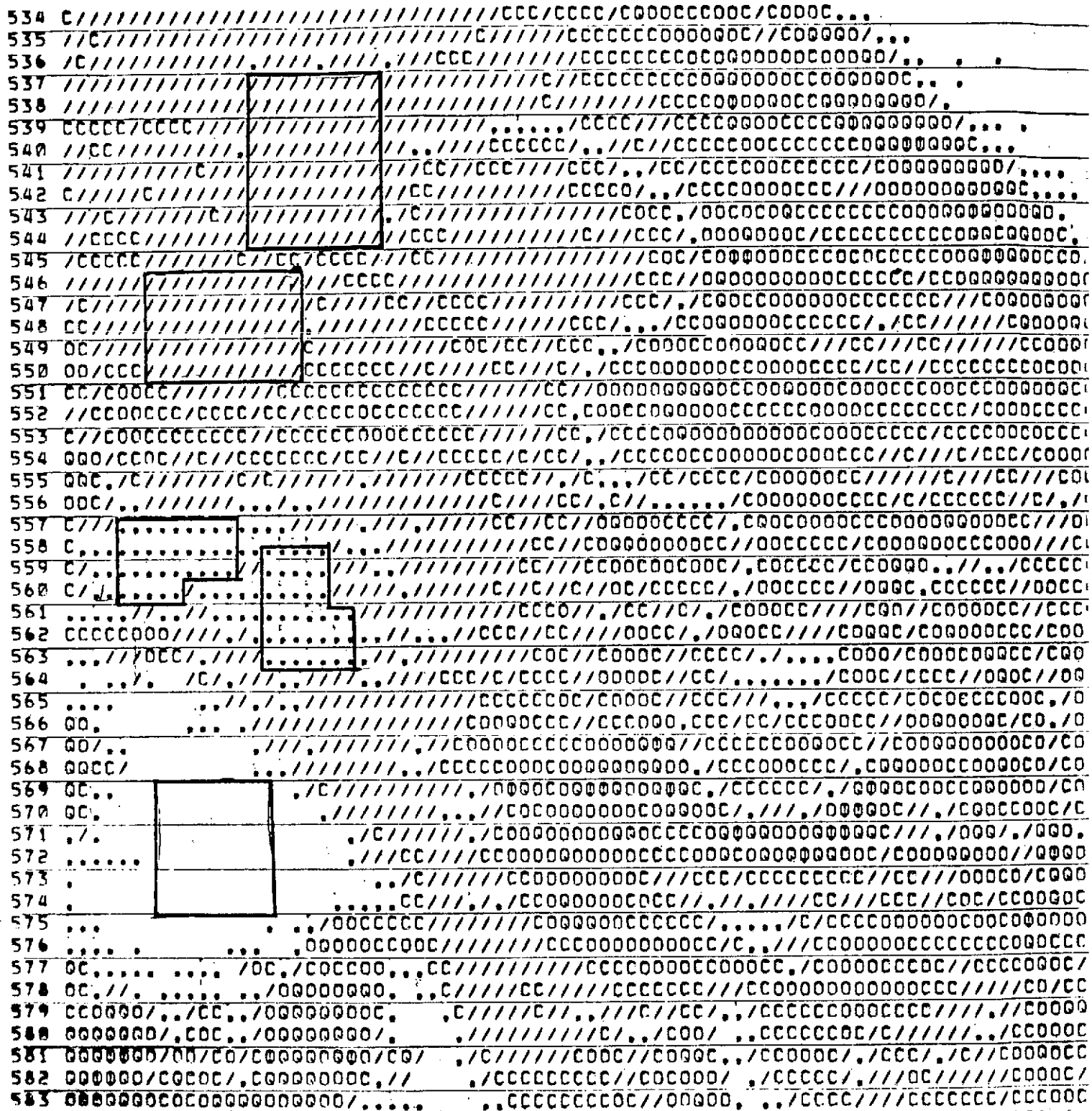
CATEGORY	Forest	Wetlands	Water	Agriculture	Urban (CARETS ONLY)
Forest	81.5%	00.0%	00.0%	18.5%	00.0%
Wetlands	00.0	97.8	00.0	2.2	00.0
Water	00.0	00.0	87.9	00.0	12.1
Agriculture	.8	00.0	00.0	90.2	9.0

TABLE 5.5

Compared with NASA-RB-57 Photography
Scale = 1: 60,000

CATEGORY	Forest	S. alt.	S. pat.	Water	Agriculture
Forest	89.9%	00.0%	4.5%	00.0%	5.6%
S. alt.	00.0	93.7	5.7	.6	00.0
S. pat.	00.0	7.7	87.0	2.2	3.0
Water	00.0	2.6	3.9	93.5	00.0
Agriculture	3.5	.3	2.1	00.0	94.1

FIGURE 5.1



Portion of grey-scale printout (ERTS band 7) showing training sets selected for:

/// - *Spartina alterniflora*

::: - Mud (tidal flats)

- Fresh water impoundment

ORIGINAL PAGE IS
OF POOR QUALITY

CANONICAL ANALYSIS: TARGET GROUP IS 2 25-JAN-74 12:17:42 Target group 2 = Spartina alterniflora
 INCLUDED VARIABLES 1(ERTS-4) 2(ERTS-5) 3(ERTS-6) 4(ERTS-7)
 MEANS(reflectance) 70.02500 50.95000 67.07500 62.65000
 STD DEV 2.39771 2.02421 3.84642 5.05741
 DETERMINANT 0.350761E 04

EIGENVALUES
 1 094.15567
 2 117.11095
 3 3.89422
 4 2.80675

CANONICAL VARIABLES		1	2	3	4			1	2	3	4
CONSTANTS		-38.835	2.034	10.327	11.222						
VAR	IVN	COEFFICIENTS				BANDS	CONTRIBUTION				
1	1	0.130	0.002	-0.230	-0.352	4	1.336	0.023	2.288	3.373	
2	2	0.368	-0.273	0.234	0.150	5	2.977	2.207	1.893	1.214	
3	3	0.049	0.088	-0.273	0.237	6	0.747	1.353	4.200	3.654	
4	4	0.113	0.092	0.204	-0.162	7	2.289	1.871	4.124	3.282	

CANONICAL VARIABLES EVALUATED AT GROUP MEANS

		WEIGHT	1	2	3	4
GROUP	1	1.000	1.723	14.069	1.844	0.793
GROUP	2	0.000	0.000	-0.000	0.000	0.000
GROUP	3	1.000	-3.322	-4.218	-0.684	0.448
GROUP	4	1.000	-11.761	-4.190	-0.476	0.804
GROUP	5	1.000	10.600	8.148	-0.931	-0.478
GROUP	6	1.000	12.144	9.872	-1.056	0.535
GROUP	7	1.000	-9.752	-7.057	-0.071	-1.072
GROUP	8	1.000	4.484	-6.921	0.560	0.093
GROUP	9	1.000	16.579	17.407	-3.322	1.236
GROUP	10	1.000	10.759	16.114	1.102	-1.006
GROUP	11	1.000	68.240	-15.036	0.397	-0.332
GROUP	12	1.000	3.742	13.258	3.181	0.455
GROUP	13	1.000	16.012	9.915	-0.804	-3.138
GROUP	14	1.000	22.381	-1.694	0.167	2.194
GROUP	15	1.000	16.026	6.390	1.044	0.923

ORIGINAL PAGE IS
 OF POOR QUALITY

Canonical analysis printout

FIGURE 5.2

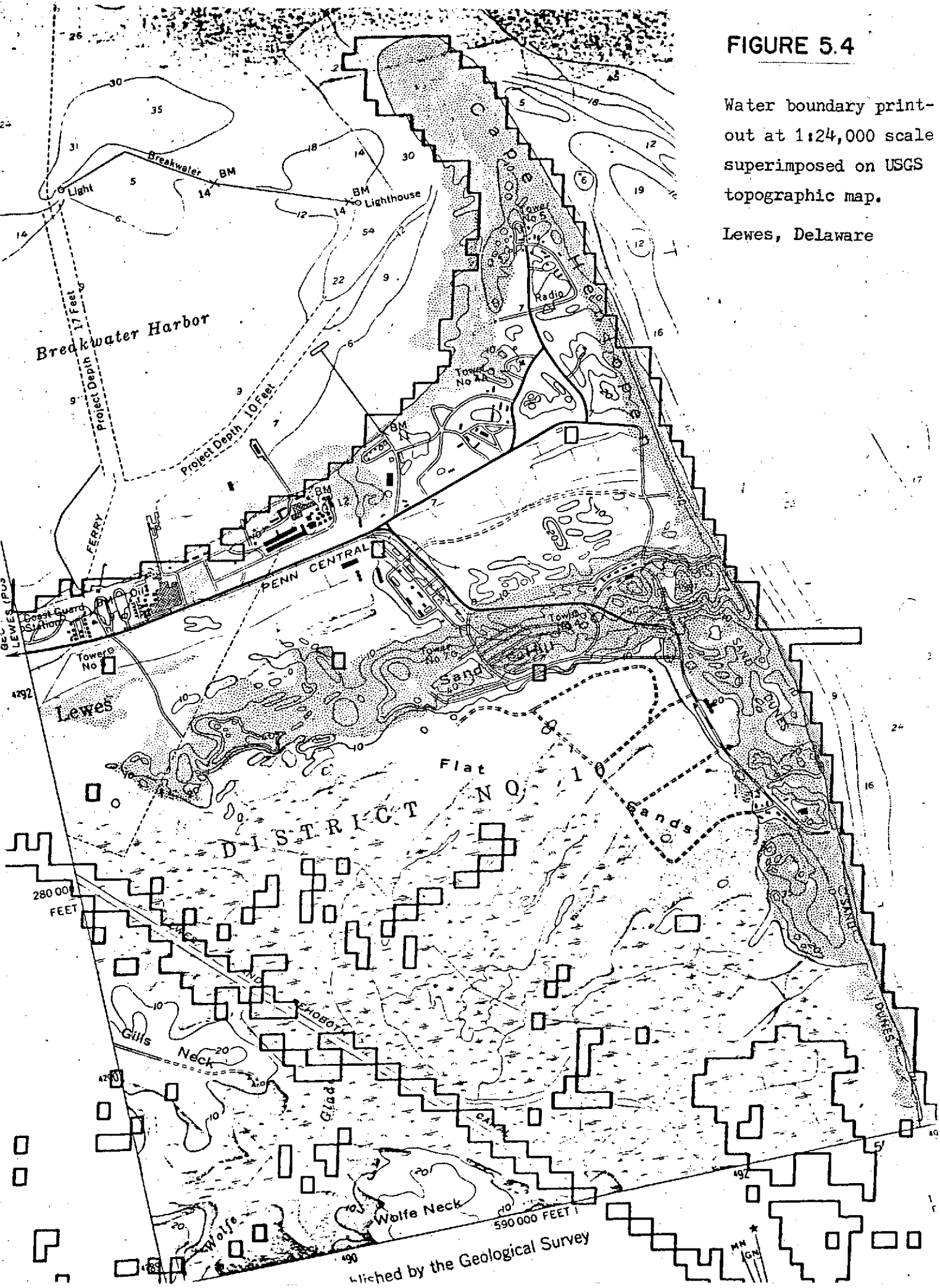
Delaware Bay - decision land-use and vegetation image



FIGURE 5.4

Water boundary print-out at 1:24,000 scale superimposed on USGS topographic map.

Lewes, Delaware



6.0 CONCLUSIONS

Under atmospheric conditions encountered along the East Coast of the United States, MSS band 5 seemed to give the best representation of sediment load in the upper one meter of the water column. Maps of suspended sediment concentration were prepared by relating the measured sediment concentration values to the radiance in band 5 and fitting the data to an exponential by a non-linear regression. Band 4 was masked by haze-like noise, while band 6 did not penetrate as deeply into the water column. ERTS-1 image radiance (microdensitometer trace) correlated well with Secchi depth and suspended sediment concentration. Color density slicing of 70mm transparencies helped delineate the suspended sediment patterns more clearly and differentiate turbidity levels. Sediment pattern enhancements obtained by additive color viewing of the four ERTS-1 MSS band transparencies did not noticeably improve the contrast beyond that seen in the best band, i.e., MSS band 5. However, digital enhancement techniques produced improved thematic maps.

Current circulation patterns were observed during different parts of the tidal cycle, using suspended sediment as a natural tracer. The current direction in the ERTS-1 imagery agreed well with predicted and measured currents throughout Delaware Bay, except on those days when the wind caused surface currents to differ from predicted tidal currents. During flood tide the suspended sediment as seen from ERTS-1 also correlated with the depth profile since most of turbidity during flood tide seems to be caused by sand particles brought into temporary suspension by currents and waves over shallow parts of the bay. As expected, no such correlation was found during ebb tide, when smaller particles of silt and clay are carried down the river in a state of nearly permanent suspension.

Convergent shear boundaries between different water masses have been observed from ERTS-1, with foam lines containing high concentrations of lead, mercury, and other toxic substances. The dispersion and movement of plumes of acid and sludge dumped at various intervals before ERTS-1 and Skylab overpasses have been studied.

As expected, Skylab imagery contains better spectral and spatial resolution than that from ERTS-1. Based on high-contrast targets, such as pier clusters and street patterns, the ERTS-1 MSS seems to have a resolution of 70 to 100 meters, Skylab's S-190A about 20 to 40 meters, and its S-190B about 10 to 20 meters. On the other hand, the regular eighteen-day cycle of ERTS-1 permits observation of important man-made and natural changes, and facilitates collection of ground truth.

Digital land-use analysis of ERTS data shows great potential as an inventorying and planning tool on the state, regional and federal level. While resolution problems generally restrict analysis to scales smaller than 1:100,000, ERTS data have the considerable advantages of regular, frequent coverage and easy, rapid data handling. Further, the digital techniques developed for use with ERTS data can be easily applied to data at larger scales if necessary.

Land-use data can be accumulated and updated at a fraction of the time and cost of conventional techniques. The ERTS digital format allows rapid, inexpensive data handling and offers the potential for automated change detection. Data products produced are generally cartographically precise and presented in a variety of formats easily used by planners and other government officials.

Ten vegetation and land-use discrimination classes were selected as follows:

1. Forest Land
2. Phragmites communis (Reed Grass)
3. Spartina patens and Distichlis spicata (Salt Marsh Hay and Spike Grass)
4. Spartina alterniflora (Salt Marsh Cord Grass)
5. Cropland
6. Plowed Cropland
7. Sand and Bare Sandy Soil
8. Bare Mud
9. Deep Saline Water
10. Sediment-laden and Shallow Saline Water

Canonical analysis showed that classification accuracy was quite good with Spartina alterniflora, exposed sand - concrete, and forested land - all discriminated with between 94% and 100% accuracy. The shallow water-mud and deep water categories were classified with accuracies of 88% and 93% respectively with all errors in classification occurring as one water category being classed as the other, a condition which is neither surprising nor bothersome with the overlap which these two classes exhibit no matter what the measurement technique used. Phragmites communis showed a classification accuracy of 83% with all confusion occurring with Spartina patens which may be due to use of mixed stands of these species as training sets. Both species occupy similar environments within the coastal zone. Discrimination of Spartina patens was very poor (accuracy = 52%) due, almost certainly, to difficulties in locating large, pure stands of S. patens for use as training sets. Classification accuracy for agriculture was also very poor (51%). Limitations of time and available class-memory space resulted in limiting the analysis of agriculture to very gross identification of a class which actually consists of many, varied signature classes. Table 5.1 shows that each of the four cropland categories were spectrally distinct (86%, 100%, 99% and 91% predicted classification accuracies) and so could have been broken out if class-memory space had been available. For this reason there is no doubt in the investigators' minds that if crop inventory had been the primary objective of the study, substantially better results could have been achieved in discriminating agricultural land categories.

Abundant ground truth was available in the form of vegetation maps compiled from NASA-RB-57 photography and in the photos themselves - both color and color-IR. Blow-ups of portions of the thematic maps digitally derived from ERTS data showed very good correlation with known sites. Cal-comp plots of thematic data at scales up to 1:24,000 showed excellent cartographic precision when overlaid onto existing maps.

It is believed that with further refinement of training set selection, sufficiently accurate results can be obtained for all categories producing a useful planning and management tool.

7.0 RECOMMENDATIONS

1. To continue monitoring environmental properties with ERTS-1 or ERTS-B in order to determine man-made and natural changes from the baseline provided by ERTS-1 and other systems, and to extrapolate environmental impact towards future, more intense development.
2. To launch a stationary, synchronous orbit satellite which would enable the continuous observation of current circulation and other water properties over complete tidal cycles under different wind, flow and wave conditions. Such operational systems would also significantly improve our ability to detect, track and clean-up accidental oil spills and provide flood warnings.
3. To add a thermal infrared mapping capability to the next satellite that is launched.
4. To develop an all-weather observation capability from future Earth Resources Observation Satellites.
5. To develop sensors which will help penetrate coastal waters more effectively and thus reduce the number of boats required for intensive oceanographic studies.
6. To accelerate the dissemination of ERTS imagery and digital tapes to users and investigators.

8.0 References

1. Klemas, V., Daiber, F., Bartlett, D., Crichton, O., Fornes, A., in Photogrammetric Engineering, Am. Soc. of Photogrammetry, Apr., 1974.
2. Klemas, V., Otley, M., Wethe, C., Robers, R., Application of ERTS-1 to the Management of Delaware's Coastal Resources, Proceedings NASA Third ERTS-1 symposium, Washington, D. C., December 10-14, 1973.
3. Bopp, Frederick, III, and Biggs, Robert B., Delaware Bay Rept. Series, Vol. 3, Trace Metal Geochemistry of Estuarine Sediments, Rept. No. 2, Trace Metal Environments Near Shell Banks in Delaware Bay, 45 pages, College of Marine Studies, University of Delaware, Spring 1973.
4. Oostdam, B. L., Suspended Sediment Transport in Delaware Bay, Ph.D. dissertation, University of Delaware, May, 1971.
5. Ketchum, B. H., The Distribution of Salinity in the Estuary of the Delaware River, Woods Hole Oceanographic Institute, Ref. No. 52-103, 38 pages, 1952.
6. Harleman, D. R. F., Tidal Dynamics in Estuaries, Estuary and Coast-line Hydrodynamics, A. T. Ippen, Ed., McGraw-Hill, New York, 1966.
7. Kraft, J. D., A Guide to the Geology of Delaware's Coastal Environment, College of Marine Studies Publication, University of Delaware, 1971.
8. Bowker, D. E., P. Fleischer, T. A. Gosink, W. J. Hanna, and J. Lucwicz, Correlation of ERTS multispectral imagery with suspended matter and chlorophyll in lower Chesapeake Bay, Symp. Significant Results Obtained from ERTS-1 NASA Goddard Space Flight Center, Greenbelt, Maryland, March 5-9, 1973.
9. Klemas, V., Borchardt, J. F., Treasure, W. M., Suspended Sediment Observation from ERTS-1 Remote Sensing of Environment, Vol. 2, 1973.
10. McCluney, W. R. NASA Goddard Space Flight Center, Personal Communication, 1974.
11. Williamson, A. N., and Grabau, W. E., "Sediment Concentration Mapping in Tidal Estuaries," Proceedings of the Third ERTS Symposium December 10-14, 1973, Washington, D. C.
12. Symposium of Significant Results Obtained from the Earth Resources Technology Satellite-1; 5 through 9 March 1973; Goddard Space Flight Center; NASA SP-327.
13. U. S. Department of Commerce, Tidal Current Charts-Delaware Bay River, Environmental Science Services Administration, Coast and Geodetic Survey, Second Edition, 1960.

14. U. S. Department of Commerce, Tidal Current Tables, Atlantic Coast of North America, National Oceanic and Atmospheric Administration, National Ocean Survey, 1972 and 1973.
15. Kupferman, S. L., Klemas, V., D. Polis, and K. Szekiolda, Dynamics of aquatic frontal systems in Delaware Bay, A.G.U. Annual Meeting, San Francisco, California, April 16-20, 1973.
16. Szekiolda, K. H., Kupferman, S., V. Klemas, and D. F. Polis, Element Enrichment in Organic Films and Foam Associated with Aquatic Frontal Systems, J. Geophys. Res. 77, No. 27, September 20, 1972.
17. Ibid.; pg. 1015; Pennsylvania State University; H. A. Weeden et al.
18. Ibid.; pg. 1031; LARS; Purdue University; William Todd et al.
19. Ibid.; pg. 1047 Environmental Research Institute of Mich.; Irwin J. Sattinger et al.
20. A. S. Hanson and R. H. Dye; "Spectral Signature Recognition"; Bendix Technical Journal, Vol. 3, No. 2; 1970.
21. P. E. Chase and L. E. Reed; "Determine Utility of ERTS-1 to Detect and Monitor Area Strip Mining and Reclamation"; Bendix Corp. BSR 4071; NASA-CR-132100; May 1973.
22. Reimold. R. J., Gallagher, J. L., and Thompson, D. E., "Remote Sensing of Tidal Marsh," in Photogrammetric Engineering, Am. Soc. of Photogrammetry, 1973.
23. Wobber, F. T., and Anderson, R. R., "Operational Wetlands Mapping Using Multiband Aerial Photography," in Coastal Mapping Symposium, Am. Soc. of Photogrammetry, 1972.
24. Klemas, V., Bartlett, D., Daiber, F., Mapping Delaware's Coastal Vegetation and Land Use from Aircraft and Satellites, A.S.P., Symposium on Remote Sensing in Oceanography, Orlando, Fla., October 2-5, 1973.
25. Rogers, R. H., and Reed, L. E. (1973) "Automated Land Use Mapping from Spacecraft Data" - Bendix Special Report #4097.
26. Kraft, J. C., and Caulk, R. L., "The Evolution of Lewes Harbor" - College of Marine Studies Technical Report No. 10, Nov. 1972.
27. Hugg, D. S., and Williams, J. C., "Delaware Natural Resources Inventory," Delaware State Planning Office, 1970.
28. Rogers, R. H., Peacock, K., and Shah, N. J., "A Technique for Correcting ERTS Data for Solar and Atmospheric Effects," unpublished manuscript, Bendix Aerospace Systems Division, 1973.
29. Klemas, V., Bartlett, D., Rogers, R., Inventories of Delaware Coastal Vegetation and Land Use Utilizing Digital Processing of ERTS-1 Imagery., Proceedings Ninth International Symposium on Remote Sensing of Environment, Ann Arbor, Michigan, April 15-19, 1974.

9.0 List of Publications

1. Szekielda, K. H., Kupferman, S. L., Klemas, V., Polis, D. F., Element Enrichment in Organic Films and Foam Associated with Aquatic Frontal Systems, *Journal of Geophysical Research*, Volume 77, No. 27, September 20, 1972.
2. Klemas, V., Detecting Oil and Measuring Oil on Water, *Instrumentation Technology*, September, 1972.
3. Klemas, V., Srna, R., and Treasure, W., Investigation of Coastal Processes Using ERTS-1 Satellite Imagery, American Geophysical Union Annual Fall Meeting, San Francisco, California, Dec. 4-7, 1972.
4. Klemas, V., Daiber, F., Bartlett, D., Crichton, O., Fornes, A., Application of Automated Multispectral Analysis to Delaware's Coastal Vegetation Mapping, American Society of Photogrammetry Annual Meeting, Washington, D.C., March 11-16, 1972.
5. Klemas, V., Daiber, F., Bartlett, D., Identification of Coastal Vegetation Species in ERTS-1 Imagery, *Proceedings NASA ERTS-1 Symposium on Significant Results*, Washington, D. C., March 5-9, 1973.
6. Klemas, V., Srna, R., Treasure, W., Applicability of ERTS-1 Imagery to the Study of Suspended Sediment and Aquatic Fronts, *Proceedings of NASA ERTS-1 Symposium on Significant Results*, Washington, D. C., March 5-9, 1973.
7. Kupferman, S., Klemas, V., Polis, D., and Szekielda, K., Dynamics of Aquatic Frontal Systems in Delaware Bay, A.G.U. Meeting, Washington, D. C., April 16-20, 1973.
8. Klemas, V., Srna, R., Treasure, W., Assessment of Sediment Dispersal Patterns on Delaware Bay by Use of ERTS-1 Satellite Imagery, *Proceedings International Symposium on Interrelationships of Estuarine and Continental Shelf Sedimentation*, Bordeaux, France, July 9-14, 1973.
9. Klemas, V., (Invited Paper), Requirements for Laser System Used in Coastal Investigation, *Proceedings Conference on the Use of Lasers for Hydrographic Studies*, Wallops Island, Va., September 12, 1973, Sponsors NASA, NOAA, EPA, NAVY.
10. Klemas, V., Borchardt, J. F., Treasure, W. M., Suspended Sediment Observations from ERTS-1 Remote Sensing of Environment, Vol. 2, 1973.
11. Klemas, V., Srna, R., Treasure, W., and Rogers, R., Satellite Studies of Suspended Matter and Aquatic Interfaces in Delaware Bay, *Proceedings A.S.P. Symposium on Remote Sensing in Oceanography*, Orlando, Florida, October 2-5, 1973.

12. Klemas, V., Bartlett, D., Daiber, F., Mapping Delaware's Coastal Vegetation and Land Use from Aircraft and Satellites. Proceedings A.S.P. Symposium on Remote Sensing in Oceanography, Orlando, Florida, October 2-5, 1973.
13. Klemas, V., (Invited Paper), Satellite Studies of Turbidity, Waste Disposal Plumes and Pollution - Concentrating Water Boundaries, Proceedings Second Conference on Environmental Quality Sensors, National Environmental Research Center, Las Vegas, Nevada, October 10, 1973, (Sponsor EPA).
14. Klemas, V., Bartlett, D., Rogers, R., Leed, L., Inventories of Delaware's Coastal Vegetation and Land-Use Utilizing Digital Processing of ERTS-1 Imagery, Proceedings NASA Third ERTS-1 Symposium, Washington, D. C., December 10, 1973.
15. Klemas, V., Otley, M., Davis, G., Rogers, R., Mapping Coastal Water Properties and Current Circulation with Spacecraft, Second Joint Conference on Sensing of Environmental Pollutants, Washington, D. C., December 10-12, 1973. (EPA, NOAA, NASA, DOT, ETC.).
16. Klemas, V., Otley, M., Wethe, C., Rogers, R., Application of ERTS-1 to the Management of Delaware's Coastal Resources, Proceedings NASA Third ERTS-1 Symposium, Washington, D. C., December 10-14, 1973.
17. Klemas V., Otley, M., Philpot, W., Rogers, R., Correlation of Coastal Water Turbidity and Circulation with ERTS-1 and Skylab Imagery. Proceedings Ninth International Symposium on Remote Sensing of Environment, April 15-19, 1974, Ann Arbor, Michigan.
18. Klemas, V., Bartlett, D., Rogers, R., Inventories of Delaware Coastal Vegetation and Land Use Utilizing Digital Processing of ERTS-1 Imagery, Proceedings Ninth International Symposium on Remote Sensing of Environment, April 15-19, 1974. Ann Arbor, Michigan.
19. Klemas, V., Daiber, F., Crichton, O., Fornes, A., Application of Automated Multispectral Analysis to Delaware Coastal Vegetation Mapping. Photogrammetric Engineering, Vol. XV, No. 4., April, 1974.
20. Klemas, V., Borchardt, J., Hsu, L., Gredell, G., Wang, H., "Photo optical Determination of Shallow-Water Wave Spectra," Proceedings International Symposium on Ocean Wave Measurement and Analysis, New Orleans, La., September 9-11, 1974.
21. Klemas, V., Maurer, D., Leatham, W., Kinner, P., Treasure, W., Dye and Drogue Studies of Spoil Disposal and Oil Dispersion, Journal of Water Pollution Control Federation, Vol. 46, No. 8, August, 1974. pp. 2026-2034.

10. NEW TECHNOLOGY

A New Field Technique for Rapidly Determining the Spectral Attenuation of Light By Suspended Matter

Summary

The purpose of this effort was to investigate an inexpensive, rapid approach for continuously monitoring optical water properties along a coastal transect. The approach is based on a device referred to as a "Spectral Attenuation Board," consisting of a board with colored stripes, partly immersed in the water at an angle, surrounded by a floating structure and towed by a boat. By mounting a camera on a rigid support above the float, a series of photographs can be obtained indicating the attenuation of each color as a function of depth. In contrast to a Secchi disk, the board does not require the boat to stop completely for each reading, gives attenuation as a function of depth in various color bands and results in a more precise, permanent record, since each photograph can be analyzed by microdensitometry.

Background and Relevance

The Spectral Attenuation Board was conceived during our study of aquatic frontal systems and suspended sediment patterns. Fronts are regions of high horizontal density gradient and have often been observed in the open ocean, for example, Rao and Murty (1), Beckerle (2), Katz (3), and Cromwell and Reid (4). Observations of fronts have recently been reported in the Gulf of Mexico, at the mouth of the Mississippi, associated with the Mississippi River outflow [Wright and Coleman (5), Wright (6)]. For the past year we have been observing fronts in Delaware Bay, using STD sections, dye drops and aircraft and satellite photography (7,8,9). Fronts are a major hydrographic feature in the bay. They have been found to have a horizontal density gradient. Horizontal salinity gradients of 4‰ in one meter, and convergence velocities of the order of 0.1 m/sec have been observed. Often the fronts extend for tens of miles, generally parallel to the axis of the bay, although locally they can be aligned in almost any direction. Fronts have been observed near the mouth of the bay, and appear to be associated with the tidal intrusion of shelf water. Since the fronts

and boundaries are frequently associated by strong temperature, salinity and turbidity gradients, they seriously affect diver and sonar operations. For example, as one of the boundaries passed divers working on towers at 18-foot depth at the wave test site near Indian River Inlet, the visibility changed from about 0.5 meter to 2.0 meters (8).

The Spectral Attenuation Board (SAB), described in the next section, offers the following advantages to investigations of regional optical water properties, suspended matter or aquatic fronts;

- a) It represents a rapid means for obtaining equivalent Secchi depth on a continuous transect, greatly decreasing the time spent on a station by eliminating the need to lower a Secchi disk.
- b) The SAB can be towed by a boat to get a continuous reading, complementing a transmissometer used in a pumped flow-through mode.
- c) Stripes of different colors on the partly submerged board give an indication of absorption and scattering by suspended and dissolved matter in the selected color bands, in addition to the white band of the Secchi board (Figure 1). Difference in the ratios of light penetration depths for the colors can be related to discrete water sample analysis.
- d) A microdensitometer trace running the length of the stripes will give a curve representing the rate of attenuation of light in the water column, and provide a means for detecting non-uniform particle distribution in the water column.
- e) By matching the spectral characteristics of the color stripes to filters used in aerial photography for enhancing water features, the penetration depth of each filter can be rapidly determined.
- f) Photographing the board by a camera mounted above it provides a permanent record. Microdensitometry of the photographs gives more precision than Secchi disk disappearance monitored by eye.

Approach and Previous Accomplishments

The Secchi disk is the simplest device for determining the transmission of visible light through water. It consists of a white plate about 30 cm in diameter, fastened to hang horizontally on the end of a line marked in

meters [Tyler, (10)]. The disk is lowered into the water and the depth at which it is lost to sight is recorded as the "Secchi depth." Although the Secchi disk is a semi-quantitative device, its simplicity has attracted investigators to the extent that most of the coastal turbidity data is in the form of "Secchi depths" [Williams, Johnson, Dyer (11)]. The same is true of Delaware Bay.

Empirical relationships have been determined by several investigators [Jones and Willis (12)] relating the Secchi disk visibility to the volume attenuation coefficient as measured by more precise instruments such as transmissometers. The relationship between Secchi disk visibility D and the volume attenuation coefficient α as measured with a transmissometer has been empirically determined by various investigators, including Jones and Willis (12) who found that:

$$\frac{\alpha}{4.38} = \frac{1}{D} \quad (1)$$

In eq. (1), the constant, 4.38, was determined empirically by Jones and Willis from data on the English Channel. Although this constant has been used frequently [Biggs (13)], it must remain open till further tested in different areas.

Determination of the median "optical" grainsize from the transparency and weight data involves transforming transparency to α as follows:

$$\alpha = \frac{1}{r} \ln \frac{(Nr)}{(No)} \quad [\text{Tyler and Presisendorfer, (14)}] \quad (2)$$

where α = volume attenuation coefficient per cm

r = path length in cm

Nr = radiance at distance r from source

No = source radiance

Postma (15) found that the relationship between Secchi disc visibility, weight of seston and median size of the seston was given by:

$$\frac{1}{D} = 0.15 \frac{G}{d} \quad (3)$$

where d = particle grainsize dia. in cm

G = concentration of seston in gm/cm³

D = Secchi disc visibility in cm

Substituting the value of

$\frac{1}{D}$ from eq. (1) into eq. (3) one obtains;

$$d = \frac{.657G}{\alpha} \quad (4)$$

Thus by measuring α with a transmissometer and G in samples from the same pumped flow-through system, one can obtain the volume attenuation coefficient, concentration of suspended matter, and an estimate of the median grainsize d. If a transmissometer is not available, one can use a Secchi disk. Secchi depth measurements are always advisable, first because most existing turbidity data is in terms of Secchi depth, and secondly, as a double check on the reliability of the transmissometer.

The large lateral extent of frontal systems and their rapidly changing configuration ideally require one aircraft and two boats for thorough examination. As the aircraft takes pictures, one of the boats takes stations on either side of the boundary to obtain temperature, salinity and Secchi depth profiles, while the second boat makes continuous transects with a transmissometer, fluorometer and Secchi disk. Rapid boat take Secchi depth measurements. Therefore, a Spectral Attenuation Board was developed which can give an equivalent Secchi depth reading on a continuous basis. By attaching the transmissometer and fluorometer to a pumped flow-through system and towing the Spectral Attenuation Board, continuous operation was achieved without the need for intermittent stops.

As shown in Figures 2 and 3, the SAB consists of a color board, a float and a superstructure supporting a camera which views the board. The board is made of plywood, three feet wide and eight feet long. One end is attached by hinges to a float and the other is free-floating. The free-floating end has weights attached which sink the board to an angle with the surface. This angle can be adjusted by changing the guides which run from the free-floating end to floating parallel arms on the surface. The floating arms are calibrated in meters for easy calculation of equivalent Secchi depth (knowing the angle of the board and distance along the arms). The semi-submerged visible surface of the board has white, green and red stripes, each one foot wide, running parallel to the long dimension of the board.

The white paint was chosen to resemble the flat white appearance of Secchi disks. Since red and green filters are frequently used to enhance suspended sediment and chlorophyll in aircraft imagery, the two colored stripes were matched approximately to the spectral transmittance of the "red" Kodak Wratten No. 25A and "green" No. 58 filters.

A camera positioned ten feet above the board on a rigid tripod is used to record the distance at which each color stripe becomes invisible. Since the inclination angle of the board is known, the visible length of each stripe can be converted to a depth. By using a camera, a more precise measurement of light penetration for each of the three colors is achieved. A color standard held above the water permits compensation for differences in film and lighting conditions. The camera provides a permanent record in addition to giving a more precise measurement than a Secchi disk viewed by the eye. The same color board has also been photographed from an aircraft flying at low altitude above the towed board.

Recommendations

To fully establish the applicability of the Spectral Attenuation Board to the study of optical water properties, suspended matter, and aquatic frontal systems, the following tasks need to be accomplished in the future:

1. Measure visibility depth of the white line on the Spectral Attenuation Board (SAB) and correlate with the visibility depths obtained with a Secchi disk. This step essentially calibrates the board in terms of "equivalent Secchi depths".
2. Experimentally determine the constant relating the volume attenuation coefficient as obtained from transmissometer readings to the visibility depth measured by the Spectral Attenuation Board. If such a constant can be defined for Delaware Bay, we will estimate medium grainsize of suspended matter using SAB visibility depth and the concentration as obtained from sample analysis.
3. Closely match colors of stripes on the SAB to the transmission bands of filters used in ERTS-1. Compare the penetration depths of the white stripe observed by a camera with filters to colored stripes photographed on color film without filters.

4. Determine relationships existing between depth of light penetration as a function of color and the color active content of the water column.

5. Evaluate the feasibility of microdensitometer traces of the board as a means of detecting non-homogeneous particle distribution.

6. Evaluate the effect of illumination and viewing conditions on the accuracy of the SAB, including the influence of sun angle, cloud conditions, water surface reflection and camera film response.

7. Assess the reliability of SAB measurements under different wave conditions. When wavelengths were of the same order of magnitude as the dimensions of the board, unreliable results were obtained in the past.

8. Improve the configuration of the SAB to permit higher towing speeds.

References

1. Rao, G. V., and T. S. Murty, 1973. Some case studies of vertical circulations associated with oceanic fronts, *J. Geophys. Res.*, 78 (3), 549.
2. Beckerle, J. C., 1972. Prediction of mid-oceanic frontal passage confirmed in near-surface current measurements, *J. Geophys. Res.*, 77, 1637.
3. Katz, E. J., 1969. Further study of a front in the Sargasso Sea, *Tellus*, 21, 259.
4. Cromwell, T., and J. L. Reid, Jr., 1956. A study of oceanic fronts, *Tellus*, 8, 94.
5. Wright, L. D., and J. M. Coleman, 1971. Effluent expansion and interfacial mixing in the presence of a salt wedge, Mississippi River Delta, *J. Geophys. Res.*, 76, 8649.
6. Wright, L. D., 1970. Circulation, effluent diffusion and sediment transport, mouth of South Pass, Mississippi River Delta, Coastal Studies Series Number 26, 56 pages, Coastal Studies Institute, Louisiana State University.
7. Szekiolda, K. H., S. L. Kupferman, V. Klemas, and D. F. Polis, 1972. Elemental enrichment in organic films and foam associated with aquatic frontal systems, *J. Geophys. Res.* 77, (27), 5278-5282.
8. Klemas, V., R. Srna, and W. Treasure, 1972. Investigation of coastal processes using ERTS-1 satellite imagery, American Geophysical Union Annual Fall Meeting, San Francisco, California, December 4-7.
9. Kupferman, S., V. Klemas, D. Polis, K. Szekiolda, 1973. Dynamics of aquatic frontal systems in Delaware Bay, A.G.U. Annual Meeting, Washington, D. C., April 16-20.
10. Tyler, John, 1968. The Secchi disc, limnology and oceanography, Vol. XIII, No. 1, January 1968.
11. Williams, J., E.R. Fenimore Johnson, and A.C. Dyer, 1960. Water Transparency Observations Along the East Coast of North America, Smithsonian Misc. Collections, Vol. 139, No. 10, October.
12. Jones, D., and M.S. Willis, 1956. The attenuation of light in the sea and estuarine waters, *J. Marine Biol. Ass.* 35: 431-444.

13. Biggs, R.B., 1968. "Optical Grainsize" of suspended sediment in Upper Chesapeake Bay, *Chesapeake Science*, Vol. 9, No. 4, p. 261-266, December.
14. Tyler, J.E., and R. W. Presisendorfer, 1962. *Light in the Sea*, N.H. Hill, ed. Vol. 1: 397-449.
15. Bond, G.C., R. H. Meade, 1966. Size distribution of mineral grain suspended in Chesapeake Bay and nearby coastal waters, *Chesapeake Sci.* 7 (4): 208-212.
16. Postma, H., 1961. Suspended matter and Secchi disc visibility in coastal waters, *Netherlands Journal Sea Res.* 1 (3): 359-390.
17. Burt, W.V., 1955. Interpretation of spectrophotometer readings on Chesapeake Bay waters, *J. Mar. Res.* 14 (1): 33-46.
18. Oostdam, B.L., 1971. Suspended sediment transport in Delaware Bay, Ph.D. dissertation, University of Delaware, May.
19. Ruggles, F. H., 1973. Plume Development in Long Island Sound Observed by Remote Sensing, Symposium on Significant Results Obtained from ERTS-1, NASA Goddard S.F.C., Greenbelt, Maryland, March 5-9.
20. Bowker, D.E., P. Fleischer, T.A. Gosink, W.J. Hanna and J. Ludwig, 1973. Correlation of ERTS multispectral imagery with suspended matter and chlorophyll in Lower Chesapeake Bay, Symposium on Significant Results Obtained from ERTS-1, NASA Goddard S.F.C., Greenbelt, Maryland, March 5-9.

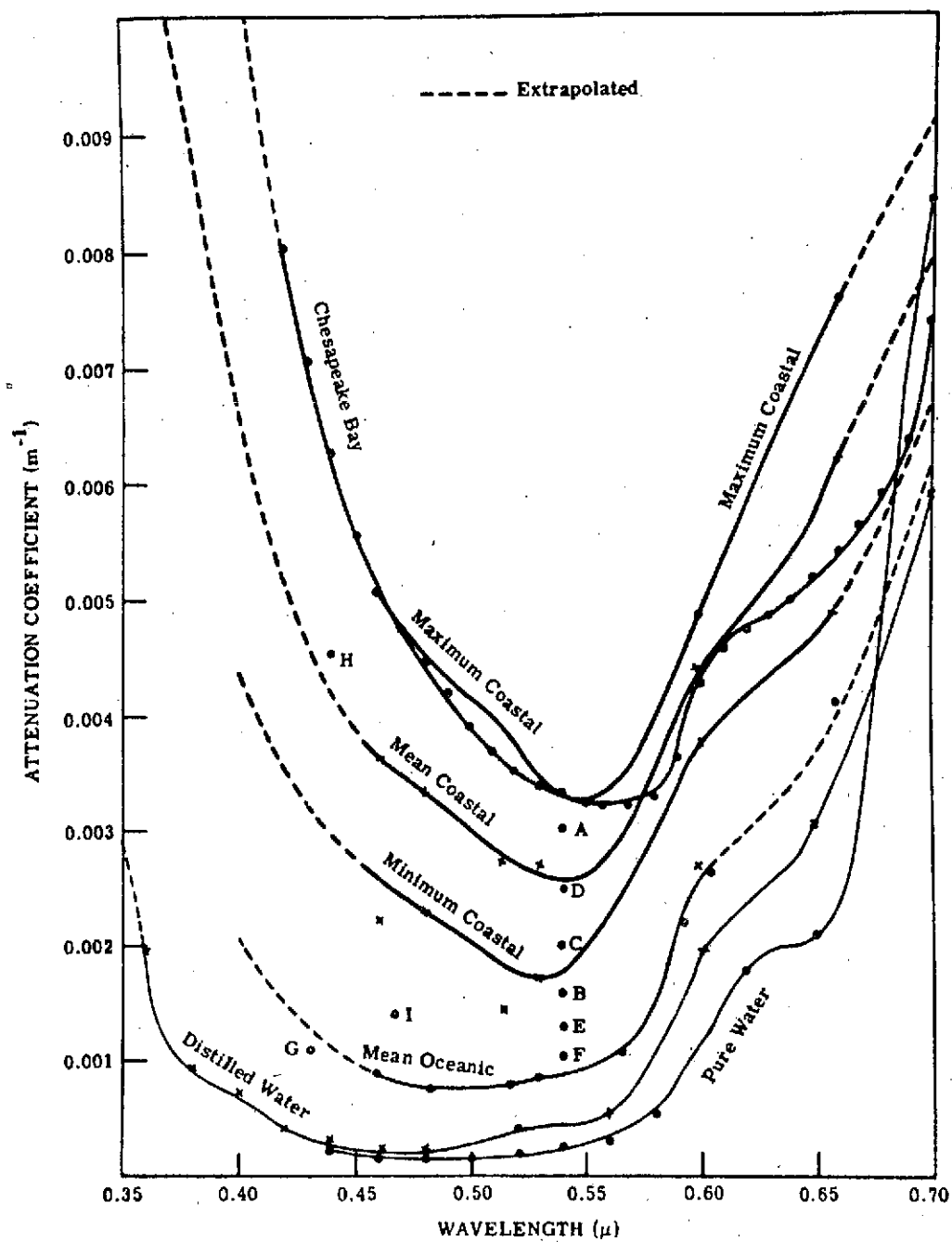


Figure 10.1 ATTENUATION COEFFICIENT VERSUS WAVELENGTH FOR PURE WATER AND SEA WATER

ORIGINAL PAGE IS
OF POOR QUALITY

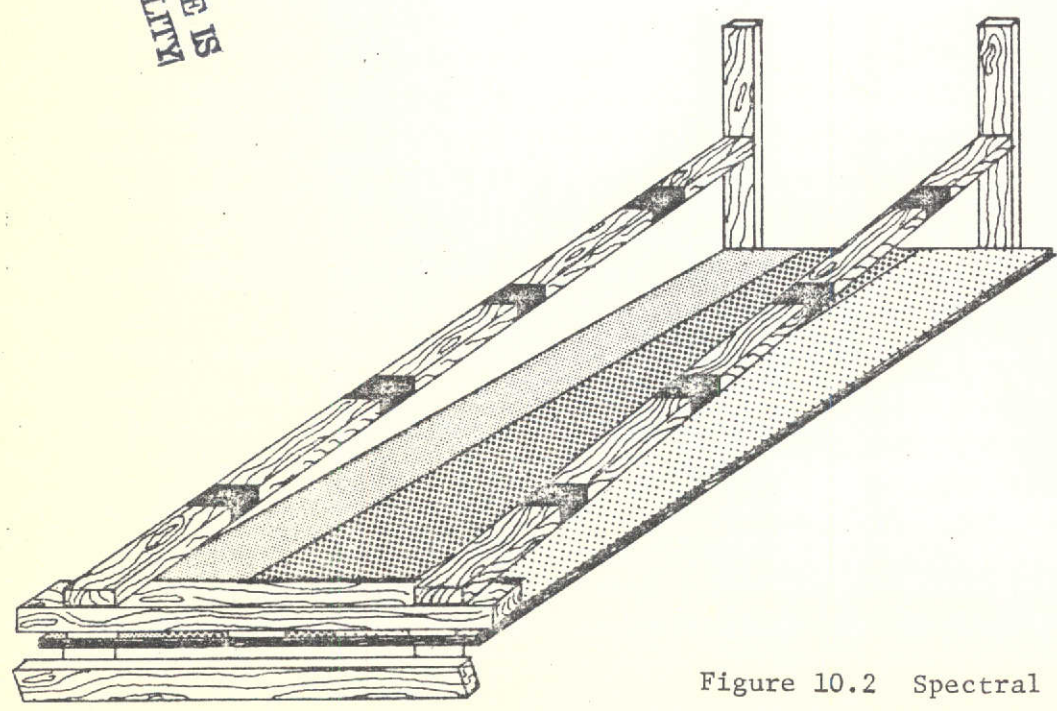
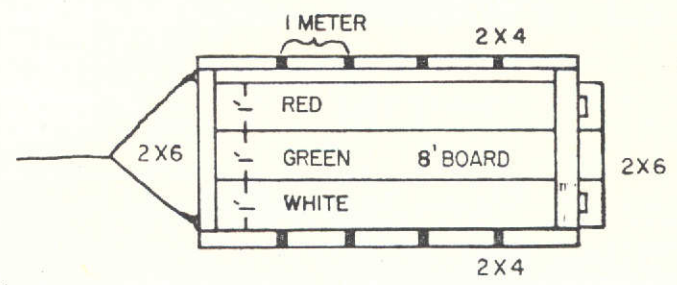


Figure 10.2 Spectral Attenuation Board

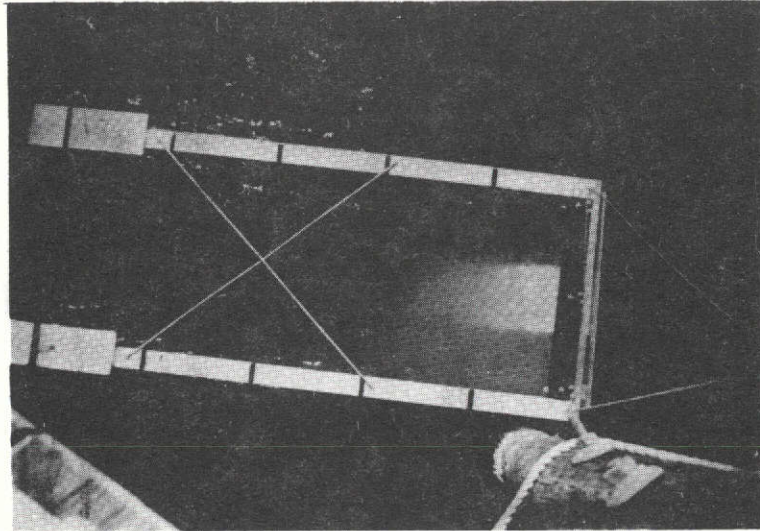


Figure 10.3 Spectral Attenuation Board with green, white, and red stripes in water adjacent to Henlopen fishing pier, without camera support structure on float

11.0 GROUND TRUTH DATA FOR ERTS-1 INVESTIGATIONS OF DELAWARE BAY

Ground truth data was collected from several types of ocean-going platforms during ERTS-1 overpasses in the Delaware Bay. The parameters of: suspended sediment and transport, Secchi depth, transmissibility, temperature, salinity, water color, Bay floor contours, and particle size were measured in an attempt to correlate their respective characteristics with the ERTS-1 imagery. Phenomena such as sediment transport, boundaries, fronts, salt water intrusions, water masses of different temperatures, bottom topography effects (e. g., ship channels, shoals, beaches, holes, ridges, and river mouth configurations), seem to agree well with the ground data and the imagery.

Most ground truth collection transects (point A to point B) were scheduled to have the overpasses and underpasses at their midpoint in time. The following table describes the various transects.

<u>Date</u>	<u>EST Time Span</u>	<u>Location</u>	<u>Type of Vehicle</u>
Oct. 22, 1972	1145-1308	Cape Henlopen to Cape May	R/V Wolverine
Jan. 26, 1973	0950-1050	Bombay Pt. to Cohansey River	Whaler
May 14, 1973	0906-1319	Cape Henlopen to Cape May	R/V Skimmer
June 1, 1973	0958-1030	Bombay Pt. to Cohansey River	Whaler
July 7, 1973	1010-1043	Bombay Pt. to Cohansey River	Whaler
July 7, 1973	0829-0851	Cape Henlopen to Cape May	Helicopter
July 7, 1973	1006-1036	Bowers to Egg Island Point	Helicopter
July 7, 1973	0920-1108	Cape Henlopen to Cape May	R/V Skimmer
July 25, 1973	1008-1253	Cape Henlopen to Cape May	R/V Wolverine
Aug. 29, 1973	0922-0942	Cape Henlopen to Cape May	Helicopter
Aug. 29, 1973	0901-1033	Cape Henlopen to Cape May	R/V Skimmer
Oct. 22, 1973	0927-1238	Cape Henlopen to 10 miles out into the ocean	R/V Skimmer
Oct. 23, 1973	0944-1243	Cape Henlopen to Cape May	R/V Skimmer
July 2, 1974	1000-1300	Joe Flogger Shoals to Hen and Chicken Shoals	Individual Boaters

Ground truth collection employs the use of either the Research Vessel Skimmer, or the Research Vessel Wolverine, a sixteen-foot Boston Whaler; a Cessna 172 airplane; an Army NASA jet-powered Bell-Huey Helicopter, and interested pleasure boaters. The R/V Skimmer is a forty-two foot aluminum-hulled craft equipped for plankton trawls, dredging, geologic and hydrographic sampling, Seismic profiling, and Loran positioning. It has a top speed of twelve kts. and can withstand moderate (3'-4') swells. It also has a three-foot draft which allows shallow work around shoaled areas. The R/V Wolverine is a forty-eight foot wooden-hulled trawler equipped for exploratory fishing, geological sampling, and limited hydrographic work. The Boston Whaler is

sixteen feet long, powered by a fifty-five horsepower engine. The Cessna airplane employed is a 172 four-seater with high wings, which allows easy access to photography of the ground. It can bank sixty degrees which gives fairly vertical pictures. The NASA helicopter is a jet-powered Bell-Huey piloted by a two-man NASA team from Wallops Island, Virginia. It is equipped with pontoons and many navigational tools. It can hover for short periods and travel from station to station at approximately 90 mph. which facilitates speedy sampling during the overflights. The scientist can be harnessed directly to the pontoon to work from that position during hovers and high-speed traveling.

Although more widely dispersed water samples can be obtained from a hovering helicopter than by boat, to further increase the number and dispersion of samples at the exact time of the ERTS-1 pass over Delaware Bay, pleasure crafts were organized to obtain samples over the entire test site. Problems in the past with using boaters were that they were asked to be at a specific location and to sample over several hours. We eliminated this problem by asking the boaters to take only two samples between 11 and 11:15 and to take them wherever they were at the time.

On the ERTS-1 pass of July second, scientists were stationed at three public boat launches along the bay (Woodland Beach, Bowers Beach, and the Lewes Public Boat Ramp) to hand out sampling packets to interested boaters. The packets contained two litre sampling bottles, a map, data card, and a pen. After filling the two bottles at the appropriate time the boaters were asked to mark their location on the map and fill out the data card with the time and their name and address. Boxes were placed at the ramps for the return of the bottles.

The two packets handed out at Woodland Beach, were either not returned or removed from the drop off point before we could pick them up. At Bowers Beach 19 packets were handed out and 16 had been returned by evening (84.2%). In Lewes 28 packets were handed out of which 24 came back (85.7%). A total of 49 packets were handed out and 40 of these were returned. Only 4 (10%) of the 40 were not in the allotted time range. This gave 36 (90% of packets returned, 73% of packets handed out) real time data points covering approximately 30 nautical miles. In the future, pleasure craft sampling will be

used in conjunction with other sampling techniques discussed previously to further increase our amount of sea truth.

Instrumentation and Sampling Techniques

The instrumentation utilized in analyzing ground truth samples includes a transmissometer, a Bendix radiant power measuring instrument, an interoceanic Marine Illuminous meter, Secchi discs, Pentax Spotmatic cameras, centigrade bucket thermometers, Loran, a sonar bathymetry transducer, analyzer.

A Hydro-Products Model 612S transmissometer system was used in situ for turbidity measurements. The instrument consists of a projector light source, a ten-cm cell path, and a photo cell detector. The housing chamber is baffled to eliminate external stray light. Optics in the projector housing present a lightbeam which is collimated sufficiently to illuminate only the detector optics. The detector optics are such that only light coming directly from the projector is "seen". This optical arrangement minimizes effects of forward and backscatter due to ambient light and divergent beam light. The sensor is designed to allow the water sample to circulate freely into the optical path where transmissivity is determined (%T) such that:

$$T = \frac{I_2}{I_1} \times 100$$

where: T = % Transmission
I₁ = intensity at projector
I₂ = intensity at detector

This measurement is related to the average optical attenuation coefficient of the water (α) by the equation:

$$T = 100e^{-\alpha d}$$

where: α = attenuation coefficient in Ln/Meter
d = cell path lengths in meters.

The 612 Sensor was designed for lowering from a static platform or it can be towed from a moving boat at speeds up to 5 knots, but our needs required a more sophisticated sampling technique in order to cover a large surface area in a short amount of time. The transmissometer was placed in a flow-

through pump system on board the R/V Skimmer for use with ERTS-1 data gathering (see Fig. 3.1). The ship's bilge pump supplied ocean water from a constant depth of 3 feet to the case which housed the instrument sensors. The case was air-tight which allowed a great volume of water to be passed through the sensor in a short period of time. This allowed the boat to travel its course at high speeds (10 kts.). The %T values represented integrated masses of water from point A to point B along the transect. In other words, the water sample was not at a point in the transect, but it was from a segment of water approximately 50 feet long. These average values are very realistic considering the resolution of ERTS-1 imagery.

The Bendix Radiant Power Measuring Instrument (RPMI) is a lightweight, portable instrument which is calibrated to measure down-welling and reflected radiation in each of the four ERTS MSS bands. The handle folds over to provide narrow-angle (7.0° circular) measurements from sky and ground targets as well as wide-angle sky and ground irradiance. The wide range of the RPMI allows for measurements as high as direct-beam-solar irradiance of $25\text{mw}/\text{cm}^2$ in Band 7 to as low a radiance from surface water as $0.02\text{mw}/\text{cm}^2$ in Bands 6 and 7.

The RPMI measurements are taken during the time of the ERTS pass. These measurements include, (1) global irradiance, H ; (2) sky irradiance, H_{sky} ; (3) radiance from a narrow solid angle of sky, $L_{\text{meas}}(\phi)$; and (4) direct-beam-solar irradiance, $H_{\text{sun}}(m)$. From these measurements the following parameters can be determined: beam transmittance, τ ; path radiance, L_a ; and direct-beam-solar irradiance above the atmosphere, H_0 . Now the measurements can be combined in the following equation to transform the ERTS radiance measurements, L , into absolute target reflectance units, ρ :

$$\rho = \frac{(L - L_a) \cdot \pi}{\tau (H_0 \tau^m \cos Z + H_{\text{sky}})}$$

where Z is the solar zenith angle read from the sun dial on the side of the RPMI or determined by a sextant.

The Inter-Ocean Marine Illuminance Meter (MIM) is a light, compact, and portable unit designed to measure and compare luminosity both on board and underwater. Operation is independent of any power source other than incident light on the photocells.

Once both the surface cell and the underwater cell are calibrated, relative incident radiance is measured by the surface cell and the underwater cell is lowered to the desired depth where relative radiance is again measured. When the two measurements are compared the transparency of the water is determined. Both cells are designed so that filters of different wavelengths can be attached in order that measurements can be made in the same spectral regions as the ERTS MSS bands.

White Secchi discs .49 cm in diameter, were used for relative visual turbidity readings. This size worked well in turbulent waters where swells were a few feet high. Also, green and red discs of the same diameter and color matched well with the green and red bands of the ERTS-1 MSS were employed to correlate light transmission of the scanners.

The R/V Skimmer's Loran was used to aid in transect alignment and radar aided in station positioning. These tools allowed mapping of stations to be \pm 50 feet in precision. The sonar transducer aboard the boat was utilized in plotting the bathymetry along the transect.

Bucket thermometers were used for temperature measurements. The transmissometer case had an auxillary outlet for sampling of the water for temperature, salinity, and sediment load.

During sampling runs, the R/V Skimmer sped along a transect at approximately 10 knots non-stop gathering data at equal intervals. As a result, the cape-to-cape transect took about one hour allowing data gathering to be accomplished one-half hour on each side of the overpasses. For shorter runs the Boston Whaler was used and transect runs lasted about one hour. The NASA helicopter was utilized best for long transect distances up to 25 miles. With its speed and accuracy of locating positions, 25-30 miles was easily covered in less than one hour. The helicopter would hover two feet above the surface while a scientist would sample the water with a plastic bucket. Temperature was a problem due to strong prop wash winds.

Sample Analyses

Samples collected under the ground truth program were analyzed for 1) sediment load, 2) salinity, 3) volatile content, and 4) total carbon.

The sediment load weight was determined from a one-litre sample immediately after sampling took place. This insured that bacterial action

and the formation of salts would not occur quickly enough to add error to the results. One litre was filtered through pre-dried and pre-weighed glass membrane filter pads (Gelbman) under suction. The pads and sediment were then dried at ambient temperatures and then weighed on a Mettler balance. Sediment load was then calculated in terms of weight (mg) per one litre of sample. Salinity was determined by a salinometer on fresh unfiltered samples. Volatile content of the sediment suspended in the water column was achieved by high temperature heating of the sample. The weight loss per sample weight times 100 gave % ignition loss. Total carbon was determined on a Coleman Carbon-Hydrogen Analyzer. The principle of analysis was based on the total combustion of the sample giving off CO_2 gas which was absorbed on an ascerite medium. Carbon was then calculated by converting the weight of CO_2 to weight of carbon.

Table 11.1
ERTS-1 Overpass
January 26, 1973

Transect: Bombay Pt. to Cohansey River Mouth
Whaler

<u>Station</u>	<u>Sed wt (mg/l)</u>	<u>Temp (°C)</u>	<u>Salinity (‰)</u>	<u>Secchi (cm)</u>	<u>%T</u>
1	94.6	2.5	5.894	19	NO DATA
2	85.5	2.6	5.875	24	
3	107.9	2.6	6.412	23	
4	89.2	2.9	4.465	28	
5	64.4	3.0	4.446	36	
6	35.4	2.8	4.393	45	
7	29.8	2.6	4.597	47	
8	34.0	3.3	6.253	51	
9	31.3	3.5	6.233	49	
10	38.5	3.1	6.649	46	
11	43.1	3.1	6.124	39	
12	43.9	3.0	6.308	41	
13	44.8	2.8	6.763	38	
14	76.1	2.7	6.499	29	

Table 11.2
ERTS-1 Overpass
June 1, 1973

Transect: Bombay Hook Pt. to Cohansey River Mouth
Whaler

<u>Station</u>	<u>Sed wt (mg/l)</u>	<u>Temp (°C)</u>	<u>Salinity (%)</u>	<u>Secchi (cm)</u>	<u>%T</u>
1	54.1	19.1	6.649	34	NO DATA
2	59.2	19.1	7.532	38	
3	39.7	18.8	7.003	45	
4	54.1	19.3	6.859	37	
5	101.4	18.0	6.535	27	
6	33.4	18.2	6.853	43	
7	47.8	19.1	5.512	43	
8	62.9	18.6	5.946	32	
9	53.9	19.2	5.506	29	
10	59.1	20.5	5.241	33	

Table 11.3
ERTS-1 Overpass
July 7, 1973

Transect: Bowers to Egg Island Pt.
Helicopter

<u>Station</u>	<u>Sed wt</u> <u>(mg/l)</u>	<u>Temp</u> <u>(°C)</u>	<u>Salinity</u> <u>(‰)</u>	<u>Secchi</u> <u>(cm)</u>	<u>%T</u>
1	39.7	27.2	16.852	NO DATA	NO DATA
2	34.1	27.5	18.199		
3	28.9	27.6	16.341		
4	19.5	27.0	15.061		
5	22.5	26.9	14.042		
6	21.6	26.5	9.255		
7	16.1	26.7	10.736		
8	19.0	27.0	6.401		
9	22.3	27.2	8.521		
10	22.1	26.9	10.893		
11	20.8	26.9	11.524		
12	41.1	26.8	11.860		

Table 11.4
ERTS-1 Overpass
July 7, 1973

Transect: Bombay Pl. to Cohansey River Mouth
Whaler

<u>Station</u>	<u>Sed wt (mg/l)</u>	<u>Temp (°C)</u>	<u>Salinity (‰)</u>	<u>Secchi (cm)</u>	<u>%T</u>
1	59.2	26.6	NO DATA	38	NO DATA
2	65.8	26.4		32	
3	77.8	26.4		33	
4	42.9	26.5		38	
5	53.2	26.7		35	
6	36.3	26.7		43	
7	31.9	27.0		47	
8	40.3	27.0		39	
9	44.8	27.0		34	
10	28.9	28.0		47	
11	62.7	26.9		36	

Table 11.5
ERTS-1 Overpass
July 7, 1973

Transect: Cape Henlopen to Cape May
R/V Skimmer

<u>Station</u>	<u>Sed wt (mg/l)</u>	<u>Temp (°C)</u>	<u>Salinity (%)</u>	<u>Secchi (cm)</u>	<u>%T</u>
1	32.8		20.662	133	45
2	29.5		20.476		42
3	33.8	25.1	18.527		39
4	27.0	25.1	17.797		41
5	22.0		16.648	128	40
6	28.7		20.310		46
7	28.4	24.2	20.743		44
8	42.7	24.7	24.003		46
9	33.0	23.2	26.803		54
10	31.8	23.7	26.320		57
11	33.1	23.2	26.652		58
12	43.4	23.0	25.163	204	
13	36.7	22.6	27.561	185	54
14	34.2	22.4	27.341		48
15	42.9	22.2	27.462	104	26
16	39.2	22.7	27.201	134	42
17	44.0	23.0	27.098		48
18					
19	37.1	22.7	27.287		43
20	74.5	22.4	27.759		23
21	43.9	22.4	27.899	152	45

Table 11.6
ERTS-1 Overpass
July 7, 1973

Transect: Cape Henlopen to Cape May
Helicopter

<u>Stations</u>	<u>Sed wt</u> <u>(mg/l)</u>	<u>Temp</u> <u>(°C)</u>	<u>Salinity</u> <u>(‰)</u>	<u>Secchi</u> <u>(cm)</u>	<u>%T</u>
1	35.9	23.5	23.652		
2	34.9	24.2	20.206		
3	32.0	23.5	18.742		
4	27.3	24.6	20.415		
5	25.2	24.1	19.113	NO	NO
6	30.2	23.5	25.505	DATA	DATA
7	35.3	23.7	25.622		
8	34.2	23.8	24.799		
9	38.2	24.9	23.365		
10	38.2	24.9	24.732		

Table 11.7
ERTS-1 Overpass
August 29, 1973

Transect: Cape May to Cape Henlopen
Helicopter

<u>Station</u>	<u>Sed wt</u> <u>(mg/l)</u>	<u>Temp</u> <u>(°C)</u>	<u>Salinity</u> <u>(‰)</u>	<u>Secchi</u> <u>(cm)</u>	<u>%T</u>
1	38.7	25.0	30.078		
2	33.2	24.5	30.325		
3	33.6	24.0	29.613		
4	37.6	24.0	29.755	NO	NO
5	30.4	24.5	29.639	DATA	DATA
6	38.1	23.5	29.632		
7	45.7	24.5	29.153		
8	44.1	24.5	28.282		
9	38.5	25.0	28.720		

Table 11.8
ERTS-1 Overpass
August 29, 1973

Transect: Cape Henlopen to Cape May
Skimmer

<u>Station</u>	<u>Sed wt (mg/l)</u>	<u>Temp (°C)</u>	<u>Salinity (‰)</u>	<u>Secchi (cm)</u>	<u>%T</u>
1	43.4	23.4	29.429	225	61
2	37.9	22.9	29.386		63.5
3	38.2	22.9	29.417		73
4	34.3	23.0	29.505		63.5
5	35.6	22.5	30.024		76
6	35.7	22.7	30.070		72.3
7	41.2	22.7	30.187		75
8	46.4	23.1	30.032		75
9	48.2	23.2	30.020		80
10	35.8	23.3	30.070	425	75.5
11	36.8	23.3	29.951		77
12	39.0	23.6	30.028		81
13	38.0	24.0	30.356		70
14	40.3	24.2	30.340		75.5
15	41.2	24.3	30.271	275	78
16	44.5	24.3	20.160		77

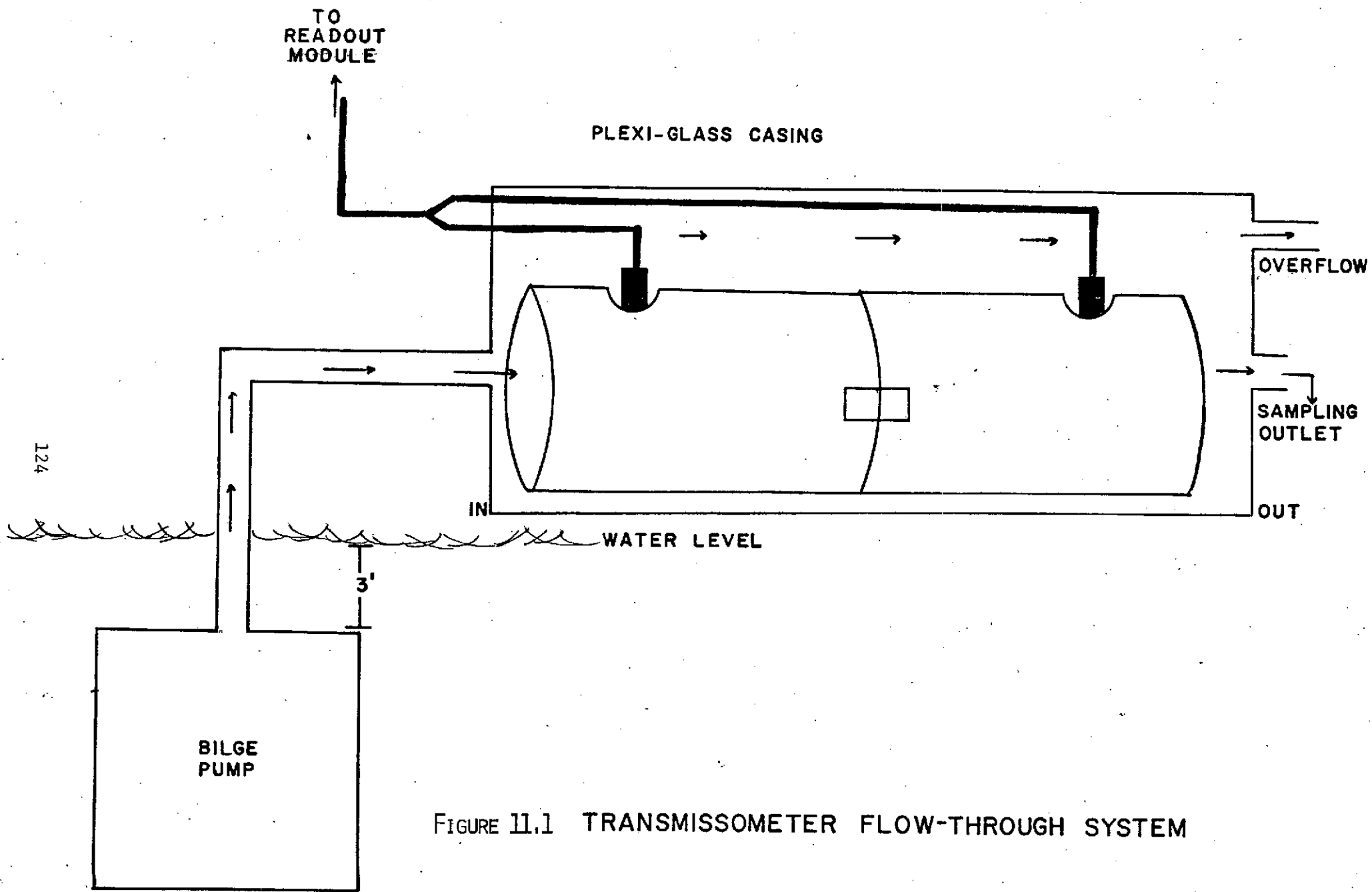


FIGURE 11.1 TRANSMISSOMETER FLOW-THROUGH SYSTEM

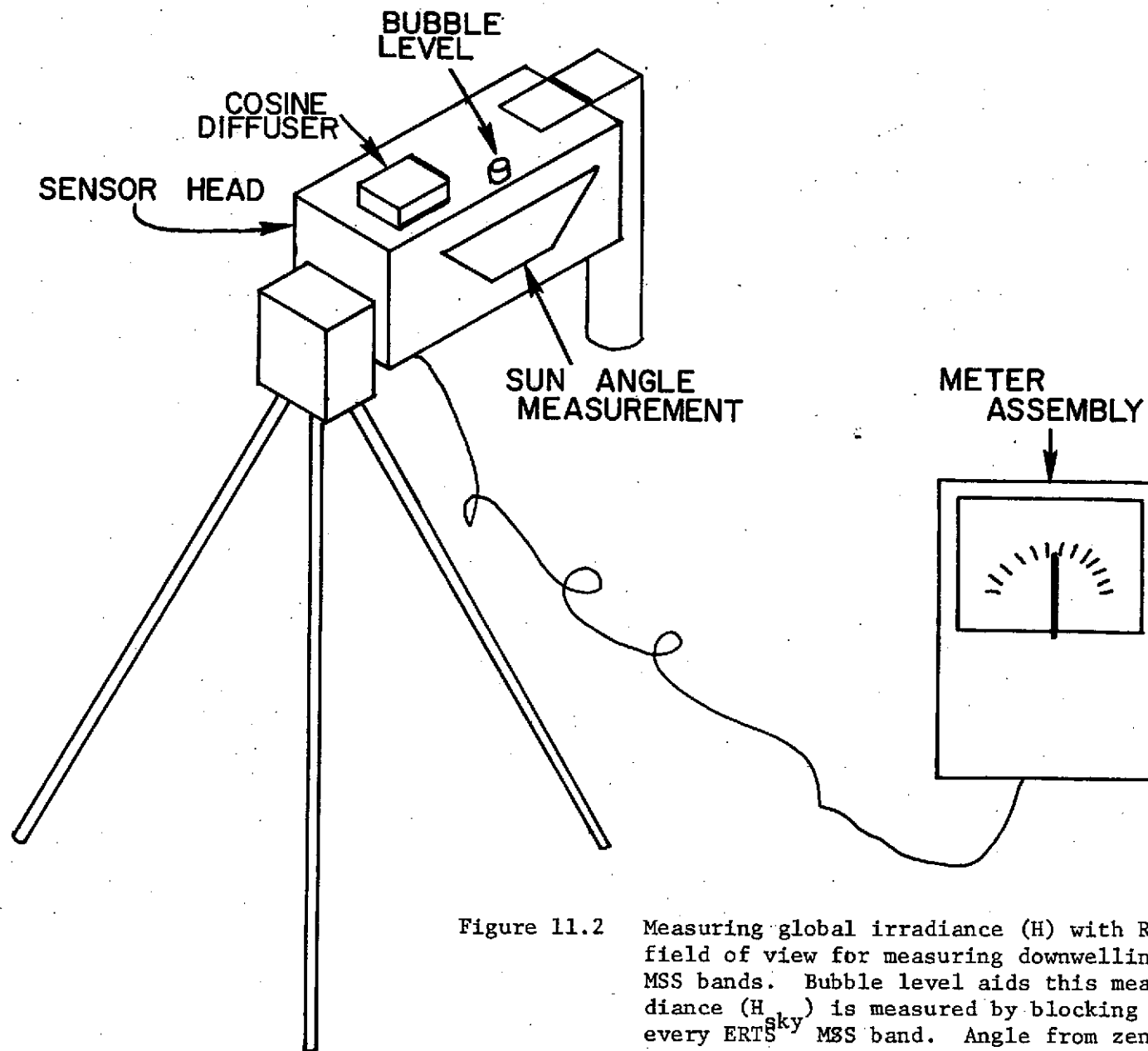
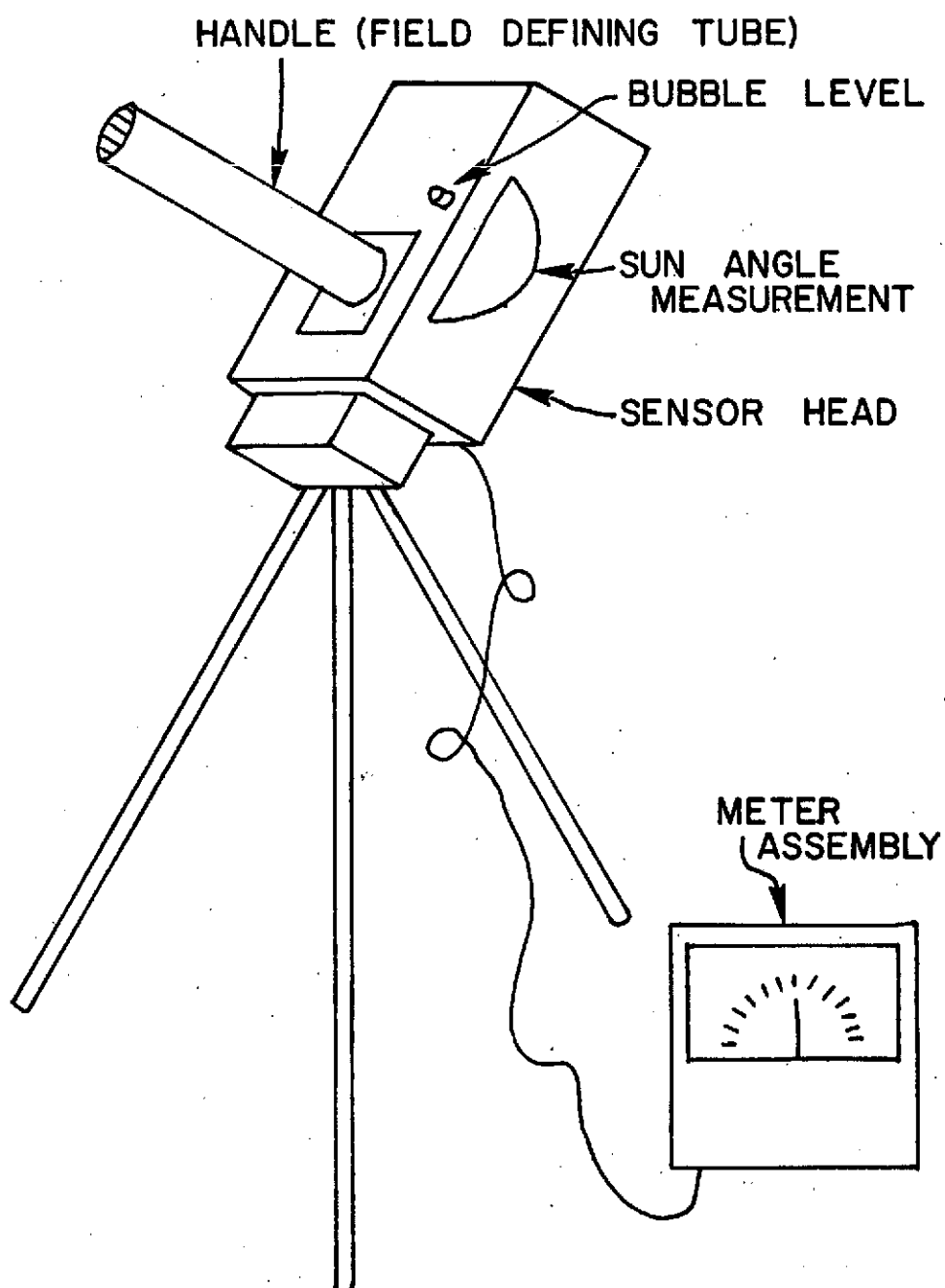


Figure 11.2 Measuring global irradiance (H) with RPMI - ZTY steradian field of view for measuring downwelling radiation in ERTS MSS bands. Bubble level aids this measurement. Sky irradiance (H_{sky}) is measured by blocking direct sunlight in every ERTS MSS band. Angle from zenith to sun is also measured in this mode by reading sun shadow on sun dial.

Figure 11.3 Radiance from narrow solid angles of sky (L_{meas}) - Handle serving as field stop, permits direct measurements through a 7.0° circular field of view. This mode also used to measure direct beam solar irradiance, H_{sun} .



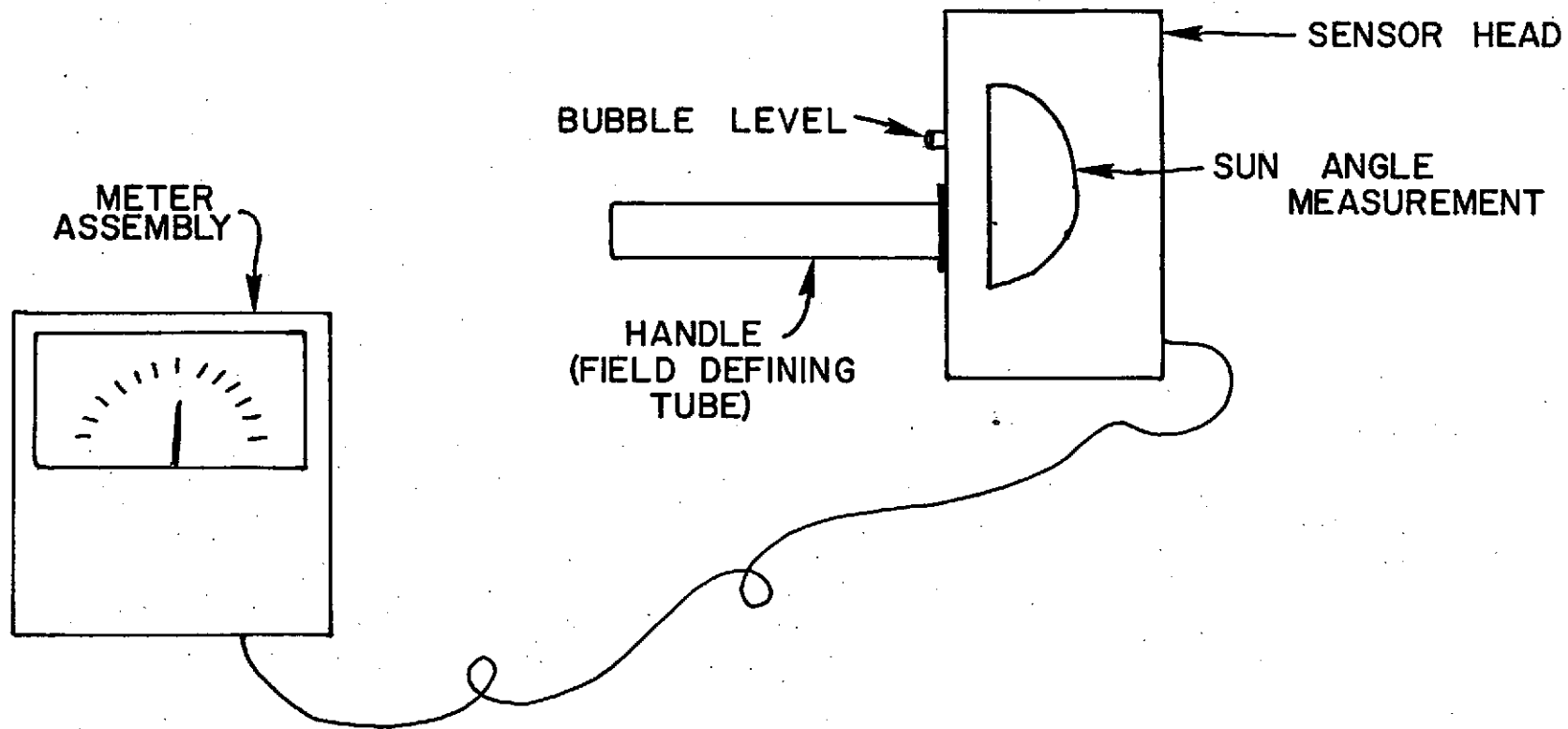


Figure 11.4 Reflected radiation measurement at ground truth site.

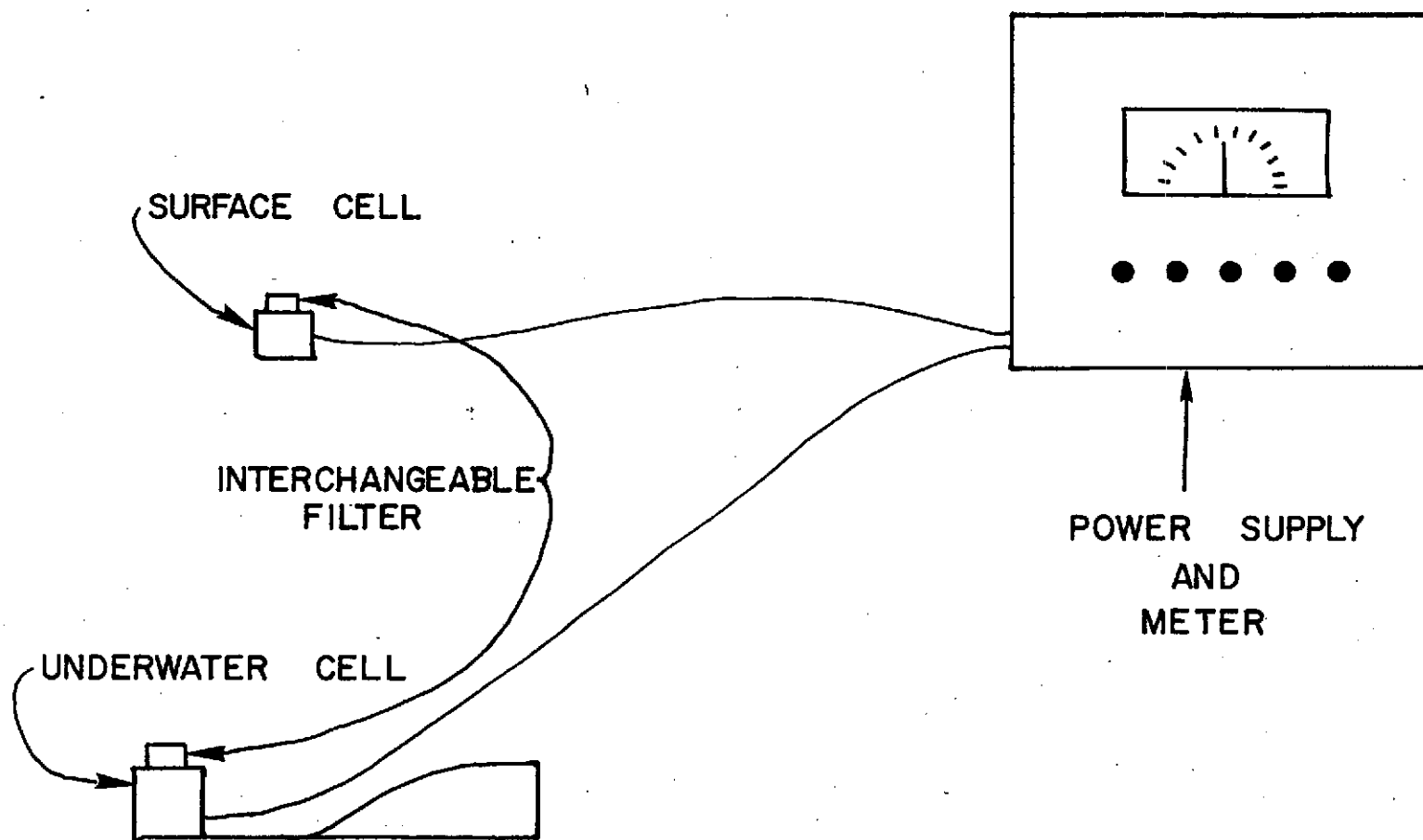


Figure 11.5 InterOcean Marine Illuminance Meter used for comparing luminosity at the surface and under water. Interchangeable filters allow for measurements in the ERTS MSS bands.